



Boronate-Based Probes for Biological Oxidants: A Novel Class of Molecular Tools for Redox Biology

Adam Sikora^{1*}, Jacek Zielonka^{2*}, Karolina Dębowska¹, Radosław Michalski¹, Renata Smulik-Izydorczyk¹, Jakub Pięta¹, Radosław Podsiadły³, Angelika Artelska¹, Karolina Pierzchała¹ and Balaraman Kalyanaraman²

¹ Faculty of Chemistry, Institute of Applied Radiation Chemistry, Lodz University of Technology, Lodz, Poland, ² Department of Biophysics and Free Radical Research Center, Medical College of Wisconsin, Milwaukee, WI, United States, ³ Faculty of Chemistry, Institute of Polymer and Dye Technology, Lodz University of Technology, Lodz, Poland

OPEN ACCESS

Edited by:

Giuseppe Vitiello,
University of Naples Federico II, Italy

Reviewed by:

Gloria Virginia López,
Universidad de la República, Uruguay
Flavia Carla Meotti,
University of São Paulo, Brazil
María Lucía Piacenza,
Universidad de la República, Uruguay

*Correspondence:

Adam Sikora
adam.sikora@p.lodz.pl
Jacek Zielonka
jzielonk@mcw.edu

Specialty section:

This article was submitted to
Chemical Biology,
a section of the journal
Frontiers in Chemistry

Received: 07 July 2020

Accepted: 12 August 2020

Published: 25 September 2020

Citation:

Sikora A, Zielonka J, Dębowska K, Michalski R, Smulik-Izydorczyk R, Pięta J, Podsiadły R, Artelska A, Pierzchała K and Kalyanaraman B (2020) Boronate-Based Probes for Biological Oxidants: A Novel Class of Molecular Tools for Redox Biology. *Front. Chem.* 8:580899. doi: 10.3389/fchem.2020.580899

Boronate-based molecular probes are emerging as one of the most effective tools for detection and quantitation of peroxynitrite and hydroperoxides. This review discusses the chemical reactivity of boronate compounds in the context of their use for detection of biological oxidants, and presents examples of the practical use of those probes in selected chemical, enzymatic, and biological systems. The particular reactivity of boronates toward nucleophilic oxidants makes them a distinct class of probes for redox biology studies. We focus on the recent progress in the design and application of boronate-based probes in redox studies and perspectives for further developments.

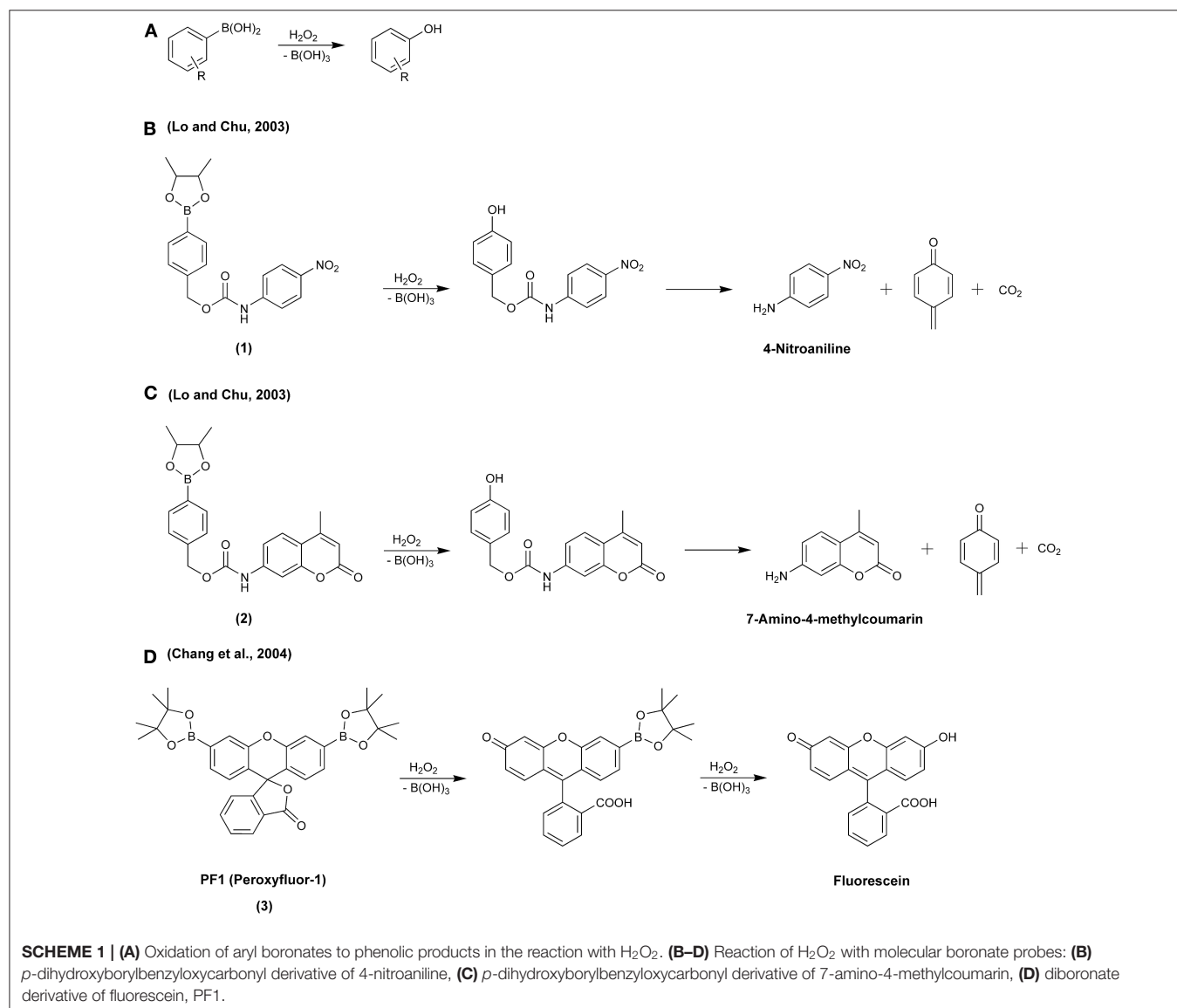
Keywords: peroxynitrite, hydrogen peroxide, hydroperoxides, hypochlorous acid, azanone, NADPH oxidases, boronic acids, molecular probes

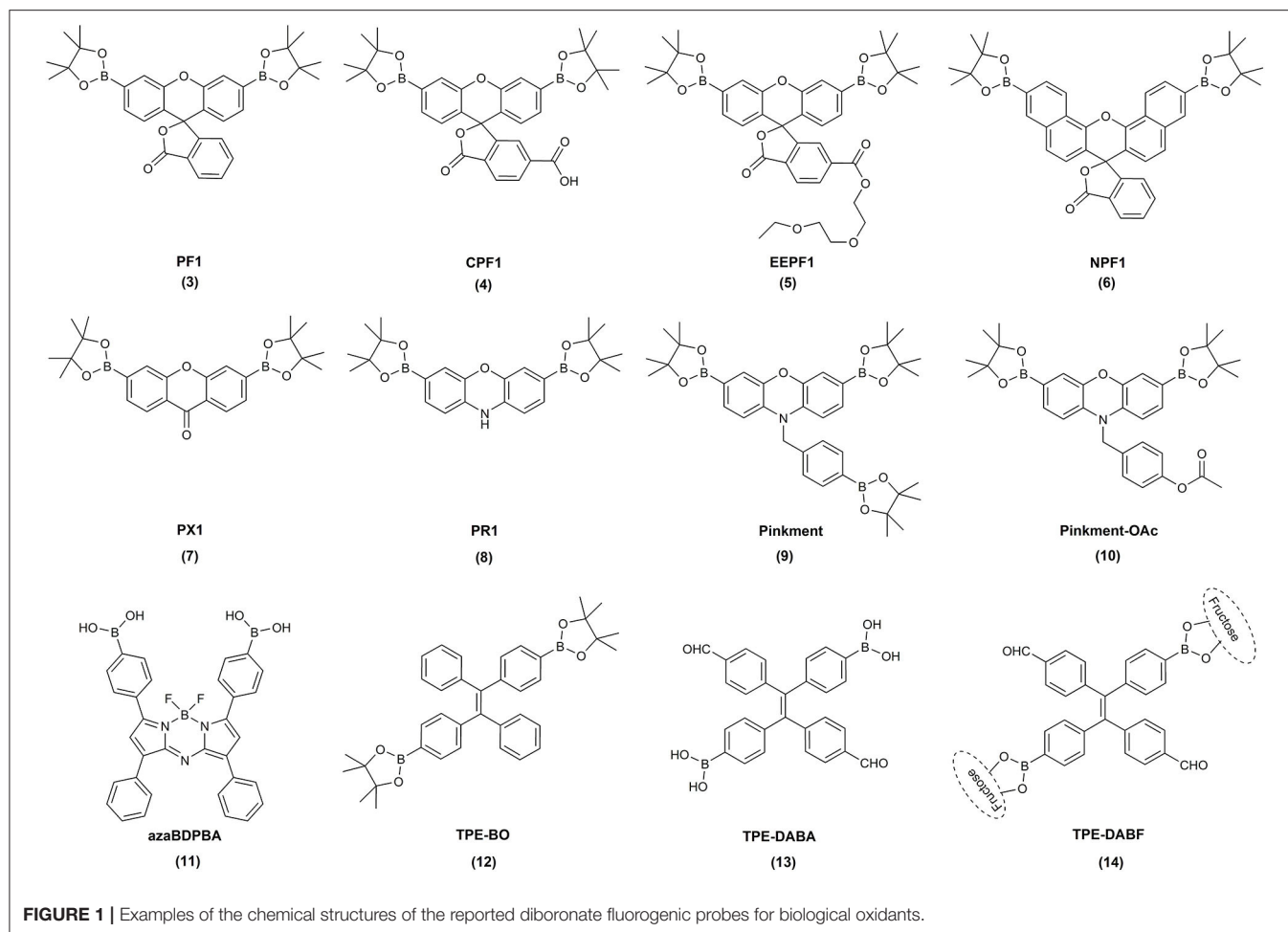
INTRODUCTION

In 1969, McCord and Fridovich discovered that erythrocyte catalyzes the dismutation of the superoxide radical anion ($O_2^{\bullet-}$) (McCord and Fridovich, 1969), and the following year Sies and Chance (1970) showed that hydrogen peroxide is formed *in vivo*. Those discoveries attracted the attention of the scientific community to the role of reactive metabolites of molecular oxygen (so called reactive oxygen species, ROS) in physiological and pathophysiological processes. Over the last 50 years, tremendous progress has been made in understanding the biological chemistry of oxidants formed *in vivo*. Among them, the most important are hydrogen peroxide (H_2O_2) (Winterbourn, 2013), hypohalous acids (HOCl, HOBr) (Winterbourn, 2002; Rayner et al., 2014), hypothiocyanous acid (HOSCN) (Hawkins, 2009; Barrett and Hawkins, 2012), nitrogen dioxide ($\bullet NO_2$), carbonate radical anion ($CO_3^{\bullet-}$) (Augusto et al., 2002), and peroxynitrite ($ONOO^-$) (Ferrer-Sueta et al., 2018). It is widely accepted that those oxidants are involved in different physiological and pathophysiological processes, but the detection and quantitation of those species remains a challenging task, mainly due to their high reactivity, short lifetime, and very low steady-state concentrations in biological systems. For that reason, fluorescent or chemiluminescent probes are widely used to study the role of biological oxidants in physiological and pathophysiological processes (Wardman, 2007; Winterbourn, 2014; Kalyanaraman et al., 2016, 2017; Hogg et al., 2017; Hardy et al., 2018). Several molecular probes that are oxidized to easily detectable and relatively stable fluorescent products have been developed, making possible real-time monitoring of the formation of biological oxidants. The latter is possible with the use of fluorescent and/or chromatographic techniques. Meaningful use of those probes, and proper interpretation of experimental data obtained, requires a good understanding of the mechanism of their action. One of the most important pre-requisites is determination of the probe reactivity pattern.

In the middle of the first decade of the 21st century, a new class of fluorogenic probes, designed for the detection of H_2O_2 and based on the oxidation of boronate derivatives of fluorescent dyes, was developed (Lo and Chu, 2003; Chang et al., 2004). The design was based on the previously reported oxidative deboronation of aryl boronates to the corresponding phenolic products (Scheme 1A) (Ainley and Challenger, 1930; Kuivila, 1954). Since then, boronate-based molecular probes have emerged as potential tools for detecting several biological oxidants: H_2O_2 (Lo and Chu, 2003; Chang et al., 2004), peroxyxynitrite (Sikora et al., 2009), hypochlorous acid (Sikora et al., 2009), organic hydroperoxides (Michalski et al., 2014), and peroxyxynoncarbonate (Truzzi and Augusto, 2017; Rios et al., 2020). This relatively simple oxidation reaction has been utilized in the design of a wide variety of redox probes, with the detection modalities including spectrophotometry

(Lo and Chu, 2003; Zhan et al., 2010; Lu et al., 2011; Choudhury et al., 2019), fluorescence (Chang et al., 2004; Miller et al., 2005, 2007; Dickinson et al., 2010; Zielonka et al., 2012b), chemiluminescence (Green et al., 2017a,b; Seven et al., 2017; Gnaïm and Shabat, 2019; Calabria et al., 2020), bioluminescence (Van De Bittner et al., 2010; Wu et al., 2014; Szala et al., 2020), high-performance liquid chromatography (HPLC) (Sikora et al., 2009, 2013; Zielonka et al., 2014), mass spectrometry (Cochemé et al., 2011; Zielonka et al., 2016b), and PET (positron emission tomography) imaging (Carroll et al., 2014). Also, theranostic (therapeutic + diagnostic) strategies to release a bioactive agent in combination with a reporting moiety (e.g., fluorescent, chemiluminescent) using a boronate group as an oxidant-sensitive trigger have been proposed (Biswas et al., 2017; Gnaïm and Shabat, 2019; Odyniec et al., 2019).





The history of the development of boronate-based probes for their use in redox biology began in 2003, when Lo and Chu (2003) proposed that *p*-dihydroxyborylbenzyloxycarbonyl derivatives of *p*-nitroaniline (1) and fluorescent 7-amino-4-methylcoumarin (2) could be used as probes for the selective detection of H₂O₂. The *p*-dihydroxyborylbenzyloxycarbonyl group, an amine protecting group that can be selectively removed by H₂O₂, has been known in organic chemistry since 1975 (Kemp and Roberts, 1975). The proposed mechanism of H₂O₂ detection was based on the oxidative deprotection of *p*-nitroaniline ($\lambda_{\text{max}} = 383$ nm, **Scheme 1B**) or fluorescent 7-amino-4-methylcoumarin ($\lambda_{\text{ex}} = 348$ nm, $\lambda_{\text{em}} = 440$ nm, **Scheme 1C**). In 2004, the synthesis and characterization of a diboronate derivative of fluorescein, PF1 (3), was described (**Scheme 1D**) (Chang et al., 2004). The probe was shown to undergo oxidation in live cells exposed to exogenously added H₂O₂, with the formation of a green fluorescent product detectable using fluorescence microscopy.

Following these reports, over the last 15 years, a great variety of boronate-based molecular probes designed for the detection of H₂O₂, hypochlorite, or peroxyxynitrite were described in the literature. The Chang laboratory pioneered the development of boronate-based fluorogenic probes. In an elegant series of studies, the Chang lab described the design,

synthesis, and characterization of several diboronate fluorogenic probes: fluorescein-based PF1 (Chang et al., 2004), resorufin-based PR1 (8) (Miller et al., 2005), xanthone-based PX1 (7) (Miller et al., 2005), and naphthofluorescein-based NPF1 (6) (Albers et al., 2008) (**Figure 1**). Introduction of two boronate groups, due to the synthetic constraints, however, limited the sensitivity of the probes in biological settings, as two consecutive oxidations were required to unmask the fluorophore (**Scheme 1D**). Therefore, the same group subsequently developed and reported the synthesis and characterization of a broad palette of monoboronate fluorogenic probes with varying emission colors: Tokyo Green-based PG1 (16) (Miller et al., 2007); resorufin-based PC1 (15) (Miller et al., 2007); and fluorescein- or rhodol-based PF2 (17), PF3 (18), PE1 (19), PY1 (20), and PO1 (21) (Dickinson et al., 2010) (**Figure 2**). This class of probes enabled monitoring of endogenously produced cellular oxidants (Miller et al., 2007).

While the chemistry of the oxidant sensing event is the same for most boronates, as shown in **Scheme 1A**, and involves oxidative deboronation that leads to the formation of the reporting molecule, at least four classes of boronate-based molecular probes can be distinguished based on their structure and the mechanism of the formation of the detectable product:

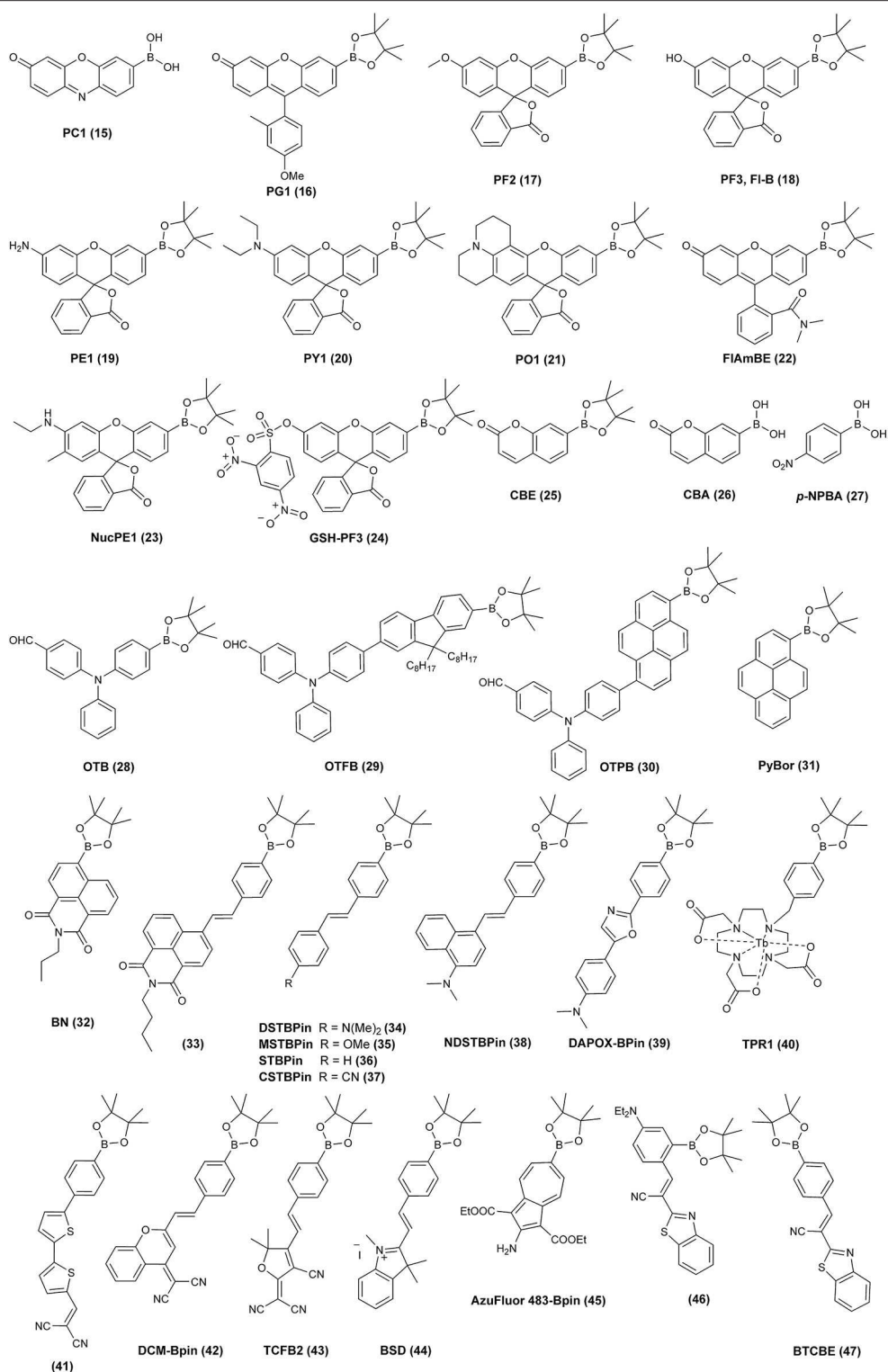
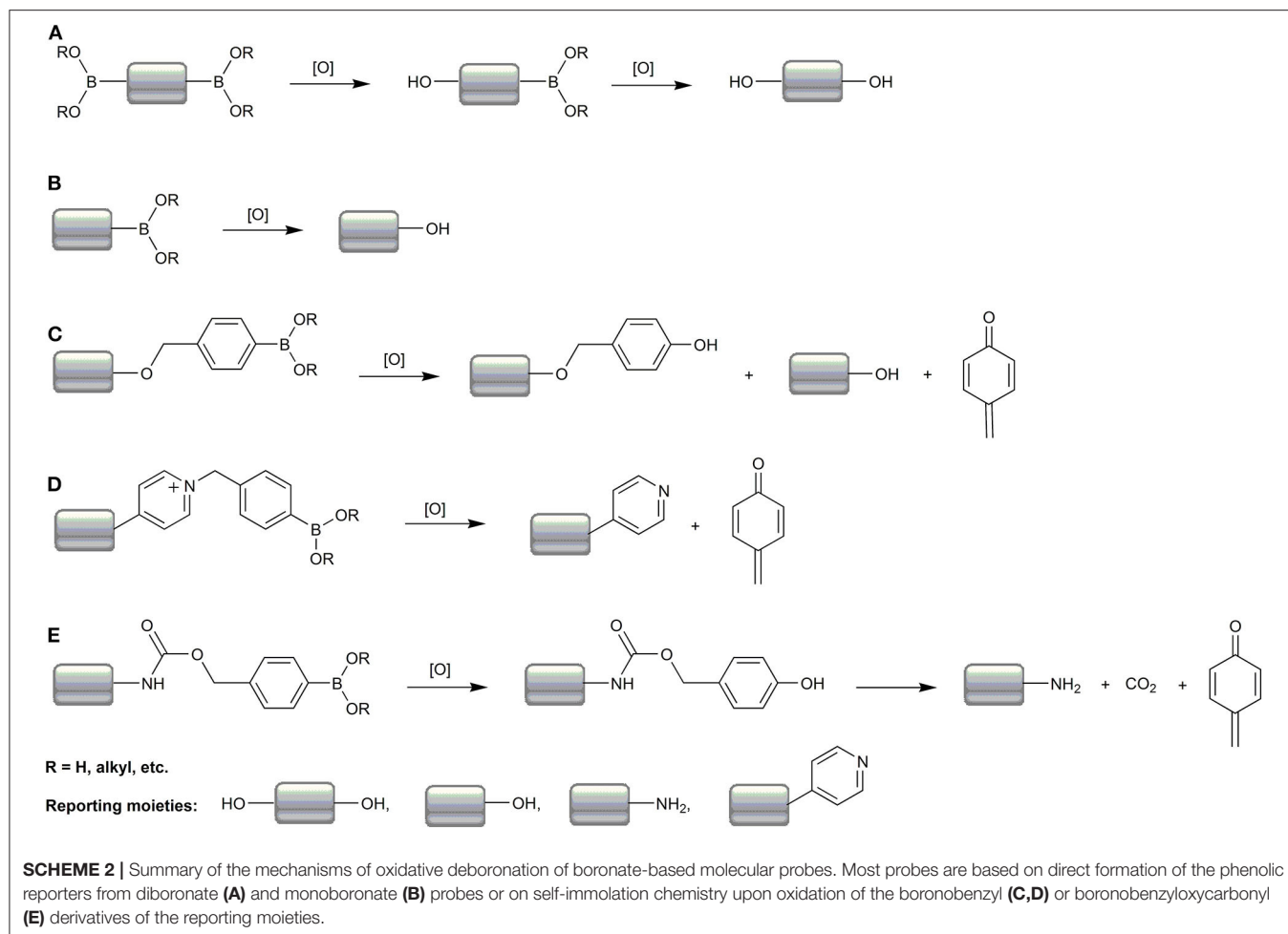


FIGURE 2 | Examples of the chemical structures of the reported monoboronate fluorogenic or colorimetric probes for biological oxidants.



- Diboronate probes, where the formation of the fluorescent reporting molecule requires oxidation of two boronate groups (**Scheme 2A**). Several examples of this class of probes are shown in **Figure 1**, and the spectroscopic properties of the detectable products are summarized in **Table 1**. The main disadvantage of these probes is their low sensitivity due to the requirement of two consecutive oxidation reactions.
- Monoboronate probes, where the direct and stoichiometric (1:1) oxidation of the probe by biological oxidant leads to the formation of the detectable (in most cases fluorescent) reporter (**Scheme 2B**). The examples of this class of probes are shown in **Figure 2**, and the spectroscopic properties of the oxidation products are summarized in **Table 1**.
- Boronobenzyl probes, where oxidation of the probe leads to the formation of 4-hydroxybenzyl derivative of the reporting molecule. The primary phenolic product undergoes subsequent spontaneous release of the fluorescent product *via* elimination of the quinone methide (QM) moiety (**Schemes 2C,D**). Examples of this class of probes are shown in **Figure 3**, and the spectroscopic properties of the end products are summarized in **Table 2**. The most important advantage of these probes is a straightforward one-step synthetic procedure using commercial materials, which enables relatively easy probe preparation.
- p*-Dihydroxyborylbenzyloxycarbonyl probes, where oxidation of the probe leads to the formation of the primary phenolic product, which upon subsequent elimination of QM and carbon dioxide (CO₂) unmasks the amine group in the reporting molecule. This typically results in an increase (“turn-on”) in the fluorescence yield (**Scheme 2E**). Examples of this class of probes are shown in **Figure 3**, and the spectroscopic properties of the products formed are summarized in **Table 2**.

SYNTHETIC APPROACHES TO BORONATE-BASED MOLECULAR PROBES

In the case of boronate-based fluorogenic probes, the introduction of a boronic acid or ester group directly or by introduction of the boronobenzyl or *p*-dihydroxyborylbenzyloxycarbonyl moieties, can be considered as fluorescence masking or a fluorescence “on/off” molecular switch. Synthetic protocols for boronate-based probes can be roughly divided into five strategies: (i) substitution of an aromatic hydroxyl group *via* triflate intermediate (**Scheme 3A**), (ii) substitution of an aromatic halogen atom (**Scheme 3B**), (iii) “boronobenylation” of a phenolic compound

TABLE 1 | Spectroscopic properties of diboronate and monoboronate molecular probes for detection of biological oxidants.

No.	Name	Probe			Oxidation product			Comment	References
		λ_{abs} (nm)	ϵ ($\text{M}^{-1}\text{cm}^{-1}$)	λ_{em} (nm); ϕ	λ_{exc} (nm)	ϵ ($\text{M}^{-1}\text{cm}^{-1}$)	λ_{em} (nm); ϕ		
DIBORONATE PROBES									
3	PF1	NA	-	NA	450 ^a	-	ca. 515 ^a		Chang et al., 2004
4	CPF1	-	-	-	450	-	520		Purdey et al., 2015
5	EEPF1	-	-	-	450	-	520		Purdey et al., 2015
6	NPF1	345 ⁱ	22 400 ^j	-	598 ⁱ	-	660 ⁱ		Albers et al., 2008
7	PX1	350 ^a	4 700 ^a	400(weak) ^a	350 ^a	-	ca. 450 ^a		Miller et al., 2005
8	PR1	NA	-	NA	530 ^a	-	ca. 580 ^a		Miller et al., 2005 Weber et al., 2018
9	Pinkment	-	-	-	545 ^b	-	ca. 580		Odyniec et al., 2018
10	Pinkment-OAC	-	-	-	545 ^b	-	ca. 580		Odyniec et al., 2018
11	azaBDPBA	655	-	682; 0.6	-	-	724 ^j		Liu et al., 2015
12	TPE-BO	-	-	-	ca. 400	-	ca. 500	AIE-fluorescence	Zhang et al., 2015
13	TPE-DABA	-	-	-	380 ^b	-	ca. 500 ^b	AIE-fluorescence	Liu et al., 2016
14	TPE-DABF	ca. 270 ca. 350	-	-	430 ^b	-	576 ^b	AIE-fluorescence	Liu et al., 2016
MONOBORONATE PROBES									
15	PC1	480 ^a	4800 ^a	584 ^a ; 0.006 ^a	550 ^a	-	-	$k(\text{H}_2\text{O}_2) \approx 1 \text{ M}^{-1}\text{s}^{-1\text{a}}$ $k(\text{HOCl}) = 1.1 \times 10^4 \text{ M}^{-1}\text{s}^{-1\text{b}}$ $k(\text{ONOO}^-) = 1 \times 10^6 \text{ M}^{-1}\text{s}^{-1\text{b}}$	Miller et al., 2007 Debowska et al., 2016
16	PG1	460 ^a	5500 ^a	510 ^a ; 0.075 ^a	450 ^a	-	-	$k(\text{H}_2\text{O}_2) \approx 1.1 \text{ M}^{-1}\text{s}^{-1\text{a}}$	Miller et al., 2007
17	PF2	n/a	n/a	n/a	475 ^a	28 600 ^a	511; 0.27 ^a	$k(\text{H}_2\text{O}_2) \approx 0.47 \text{ M}^{-1}\text{s}^{-1\text{a}}$	Dickinson et al., 2010
18	PF3, FI-B	454 ^a	24 000 ^a	521; 0.1 ^a	492 ^a	88 000 ^a	515; 0.94 ^a	$k(\text{H}_2\text{O}_2) \approx 0.38 \text{ M}^{-1}\text{s}^{-1\text{a}}$ $k(\text{H}_2\text{O}_2) = 0.65 \text{ M}^{-1}\text{s}^{-1\text{b}}$ $k(\text{HOCl}) = 4.3 \times 10^2 \text{ M}^{-1}\text{s}^{-1\text{b}}$ $k(\text{ONOO}^-) = 1.1 \times 10^6 \text{ M}^{-1}\text{s}^{-1\text{b}}$	Dickinson et al., 2010 Rios et al., 2016
19	PE1	480 ^a	16 400 ^a	519; 0.3 ^a	491 ^a	51 200 ^a	514; 0.93 ^a	$k(\text{H}_2\text{O}_2) \approx 0.81 \text{ M}^{-1}\text{s}^{-1\text{a}}$	Dickinson et al., 2010
20	PY1	494 ^a	16 200 ^a	558; 0.1 ^a	519 ^a	48 900 ^a	548; 0.12 ^a	$k(\text{H}_2\text{O}_2) \approx 0.37 \text{ M}^{-1}\text{s}^{-1\text{a}}$	Dickinson et al., 2010
21	PO1	507 ^a	13 900 ^a	574; 0.07 ^a	540 ^a	29 300 ^a	565; 0.46 ^a	$k(\text{H}_2\text{O}_2) \approx 0.52 \text{ M}^{-1}\text{s}^{-1\text{a}}$	Dickinson et al., 2010
22	FIAmBE	-	-	-	485 ^b	-	535 ^b	$k(\text{ONOO}^-) > 5 \times 10^5 \text{ M}^{-1}\text{s}^{-1}$	Zielonka et al., 2012b Zielonka et al., 2012a
23	NucPE1	468 ^a 490 ^a	27 300 ^a 26 000 ^a	530; 0.117 ^a	505 ^a	19 100 ^a	530; 0.626 ^a	$k(\text{H}_2\text{O}_2) \approx 0.82 \text{ M}^{-1}\text{s}^{-1\text{a}}$	Dickinson et al., 2011b
24	GSH-PF3	-	-	-	488	-	512	ONOO ⁻ and GSH detection	Sedgwick et al., 2018
25	CBE	-	-	-	332	-	450	-	Du et al., 2008
26	CBA	287 ^b	12 000 ^b	-	324 ^b	13 000 ^b	450 ^b	$k(\text{H}_2\text{O}_2) = 1.5 \text{ M}^{-1}\text{s}^{-1\text{b}}$; $k(\text{ONOO}^-) = 1.1 \times 10^6 \text{ M}^{-1}\text{s}^{-1\text{b}}$	Zielonka et al., 2010 Zielonka et al., 2012b
27	p-NPBA	294 ^c	-	-	405 ^c	19 400 ^c	-	Colorimetric probe	Lu et al., 2011
28	OTB	-	-	-	366	-	466	The organic thin-film fluorescence probe for sensing of hydrogen peroxide vapor	Fu et al., 2016
29	OTFB	-	-	-	-	-	-	The organic thin-film fluorescence probe for sensing of hydrogen peroxide vapor	Fu et al., 2016
30	OTPB	-	-	-	-	-	-	The organic thin-film fluorescence probe for sensing of hydrogen peroxide vapor	Fu et al., 2016

(Continued)

TABLE 1 | Continued

No.	Name	Probe			Oxidation product			Comment	References
		λ_{abs} (nm)	ϵ ($\text{M}^{-1}\text{cm}^{-1}$)	λ_{em} (nm); ϕ	λ_{exc} (nm)	ϵ ($\text{M}^{-1}\text{cm}^{-1}$)	λ_{em} (nm); ϕ		
31	PyBor	265 ^b	41 550 ^b	377,	268 ^b	55 160 ^b	396,	Yu et al., 2012	
		275 ^b	69 970 ^b	392,	280 ^b	95 610 ^b	410,		
		325 ^b	44 120 ^b	417;	350 ^b	65 280 ^b	430;		
		340 ^b	59 450 ^b	0.08 ^b	360 ^b	29 350 ^b	0.60 ^b		
32	BN	344 ^d	-	455 ^d	455 ^d	-	555 ^d	Probe designed for ACh detection Liu et al., 2014	
33	-	376 ^e	-	536; 0.54 ^e	424 ^e	-	604, 0.18 ^e	Ratiometric probe Lee et al., 2019	
34	DSTBPin	ca. 355 ^f	-	488 ^f	350 ^f	-	444 ^f	Increase in fl. intensity Lampard et al., 2018	
35	MSTBPin	ca. 330 ^f	-	405 ^f	330 ^f	-	380 ^f	Increase in fl. intensity Lampard et al., 2018	
36	STBPin	ca. 320 ^f	-	ca.360 ^f	315 ^f	-	ca. 360 ^f	Small decrease in fl. Intensity Lampard et al., 2018	
37	CSTBPin	ca. 330 ^f	-	ca. 380 ^f	330 ^f	-	ca. 380 ^f	Decrease in fl. Intensity Lampard et al., 2018	
38	NDSTBPin	360 ^f	-	525 ^f	350 ^f	-	ca. 510 ^f	Decrease in fl. Intensity Lampard et al., 2018	
39	DAPOX-Bpin	350 ^f	-	480 ^f	350 ^f	-	475 ^f	Increase in fl. intensity Lampard et al., 2018	
40	TPR1	226 ^b	6700 ^b	545; 0.029 ^b	280 ^b	-	545; 0.054 ^b	Terbium-based fluorogenic probe Lippert et al., 2010	
41		463	36 500	565	482	-	640	Ratiometric I ₆₄₀ /I ₅₆₅ ; probe designed for HOCl detection Tong et al., 2018	
42	DCM-Bpin	434	-	-	560	-	667	Wu L. et al., 2019	
43	TCF-OCI, TCFB2	400	-	590	560	-	606	Probe designed for HOCl detection Shu et al., 2015 Sedgwick et al., 2017 Choudhury et al., 2019	
44	BSD	391 ^g	-	-	522 ^g	87 000 ^g	-	Colorimetric probe Zhan et al., 2010	
45	AzuFluor 483-Bpin	327 ^f	-	-	335 ^f	-	483	Murfin et al., 2019	
46		478	61 300	-	ca. 480	>61 300	522	$k_{\text{obs}}(\text{ONOO}^-) = 4.2 \times 10^3 \text{ M}^{-1}\text{s}^{-1}$ Formation of the fluorophore via intramolecular cyclization of oxidation product Zhang J. et al., 2016	
47	BTCBE	356 ^h	-	-	441 ^h	-	522; 0.088 ^h	Shu et al., 2020a	

^a20 mM HEPES buffer, pH 7, 25°C.

^bPhosphate buffer, pH 7.4, 25°C.

^c75 mM carbonate/bicarbonate buffer, pH 9.0.

^dPhosphate buffer, pH 7.5.

^e10 mM phosphate buffer, pH 7.4, containing 50% (v/v) DMSO.

^fH₂O/CH₃OH (52.1 wt%), pH 8.2.

^gNaHCO₃/Na₂CO₃ buffer, pH 9.

^hPBS/ethanol = 7:3, pH 7.4.

ⁱ20 mM HEPES buffer, pH 7.5.

^jPBS/ethanol 1:1, pH 7.4.

(Scheme 3C) or heterocyclic nitrogen atom (represented as a pyridine nitrogen) (Scheme 3D), (iv) synthesis of a *p*-dihydroxyborylbenzyloxycarbonyl derivative of aromatic amine (Scheme 3E), and (v) miscellaneous syntheses.

Substitution of a Hydroxyl Group in an Aromatic Ring

In this strategy, the boronic moiety is introduced indirectly via transformation of an aromatic hydroxyl group (phenol) into a good leaving group in a reaction with trifluoromethanesulfonic anhydride (Demicheli et al., 2016; Zhang J. et al., 2016) or

N-phenyl-bis(trifluoromethanesulfonimide) (Albers et al., 2008; Srikun et al., 2010; Kim E. J. et al., 2014) in the presence of amines like DMAP (4-dimethylaminopyridine) (Demicheli et al., 2016), DIPEA (N,N-diisopropylethylamine) (Rios et al., 2016), or pyridine (Li et al., 2020) in anhydrous solvent under inert atmosphere at room temperature. Subsequently, the triflate derivative is substituted in a Pd(dppf)Cl₂-assisted reaction with bis(pinacolato)diboron in the presence of potassium acetate, and refluxed under anaerobic conditions (Scheme 3A) (Miller et al., 2007; Albers et al., 2008; Srikun et al., 2010).

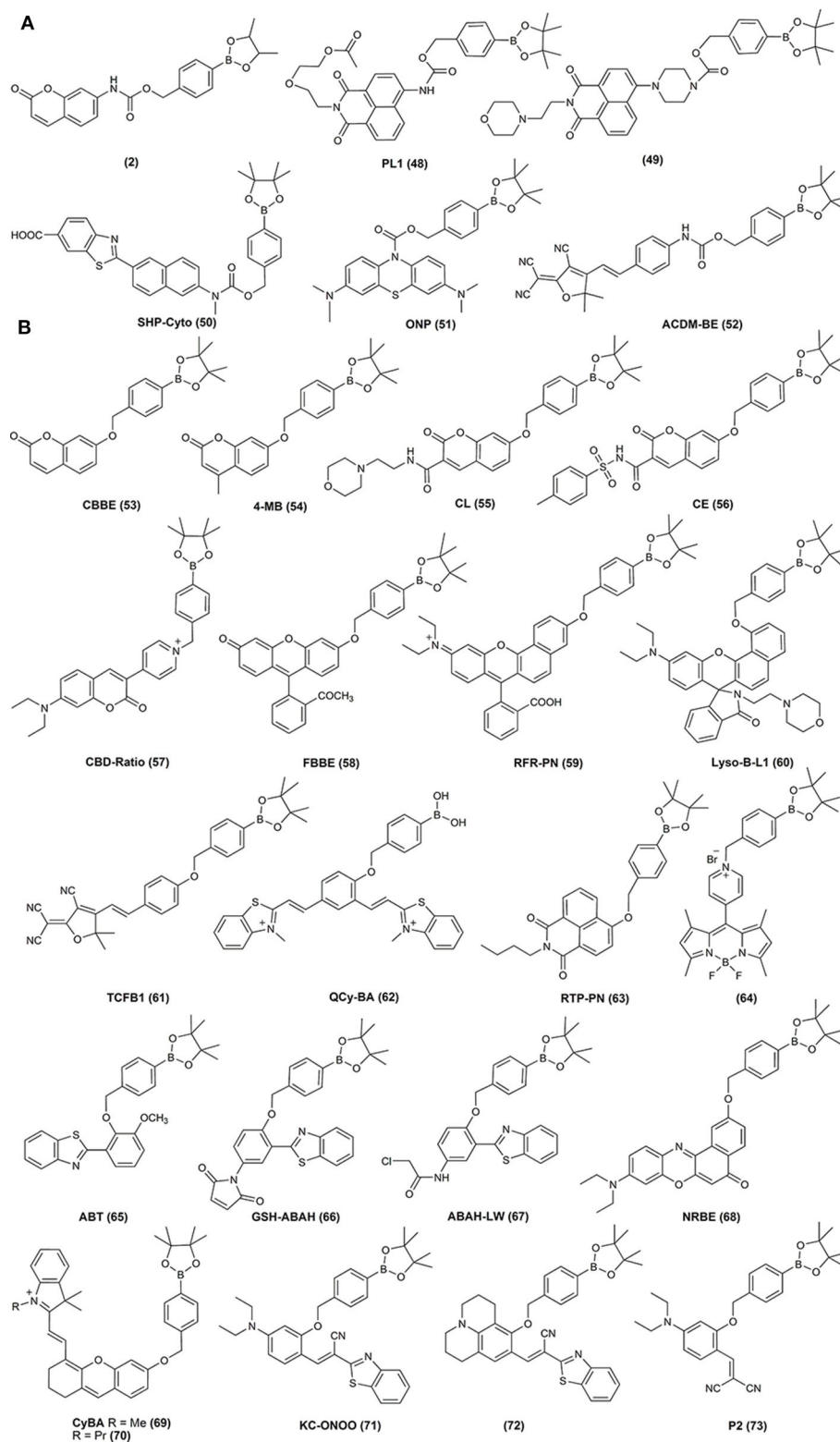


FIGURE 3 | Examples of the chemical structures of boronbenzyloxycarbonyl (**A**) and boronbenzyl (**B**) derivatives of fluorescent dyes reported as probes for biological oxidants.

TABLE 2 | Spectroscopic properties of boronobenzyl derivatives of fluorescent dyes reported as probes for biological oxidants.

No.	Name	Probe			Oxidation product			Comment	References
		λ_{abs} (nm)	ϵ ($\text{M}^{-1}\text{cm}^{-1}$)	λ_{em} (nm); ϕ	λ_{exc} (nm)	ϵ ($\text{M}^{-1}\text{cm}^{-1}$)	λ_{em} (nm); ϕ		
2		348 ^a		440 ^a	355 ^a		460 ^a		Lo and Chu, 2003
48	PL1	375 ^b	9600 ^b	475; 0.38 ^b	435 ^b	8600 ^b	540; 0.11 ^b	$k(\text{H}_2\text{O}_2) \approx 0.88$ $\text{M}^{-1}\text{s}^{-1}$; ratiometric probe	Srikun et al., 2008
49		400 ^c		528 ^c	400 ^c		528 ^c	Lysosome targetable probe; increase in fl. Intensity	Kim et al., 2015
50	SHP-Cyto	333 ^d	38,000 ^d	455; 1.00 ^d	370 ^d	21,000 ^d	528; 0.7 ^d	Ratiometric probe; two-photon also	Lim et al., 2018
51	ONP	640 ^e	29,160 ^e	692; 0.007 ^e	665 ^e		692; 0.11 ^e	Increase in fl. Intensity	Hu et al., 2019
52	ACDM-BE	ca. 445 ^f			540 ^f		604 ^f		Wang G. et al., 2020
53	CBBE	ca.330 ^g		Non-fluorescent	370 ^g		453 ^g	$k(\text{H}_2\text{O}_2) \approx 0.46$ $\text{M}^{-1}\text{s}^{-1}$	Daniel et al., 2013
54	4-MB	320 ^h		385 ^h	370 ^h		450; 0.31 ^h		Palanisamy et al., 2017
55	CL			395 ⁱ	340 ⁱ		447 ⁱ	Ratiometric probe	Weber et al., 2020
56	CE			405 ^j	340 ^j		447 ^j	Ratiometric probe	Weber et al., 2020
57	CBD-Ratio	497 ^j		565 ^j	450 ^j		500 ^j	Ratiometric probe	Li et al., 2019
58	FBBE	456 ^k 483 ^k	25,000 ^k 22,000 ^k	Non-fluorescent	494 ^k	78,000 ^k	518 ^k	$k(\text{ONOO}^-) = 2.8 \times 10^5$ $\text{M}^{-1}\text{s}^{-1}$ $k(\text{H}_2\text{O}_2) = 0.96$ $\text{M}^{-1}\text{s}^{-1}$ $k(\text{OCl}^-) = 8.6 \times 10^3$ $\text{M}^{-1}\text{s}^{-1}$	Debowska et al., 2016
59	RFR-PN	ca.577 ^l		560 ^j	480 ^j		630 ^j	Ratiometric probe	Zhu et al., 2018
60	Lyso-B-L1			Non-fluorescent	570 ^l		606 ^l		Liu et al., 2017
61	TCFB1	ca.440 ^m			560 ^m		606; 0.002 ^m		Sedgwick et al., 2017
62	QCy-BA	400 ⁱ		565 ^j	ca. 480 400 (with DNA) ^j		ca.680 650(with DNA) ^j	Binding to DNA	Narayanaswamy et al., 2016
63	RTP-PN	372 ⁱ		450 ^j	415 ⁱ		543 ⁱ	Ratiometric probe	Wang Z. et al., 2019
64		508 ⁱ		520; 0.002 ⁱ	480 ^j		520; 0.78 ⁱ		Xu et al., 2014
65	ABT	309 ⁿ		405 ⁿ	317 ⁿ		483 ⁿ	$k(\text{ONOO}^-) = 1.16 \times 10^4$ $\text{M}^{-1}\text{s}^{-1}$ $k(\text{H}_2\text{O}_2) = 0.23$ $\text{M}^{-1}\text{s}^{-1}$ $k(\text{OCl}^-) = 4.81 \text{M}^{-1}\text{s}^{-1}$	Li and Yang, 2018
66	GSH-ABAH	326 ^o		Non-fluorescent	390 ^o		451 ^o	GSH and ONOO detection	Wu et al., 2018a
67	ABAH-LW	ca. 430,490 ^o		405 ^o	370 ^o		481 ^o	Ratiometric probe; increase in fl. Intensity	Wu et al., 2018b
68	NRBE			670; 0.01 ^p	585 ^p		670; 0.36 ^p		Diao et al., 2019
69	CyBA	610, 660			700			Photoacoustic imaging	Hariri et al., 2019
70		ca. 610, 650, 740 ^q		708 ^q	670 ^q		708 ^q	Increase in fl. Intensity	Zhang et al., 2019
71	KC-ONOO	510 ^r	33,000 ^r	<0.01 ^r	480	34,000 ^r	530; 0.24 ^r		Xia et al., 2019

(Continued)

TABLE 2 | Continued

No.	Name	Probe			Oxidation product			Comment	References
		λ_{abs} (nm)	ϵ ($\text{M}^{-1}\text{cm}^{-1}$)	λ_{em} (nm); ϕ	λ_{exc} (nm)	ϵ ($\text{M}^{-1}\text{cm}^{-1}$)	λ_{em} (nm); ϕ		
72		468 ^s	20,370 ^s	646; 0.01 ^s	500 ^s	29,500 ^s	540; 0.62 ^s	$k(\text{ONOO}^-) \approx 1.51 \times 10^4 \text{ M}^{-1}\text{min}^{-1}$ $k(\text{H}_2\text{O}_2) \approx 2.24 \text{ M}^{-1}\text{min}^{-1}$	Kim J. et al., 2014
73	P2	440 ^t		580 ^t	440 ^t		480 ^t	$k(\text{ONOO}^-) = 7.65 \times 10^3 \text{ M}^{-1}\text{min}^{-1}$ $k(\text{H}_2\text{O}_2) = 75.3 \text{ M}^{-1}\text{min}^{-1}$	Zhou et al., 2014

^a 140 mM NaHCO₃, pH 8.3, 25°C.

^b 20 mM HEPES, pH 7.4.

^c 0.1 M PBS, pH 7.4, 1% DMF.

^d 30 mM MOPS buffer, 100 mM KCl, pH 7.4.

^e 10 mM PBS, 5% CH₃CN, pH 7.4, 37°C.

^f CH₃CN/PBS (0.1 M, pH 7.4, v/v, 3/20).

^g 50 mM HEPES buffer, pH 7.5.

^h 20 mM HEPES, 1% DMSO, pH 7.4 25°C.

ⁱ PBS, pH 7.4, 25°C.

^j 20% DMSO, 20 mM PBS, pH 7.4.

^k 50 mM phosphate buffer, pH 7.4, 100 μM dtpa, 10% CH₃CN.

^l 10 mM acetate buffer, 1% DMSO, pH 4.5.

^m PBS, 20% DMSO, pH 8.0.

ⁿ 10 mM PBS, pH 7.4, 40% EtOH.

^o PBS, pH 8.2, 8% DMSO, 1 mM CTAB.

^p HEPES buffer 0.1 M, pH 7.4.

^q PBS, pH 7.4, 37°C.

^r 10 mM PBS, 10% DMSO, pH 7.4.

^s 10 mM phosphate buffer, pH 7.4, 10% C₂H₅OH, 37°C.

^t 10 mM PBS, 10% CH₃CN, pH 7.4.

Substitution of a Halogen Atom in the Aromatic Ring

This approach is more direct and, in the majority of cases, can be described as a straightforward bromide (Miller et al., 2005; Albers et al., 2006; Mohapatra and Phillips, 2012), rarely iodide (Chang et al., 2004; McQuaker et al., 2013), or chloride (Zhu B. et al., 2013), substitution in a reaction with bis(pinacolato)diboron in the presence of potassium acetate and Pd(dppf)Cl₂ in various solvents at elevated temperature and under inert atmosphere (**Scheme 3B**). It is noteworthy that, in some rare cases, a strategy in which aryl halides undergo reaction with *n*-BuLi in -78°C followed by reaction with alkylborates [e.g., trimethylborate (Lo and Chu, 2003), triisopropylborate (Yu et al., 2012), isopropylpinacolborate (Quin et al., 2010; McQuaker et al., 2013)] can be used to obtain corresponding boronic acid derivatives.

Boronbenzylation of Phenols or Heterocyclic Nitrogen

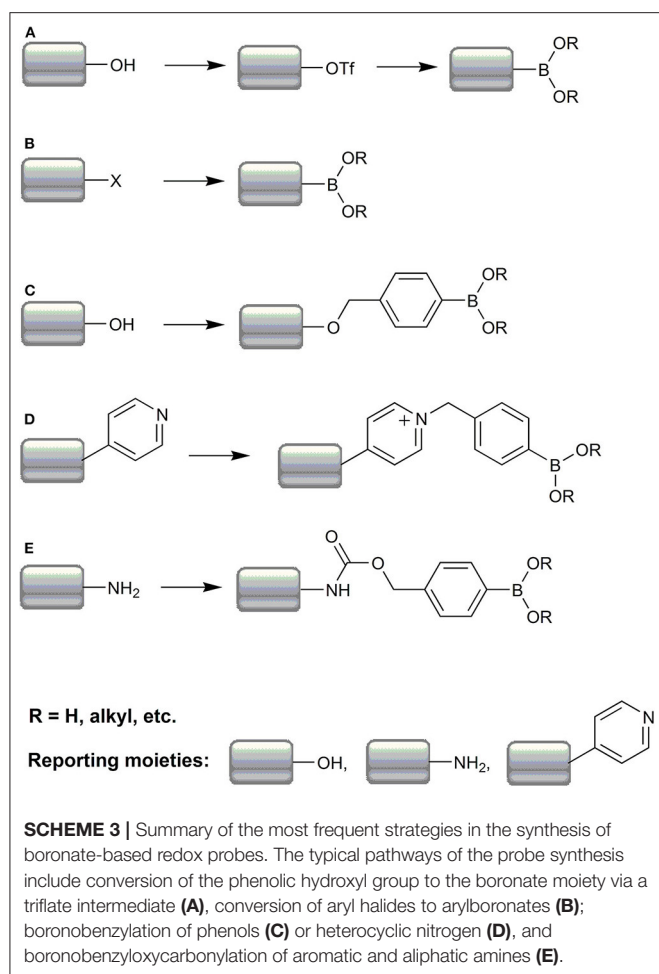
The most broadly used reaction in syntheses of the desired boronic probes consists of the so-called boronbenzylation, in which a phenol residue reacts, usually in an inert atmosphere, with 2-(4-bromomethylphenyl)-4,4,5,5-tetramethyl-[1,3,2]dioxaborolane (also known as 4-bromomethylphenylboronic acid pinacol ester) in the presence of a base, typically K₂CO₃ (Karton-Lifshin et al., 2012; Kim

J. et al., 2014; Zhou et al., 2014) or Cs₂CO₃ (Van De Bittner et al., 2010; Qian et al., 2012; Yuan et al., 2012), in an anhydrous medium (**Scheme 3C**). There are also few literature examples of a 4-iodo-derivative usage (Karton-Lifshin et al., 2012; Debowska et al., 2016; Narayanaswamy et al., 2016). A variety of solvents can be used and usually the reaction is performed under reflux during a couple of hours or is left at room temperature until completion.

There are also examples of a probe synthesis in which the boronobenzyl moiety is introduced directly to an aromatic ring nitrogen in a pyridine (Xu et al., 2014; Li et al., 2019) or quinoline (He et al., 2018) system as well as onto aliphatic amine nitrogen (**Scheme 3D**) (Sun et al., 2014; Li K.-B. et al., 2017; Han et al., 2018). However, in the rearmost examples, 2-bromomethyl-derivative is used.

Synthesis of Carbamate Type Boronic Probes

The fluorescence emitting form of some probes consists of an aniline-type, exocyclic nitrogen atom. In such cases, the amine group is often masked with a carbamic acid 4-(4,4,5,5-tetramethyl-[1,3,2]dioxaborolan-2-yl)-benzyl ester moiety (**Scheme 3D**), decreasing the electron density on the nitrogen atom. The typical procedure to introduce such a residue exploits the 4-hydroxymethylphenylboronic acid pinacol ester in which the hydroxyl group is converted, often



in situ, into an acid chloride in a reaction with triphosgene (Srikun et al., 2008; Chung et al., 2011; Zhu D. et al., 2013) in the presence of a base in various solvents, which reacts further with the target amino group. There are some examples in which this approach is also used to mask the nitrogen atom on biotin (Chung et al., 2018; Wu Y. P. et al., 2018) or methylene blue (Hu et al., 2019) or in aliphatic systems (Lippert et al., 2010; Zhu D. et al., 2013; Yik-Sham Chung et al., 2018).

Miscellaneous Syntheses

In this review, we would be remiss to omit some examples of formylphenylboronic ester/acid usage in carbon-carbon bond formation. In those reactions, which are performed mostly in boiling anhydrous ethanol (Wang et al., 2013; Guo et al., 2018), the oxygen atom of the aldehyde group serves as a base (in some cases, DIPEA (Shu et al., 2020a,b) or piperidine (Wu L. et al., 2019) is added), which abstracts an acidic proton from the reaction partner and the negatively charged carbon atom obtained attacks the protonated carbonyl group with subsequent double bond formation. For example, a single bond formation serves the reductive amination reaction in which a 2-(2-aminophenyl)benzothiazole reacts with

the 4-formylphenylboronic pinacol ester in the presence of $\text{NaBH}(\text{OAc})_3$ (Sedgwick et al., 2016).

Also, the Wittig reaction is applied in double bond formation (Das et al., 2009; Lee et al., 2019). In this approach, the 4-bromophenylboronic pinacol ester is transformed into an ylide in a direct reaction with triphenylphosphine, carried out in reflux under anaerobic conditions in the dark, which is used in the subsequent reaction with an aldehyde group of the reporter residue.

SUBCELLULAR TARGETING OF BORONATE PROBES

Fluorescence microscopy enables spatial resolution at the level of cellular organelles, and many boronate probes have been designed to accumulate in a specific organelle for site-specific detection of H_2O_2 . Typically, an organelle-targeting moiety is covalently attached to a probe for that purpose (Xu W. et al., 2016; Zhu et al., 2016; Gao et al., 2019). Examples of the cellular organelles that have been targeted to accumulate boronate-based redox probes include mitochondria (see below), nucleus (Dickinson et al., 2011b; Wen et al., 2014), endoplasmic reticulum, Golgi apparatus (Wu et al., 2018b; Wang H. et al., 2019), and lysosomes (Kim et al., 2015; Liu et al., 2017; Ren et al., 2017). Also, simultaneous monitoring of H_2O_2 in mitochondria and endoplasmic reticulum has been reported using a combination of targeted probes, yielding products of different fluorescence parameters (Xiao et al., 2016). In addition to targeting a specific organelle, boronate redox probes designed for intracellular accumulation and retention have been developed, with the aim of differentiating between intracellular and extracellular oxidants (Miller et al., 2010; Dickinson et al., 2011a).

By far, the highest number of targeted boronate redox probes was designed and reported for the detection of mitochondrial oxidants. Detection and quantitation of biological oxidants produced inside mitochondria remain challenging, and numerous mitochondria-targeted redox probes were designed and synthesized for that purpose (Zielonka et al., 2017b; Cheng et al., 2018), among them a series of boronate-based molecular probes. Mitochondria are regarded as one of the major cellular sources of $\text{O}_2^{\bullet-}$, which undergoes spontaneous or superoxide dismutase-catalyzed dismutation to H_2O_2 . It is also possible that $\text{O}_2^{\bullet-}$ reacts in mitochondria with nitric oxide ($\bullet\text{NO}$), as $\bullet\text{NO}$ can easily diffuse across lipid membranes, to produce peroxynitrite—a significantly faster oxidant of the boronate probes. The ability to directly and stoichiometrically react with H_2O_2 or ONOO^- , without the requirement of a catalyst is a significant advantage of the boronate-based probes, as compared with many other probes used for the detection of mitochondrial oxidants.

The first reported mitochondria-targeted boronate probe, called “mitochondria-targeted Peroxy Yellow 1” (MitoPY1 (74), **Figure 4**), was a boronate derivative of a rhodol fluorescent dye linked to a triphenylphosphonium cationic moiety (TPP^+) *via* $-(\text{CH}_2)_4-$ alkyl chain (Dickinson and Chang, 2008; Dickinson et al., 2013). Linking compounds to the TPP^+

moiety is the most common strategy to target and accumulate chemical agents in cell mitochondria (Zielonka et al., 2017b). Oxidative deboronation of MitoPY1 leads to the formation of strongly fluorescent dye, MitoPY1ox, with the reaction rate constant of $0.2 \text{ M}^{-1}\text{s}^{-1}$ (Dickinson and Chang, 2008) (Figure 4A). A different approach to detect mitochondrial H_2O_2 came from the Murphy's lab (Cochemé et al., 2011, 2012). The TPP^+ -conjugated simple phenylboronic acid, (3-boronobenzyl)triphenylphosphonium bromide (75), called MitoB (Figures 4B,C), was proposed for *in vivo* measurements of mitochondrial H_2O_2 production in living *Drosophila*. Both the probe and the products were detected and quantified by liquid chromatography–mass spectrometry (LC–MS)-based analyzes of the homogenates after the incubation with the probe, with the use of deuterated internal standards for most accurate quantification. It has been shown, that MitoB accumulates within mitochondria where it is oxidized to the corresponding phenol, (3-hydroxybenzyl)triphenylphosphonium cation (MitoP) (Figure 4B). The differences in H_2O_2 production was evaluated by the comparison of MitoP/MitoB ratios (to correct for changes in the distribution of the MitoB probe and MitoP phenolic product in the tissue under consideration). During the last decade, the MitoB probe has been applied in numerous studies on the production of mitochondrial H_2O_2 (Logan et al., 2014; Salin et al., 2015, 2017, 2018; Gallego-Villar et al., 2016; He et al., 2019). Also a TPP^+ -linked probe isomeric to MitoB, called *o*-MitoPhB(OH)₂ (76), was shown to react with H_2O_2 and ONOO[−], with the advantage of being able to distinguish those two oxidants, based on the product profiles, as discussed below (Sikora et al., 2013; Zielonka et al., 2015, 2016b). MS/MS detection parameters for both MitoB and *o*-MitoPhB(OH)₂ probes, their oxidation products, and internal standards used are listed in Supplementary Table 1.

Several other mitochondria-targeted boronate-based fluorogenic probes were reported for the detection of H_2O_2 and ONOO[−], including SHP-Mito (78) (Masanta et al., 2012; Kim and Cho, 2013), Mito- H_2O_2 (79) (Xu J. et al., 2016), pep3-NP1 (86) (Wen et al., 2015), MI- H_2O_2 (80) (Xiao et al., 2016), CBZ- H_2O_2 (81) (Zhang K. et al., 2016), HKB (83) (He et al., 2018), HBTBPB (84) (Tang et al., 2018), Mito-NP (88) (Liang et al., 2019), MBTBE (89) (Shu et al., 2020b), and CM (90) (Weber et al., 2020) (Figure 4C, Table 3).

It should be noted that detection of cellular oxidants requires competition with other pathways of their cellular elimination. For example, peroxiredoxins are assumed as major enzymatic scavengers of H_2O_2 and ONOO[−] (Cox et al., 2009; Trujillo et al., 2017; De Armas et al., 2019; Zeida et al., 2019). Taking into account the estimated lifetime of both oxidants in the range of 0.3–1.6 ms both in the cytosolic and mitochondrial compartments (Trujillo et al., 2017), when present at 10 mM concentration, boronates would scavenge <0.001% (!) of intracellular H_2O_2 produced. On the other hand, at this concentration, boronates may efficiently compete for ONOO[−] and intercept >50% of ONOO[−]. When used at a 10 μM concentration (extracellular), positively charged boronate probes are expected to reach the 100 μM level in the cytosol and $\sim 10 \text{ mM}$ in the mitochondrial matrix, driven by cellular

plasma and mitochondrial membrane potentials (Zielonka et al., 2017b), thus demonstrating their feasibility to sensitively detect mitochondrial ONOO[−]. In case of the detection of cytosolic or mitochondrial H_2O_2 , only a miniscule fraction of H_2O_2 can be directly detected by boronate probes; thus, a highly sensitive detection method would be required, and the yield of the phenolic product is expected to be a linear function of the probe's intracellular concentration. Additional factors, including the conversion of H_2O_2 into another oxidizing species of higher lifetime in cells and/or higher reactivity toward boronates (e.g., peroxymonocarbonate), may increase the efficiency of H_2O_2 -induced cellular probe oxidation.

BIOLOGICAL OXIDANTS: HYDROGEN PEROXIDE, PEROXYNITRITE, ORGANIC HYDROPEROXIDES, AND HYPOCHLOROUS ACID

Before discussing the chemical reactivity of the boronate-based redox probes toward biological oxidants, it is important to understand the basic chemical properties, biological fates, and currently used detection methods for those oxidants. In this section, we provide an overview of the chemical characteristics of H_2O_2 , ONOO[−], organic hydroperoxides, and HOCl, as these oxidants have been demonstrated to be formed in biological systems and to be able to oxidize the arylboronic compounds (Ainley and Challenger, 1930; Kuivila et al., 1962; Sikora et al., 2009; Lippert et al., 2011; Zielonka et al., 2012a; Michalski et al., 2014).

Hydrogen Peroxide

Hydrogen peroxide can be generated *in vivo* in numerous biological processes, and perhaps is one of the most important redox messengers (Winterbourn, 2013; Forman et al., 2014). It can be generated directly, by enzymatic two-electron reduction of O_2 , or from dismutation of $\text{O}_2^{\bullet -}$. Several enzymes produce H_2O_2 : L-amino acid oxidase, urate oxidase, glycolate oxidase, and monoamine oxidase. The most important sources of H_2O_2 in cells are NADPH oxidases (Nox family of enzymes) and mitochondria. H_2O_2 is a strong two-electron oxidant [$E^\circ(\text{H}_2\text{O}_2/\text{H}_2\text{O}) = 1.32 \text{ V}$ at pH 7], but due to the kinetic reasons (high activation energy barriers), it reacts slowly or not at all with most biological molecules. Due to the high pK_a -value of H_2O_2 ($\text{pK}_a = 11.6$), at a physiological pH, <0.01% of hydrogen peroxide is present in the deprotonated, nucleophilic anionic form, HOO[−]. H_2O_2 oxidizes thiols to form sulfenic acids, but the reaction is slow in the case of most biothiols, with the family of peroxiredoxins enzymes being the major exception. H_2O_2 reacts rapidly with heme peroxidases (e.g., myeloperoxidase or eosinophil peroxidase) with the second order rate constants in the range of 10^7 – $10^8 \text{ M}^{-1}\text{s}^{-1}$, but these peroxidases are mostly restricted to host defense mechanisms, rather than cellular signaling. Due to the high cellular abundance and high reactivity toward H_2O_2 , peroxiredoxins and to a smaller extent glutathione peroxidases represent the major cellular targets and enzymatic scavengers of H_2O_2 . Another H_2O_2 -scavenging enzyme, catalase,

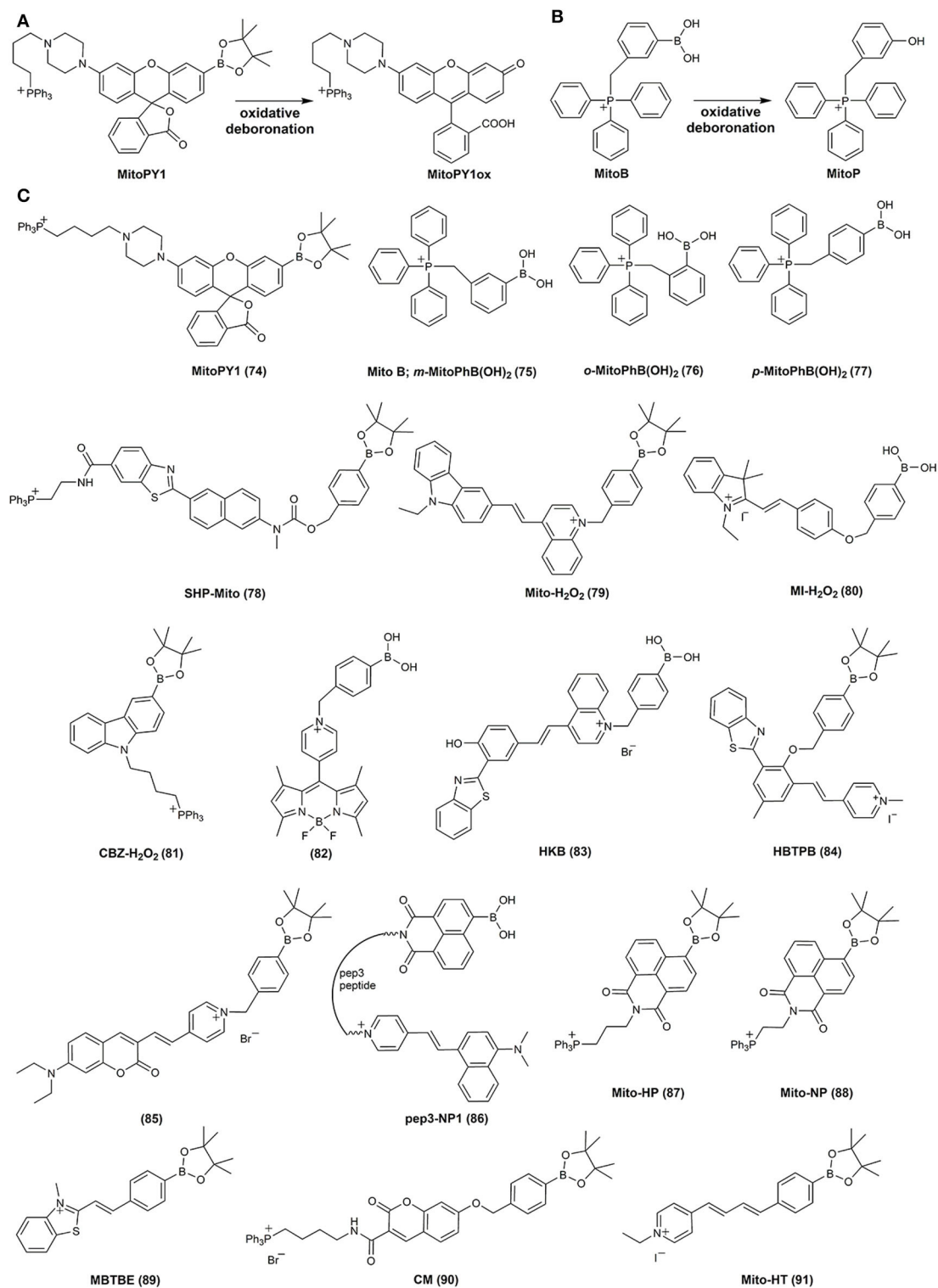


FIGURE 4 | Oxidative deboronation of MitoPY1 (A) and MitoB (B). Chemical structures of mitochondria-targeted boronate-based redox probes (C).

TABLE 3 | Mitochondria-targeted boronate-based molecular probes for detection of biological oxidants.

No.	Name	Probe			Oxidation product			Comment	References
		λ_{abs} (nm)	ϵ ($\text{M}^{-1}\text{cm}^{-1}$)	λ_{em} (nm); ϕ	λ_{exc} (nm)	ϵ ($\text{M}^{-1}\text{cm}^{-1}$)	λ_{em} (nm); ϕ		
74	MitoPY1	489 ^a 510 ^a	14,300 ^a 14,200 ^a	540; 0.019 ^a	510 ^a	22,300	528, 0.405 ^a	$k(\text{H}_2\text{O}_2) \approx 0.201 \text{ M}^{-1}\text{s}^{-1}$	Dickinson and Chang, 2008
75	MitoB, <i>m</i> - MitoPhB(OH) ₂	-	-	-	-	-	-	HPLC detection: $\lambda_{\text{Abs}} = 268 \text{ nm}$ or LC-MS detection ^f ; $k(\text{H}_2\text{O}_2) \approx 3.8 \text{ M}^{-1}\text{s}^{-1\text{b}}$ $k(\text{ONOO}^-) = 1 \times 10^6 \text{ M}^{-1}\text{s}^{-1}$	Cochemé et al., 2011 Sikora et al., 2013
76	<i>o</i> - MitoPhB(OH) ₂	-	-	-	-	-	-	HPLC detection: $\lambda_{\text{Abs}} = 268 \text{ nm}$ or LC-MS detection ^f ; $k(\text{ONOO}^-) = 3.5 \times 10^5 \text{ M}^{-1}\text{s}^{-1}$	Sikora et al., 2013
77	<i>p</i> - MitoPhB(OH) ₂	-	-	-	-	-	-	HPLC detection: $\lambda_{\text{Abs}} = 268 \text{ nm}$ or LC-MS detection; $k(\text{ONOO}^-) = 1 \times 10^6 \text{ M}^{-1}\text{s}^{-1}$	Sikora et al., 2013
78	SHP- Mito	342 ^d	17,000 ^d	470; 0.13 ^d	383 ^d	15,000 ^d	545; 0.12 ^d	Ratiometric probe; Two-photon probe; $k(\text{H}_2\text{O}_2) \approx 1.0\text{--}1.2 \text{ M}^{-1}\text{s}^{-1\text{d}}$	Masanta et al., 2012
79	Mito- H ₂ O ₂	490 ^e	-	527; 0.003 ^e	376 ^e	-	527 ^e	Increase in fl. intensity	Xu J. et al., 2016
80	MI-H ₂ O ₂	425 ^f	-	0.0087 ^f	525 ^f	-	555; 0.11 ^f	$k(\text{H}_2\text{O}_2) \approx 4.35 \text{ M}^{-1}\text{s}^{-1\text{f}}$	Xiao et al., 2016
81	CBZ- H ₂ O ₂	340 ^g	-	ca. 400 ^g	350 ^g	-	430 ^g	-	Zhang K. et al., 2016
82	-	507 ^h	-	0.002 ^h	495 ^h	-	515; 0.213 ^h	Probe designed for HOCl detection	Li G. et al., 2017
83	HKB	564 ⁱ	-	666 ⁱ	440 ⁱ	-	594 ⁱ	Ratiometric probe; $k(\text{H}_2\text{O}_2) \approx 1.07 \text{ M}^{-1}\text{s}^{-1\text{i}}$	He et al., 2018
84	HBTPB	312 ^j	-	539 ^j	373 ^j	-	669 ^j	Ratiometric probe; ESIP-T-based probe	Tang et al., 2018
85	-	500 ^k	-	640 ^k	500 ^k	-	535 ^k	Ratiometric probe	Shen et al., 2018
86	pep3- NP1	352 455 ^l	9020 10,700 ^l	646; 0.033 ^l	455 ^l	-	555; 0.058 ^l	$k(\text{H}_2\text{O}_2) \approx 0.487 \text{ M}^{-1}\text{s}^{-1\text{l}}$; DNA-binding probe	Wen et al., 2015
87	Mito-HP	358 ^m	-	543 ^m	446 ^m	-	543 ^m	Increase in fl. intensity	Dai et al., 2018
88	Mito-NP	360 ⁿ	-	-	460 ⁿ	-	553 ⁿ	ICT-based probe; $k(\text{H}_2\text{O}_2) \approx 3.5 \text{ M}^{-1}\text{s}^{-1}$	Liang et al., 2019
89	MBTBE	380 ^o	-	0.018 ^o	520 ^o	-	569; 0.097 ^o	-	Shu et al., 2020b
90	CM	-	-	400 ^p	340 ^p	-	ca. 450 ^p	Ratiometric probe	Weber et al., 2020
91	Mito-HT	380 ^q	-	493; 0.39 ^q	395 ^q	-	562; 0.43 ^q	Ratiometric probe	Wang C. et al., 2020

^a20 mM HEPES, pH 7, 25°C.^bKCl medium, pH 8.0, 25°C.^c50 mM phosphate buffer, pH 7.4, 1 M CH₃OH, RT.^d30 mM MOPS, 100 mM KCl, pH 7.4.^e20 mM phosphate buffer, pH 7.4, 1% DMSO, 25°C.^f10 mM PBS, pH 8.0.^g20 mM PBS, pH 7.4, 20% DMSO.^h20 mM PBS, pH 7.4, 1% DMSO.ⁱ10 mM PBS, pH 7.0, 30% CH₃CN.^j10 mM HEPES/CH₃CN (1/1, v/v), pH 7.4.^kPBS/CH₃CN, (1/9, v/v), pH 7.4.^lTris-HCl, pH 7.2, 1% DMSO.^m10 mM PBS, pH 7.4, RT.ⁿ20 mM PBS, pH 7.4.^oPBS : C₂H₅OH, 7:3, pH 7.4.^pPBS/CH₃OH (52%), pH 7.4.^q0.01 M PBS/DMSO (5/1, v/v), pH 7.4.^rMolecular ions used in MS/MS-based detection are listed in **Supplementary Table 1**.

is mostly limited to cell peroxisomes, and its contribution to total consumption of cellular H_2O_2 under most conditions may be significantly lower.

Currently, only a few reliable methods for H_2O_2 detection and quantitation exist. In cell culture studies, extracellular H_2O_2 can be quantitated with the use of peroxidase-catalyzed oxidation of fluorogenic probes (currently the probe used most often for such purposes is Amplex Red, which undergoes oxidation to red fluorescent resorufin). Extracellular H_2O_2 also can be detected with the use of fluorogenic boronate probes, without the requirement of peroxidase, but the oxidation process is slower and a kinetic assay is required to determine the rate of probe oxidation. Intracellular H_2O_2 detection is still challenging (Rezende et al., 2018), and a decades-old aminotriazol-induced catalase inactivation assay remains the method of choice for quantitative estimation of the intracellular H_2O_2 level (Chance et al., 1979; Royall et al., 1992).

Peroxynitrite

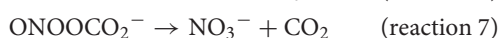
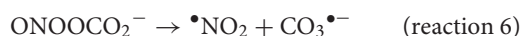
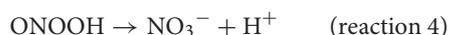
Peroxynitrite anion (ONOO^-) and peroxynitrous acid (ONOOH), a Brønsted acid-base pair ($\text{pK}_a(\text{ONOOH}) = 6.8$) (Pryor and Squadrito, 1995), are strong but unstable biological oxidants [$E^\circ(\text{ONOO}^-, 2\text{H}^+/\bullet\text{NO}_2) = 1.4\text{ V}$ and $E^\circ(\text{ONOO}^-, 2\text{H}^+/\text{NO}_2^-) = 1.2\text{ V}$ at pH 7] (Koppenol et al., 1992) formed *in vivo* through the recombination of two biologically important radicals: $\text{O}_2^{\bullet-}$ and $\bullet\text{NO}$. This reaction takes place nearly at the diffusion-controlled rate (reaction 1, $k_1 = 0.4\text{--}1.6 \times 10^{10}\text{ M}^{-1}\text{s}^{-1}$) (Huie and Padmaja, 1993; Goldstein and Czapski, 1995; Kobayashi et al., 1995; Kissner et al., 1997), and it is believed to outcompete most other cellular routes of $\bullet\text{NO}$ and $\text{O}_2^{\bullet-}$ consumption.



Recently, it has been demonstrated that ONOO^- is also formed at physiological pH in the reaction of azanone (HNO) with molecular oxygen (reaction 2, $k_2 = (1.8 \pm 0.3) \times 10^4\text{ M}^{-1}\text{s}^{-1}$) (Smulik et al., 2014). However, because HNO reacts significantly faster with cellular thiols than with molecular oxygen, the biological relevance of this reaction remains to be determined.



Peroxynitrite is a source of highly oxidizing radicals, which can be formed in fractional yields through a homolytic cleavage of the O–O bond of ONOOH ($\eta \approx 30\%$, reaction 3, $k_3 = 1.3\text{ s}^{-1}$ at 25°C) (Koppenol et al., 1992; Pryor and Squadrito, 1995; Ferrer-Sueta et al., 2018) or *via* the reaction of ONOO^- with CO_2 (reaction 5, $k_5 = 2.9 \times 10^4\text{ M}^{-1}\text{s}^{-1}$, at 25°C) (Lyman and Hurst, 1995). Peroxynitrous acid also undergoes isomerization to the nitrate anion ($\eta \approx 70\%$, reaction 4) (Pryor and Squadrito, 1995).



The unstable nitrosoperoxocarbonate anion (ONOOCO_2^-) formed from the reaction between ONOO^- and CO_2 (reaction 5) decays to the nitrogen dioxide radical ($\bullet\text{NO}_2$) and carbonate radical anion (reaction 6, $\eta = 33\%$ of initial ONOOCO_2^-) or to nitrate and CO_2 (reaction 7, $\eta = 67\%$ of the initial ONOOCO_2^-) (Augusto et al., 2019). This reaction leads to the formation of two potent one-electron oxidants - $\bullet\text{NO}_2$ and $\text{CO}_3^{\bullet-}$ (Augusto et al., 2002). The production of $\bullet\text{NO}_2$ makes ONOO^- both an oxidizing and nitrating species. The nitration of tyrosine at the 3-position causes a considerable loss of protein function and is considered as a biomarker of ONOO^- formation *in vivo* (Ferrer-Sueta et al., 2018). Because $\bullet\text{NO}_2$ can be formed via ONOO^- -independent pathways, including myeloperoxidase (MPO)-catalyzed oxidation of nitrite by H_2O_2 , detection of nitrated proteins is not sufficient to conclude the involvement of ONOO^- .

In accordance with the current knowledge of ONOO^- biological chemistry, only a few targets account for its consumption in biological systems. It is believed that CO_2 , peroxiredoxins, peroxidases, and a few metalloproteins are responsible for most ONOO^- scavenging *in vivo* (Ferrer-Sueta and Radi, 2009; Ferrer-Sueta et al., 2018).

For many years, most of the strategies for ONOO^- detection and quantification were depended on the reaction of probes, being the reduced fluorescent dyes with ONOO^- -derived radicals ($\text{CO}_3^{\bullet-}$, $\bullet\text{NO}_2$, $\bullet\text{OH}$). However, the detection of ROS and reactive nitrogen species with the use of those probes is non-specific (Wrona et al., 2005, 2008; Folkes et al., 2009). Moreover, such redox probes—dichlorodihydrofluorescein (DCFH) and dihydrorhodamine (DHR)—yield a corresponding fluorescent product by a free radical mechanism. It was demonstrated in a series of papers on the chemistry of DCFH and DHR, that the DCFH- and DHR-derived radicals—being products of their one-electron oxidation—react with molecular oxygen producing $\text{O}_2^{\bullet-}$ (Wrona et al., 2008; Folkes et al., 2009), resulting in H_2O_2 production and self-propagation of the probe oxidation (Rota et al., 1999; Bonini et al., 2006).

Organic Hydroperoxides

Organic hydroperoxides (ROOH) are compounds bearing at least one hydroperoxyl group. They can be considered structural analogs of H_2O_2 where one of the protons is substituted by an organic group. This class of compounds covers a wide range of chemical structures, ranging from small molecules, such as *tert*-butyl hydroperoxide, to high molecular weight compounds, including protein-bound hydroperoxides. Hydroperoxides are readily formed in biomolecules like lipids and proteins, in the presence of molecular oxygen and free radicals, or from excited-state species (Yin et al., 2011; Niki, 2014; Davies, 2016). Small-molecular-weight hydroperoxides are able to diffuse far from the site of their formation and can oxidize a wide variety of biological targets; thus, they are often considered reactive oxygen species.

The two-electron reduction potential of the organic hydroperoxyl group was estimated to be close to that of HOCl [$E^\circ(\text{ROOH}, \text{H}_2\text{O}/\text{ROH}) = 1.28\text{ V}$] (Merenyi et al., 1994), but the reactivity of those species is largely dependent on the nature of the organic part as well as on the pK_a of the

hydroperoxyl group. Isolated hydroperoxides are relatively stable and undergo slow decomposition to appropriate alcohols, but under physiological conditions they are reduced by thiols (e.g., glutathione) and ascorbate or removed by antioxidant enzymes, including peroxiredoxins and glutathione peroxidases (Peskin et al., 2010; Davies, 2016).

Hydroperoxides can be detected by titration and colorimetric methods based on iodide or ferrous ion oxidation (e.g., FOX assay), but these methods are non-specific and suitable mostly for hydroperoxides detection in simple chemical systems due to competing reactions of both assays with other biomolecules present in samples (Jessup et al., 1994; Bou et al., 2008; Michalski et al., 2014). The use of fluorescent probes like diphenyl-1-pirenyl phosphine or boronate probes is a more specific approach; however, those probes still can be oxidized by other ROS generated in the investigated system (Santas et al., 2013; Michalski et al., 2014). In the case of sterically isolated hydroperoxides (e.g., buried inside the tertiary structure of protein), there is always an uncertainty as to whether all hydroperoxyl species were scavenged by the probe, as some of the protein-derived hydroperoxides remain intact even after enzymatic digestion (Davies, 2016).

Detection of organic hydroperoxides is a challenging task. The use of fluorescent probes, rather than the onerous method requiring extraction of organic hydroperoxides from the biological matrix, enables high-throughput and kinetic studies.

Hypochlorous Acid

Hypochlorous acid (HOCl) is another important ROS. This potent oxidizing and chlorinating agent is generated *via* the reaction of H₂O₂ with chloride ions, catalyzed by the heme enzyme MPO (Davies et al., 2008). The pK_a of HOCl is equal to 7.5 (Morris, 1966); thus, both HOCl and the hypochlorite anion (OCl⁻) are present at nearly equimolar concentrations at physiological pH.

HOCl is a strong two-electron oxidizing [$E^{\circ}(\text{HOCl}, \text{H}_2\text{O}/\text{Cl}^-) = 1.28 \text{ V}$] (Arnhold et al., 2006) and chlorinating agent. It reacts rapidly with nucleophiles such as thiols and amines; thus, cysteine residues in proteins and glutathione (GSH) are the main targets for cellular HOCl (Davies et al., 2008). Due to the high reactivity of HOCl toward thiols and amines, its intracellular detection is difficult. In most cases, the probe would be able to intercept only a small fraction of the total amount of HOCl produced and/or react with the products of the interaction of HOCl with biomolecules.

There are numerous reported examples of fluorescent probes designed for the detection of HOCl utilizing the strong oxidizing character of HOCl and specific redox reactions of HOCl (Zhang et al., 2018; Wu D. et al., 2019). Nonetheless, in most cases, the chemistry of those probes has not been fully characterized, and their biological validation should include an independent and established method of HOCl detection. One of the reasonable approaches for selective monitoring of HOCl in biological systems can be the detection of products of HOCl-induced chlorination. The conversion of a hydroethidine probe to 2-chloroethidium represents a detection strategy, utilizing both the oxidizing and chlorinating potential of HOCl (Maghzal

et al., 2014; Talib et al., 2016). It has been shown that boronate probe peroxy-caged luciferin (PCL-1) reacts with HOCl, forming a phenolic product that further undergoes chlorination producing 7'-chloroluciferin (Kalyanaraman et al., 2016; Zielonka et al., 2016a). It is well-established that arylboronates react stoichiometrically with HOCl to produce phenolic products (Sikora et al., 2009). Although the use of boronic probes for HOCl monitoring in cellular studies is not without caveats, due to their moderate reactivity toward HOCl ($^2k \sim 10^4 \text{ M}^{-1}\text{s}^{-1}$) and the high reactivity of HOCl toward endogenous thiols and amines, boronate redox probes can be used in cell-free-based screening assays for MPO inhibitors. Also, boronate probes may be able to intercept HOCl in the cell culture/assay medium, where the lifetime of HOCl may be significantly higher than inside the cells.

CHEMICAL REACTIVITY OF BORONATES TOWARD BIOLOGICAL OXIDANTS

Biological Oxidants Reported to React With Arylboronates

Since the first reports on the development of boronate-based redox probes (Lo and Chu, 2003; Chang et al., 2004; Akhavan-Tafti et al., 2005), numerous authors have claimed the selectivity of this class of probes toward H₂O₂. However, analysis of the scientific literature on the chemical reactivity of arylboronates clearly points to the ability of other nucleophilic oxidants to convert them to corresponding phenols. In 1930, phenylboronic acid was reported to react with H₂O₂, forming phenol (Ainley and Challenger, 1930). However, the same paper also showed that phenylboronic acid is oxidized to phenol in chlorine or bromine water, and it was proposed that the reacting oxidant is HOCl/HOBr (Ainley and Challenger, 1930). The oxidation of phenylboronic acids by HOCl and HOBr anions also was reported in 1962 (Kuivila et al., 1962). It was shown that arylboronates are substrates for flavin-containing cyclohexanone oxygenase, and flavin hydroperoxide was proposed as the reactive oxidant (Branchaud and Walsh, 1985). In 2009, another biologically important oxidant, ONOO⁻, was shown to react directly and rapidly with arylboronates, yielding corresponding phenols as the main products (Sikora et al., 2009). The second-order rate constants for the reaction of boronates with ONOO⁻, HOCl, and H₂O₂ were determined at pH 7.4, and it was demonstrated that ONOO⁻ reacts with boronic acids nearly a million times faster ($k \sim 10^6 \text{ M}^{-1}\text{s}^{-1}$) than H₂O₂ ($k \sim 1 \text{ M}^{-1}\text{s}^{-1}$) and more than 100 times faster than HOCl ($k \sim 10^4 \text{ M}^{-1}\text{s}^{-1}$) (Sikora et al., 2009). This high reactivity of arylboronic acids toward ONOO⁻, compared with H₂O₂, makes them potential probes for intracellular detection of ONOO⁻. Based on the substrate consumption study and the analysis of phenols formation yield, arylboronates were concluded to react with peroxynitrite at a 1:1 stoichiometry, yielding the corresponding phenol as a major product ($\eta = 80\text{--}85\%$) (Sikora et al., 2009). Also, the reaction of peroxynitrite with arylboronates was proposed to lead to the formation of radical transient species and radical-derived minor products ($\eta = 15\text{--}20\%$) (Sikora

et al., 2011). Both HOCl and H₂O₂ react stoichiometrically with boronates, yielding the corresponding phenols with a yield close to 100%. When used at excess, HOCl has been shown to cause a rapid decrease in the yield of phenol, which can be attributed to the chlorination of phenol by excess HOCl. The oxidation of boronates was observed in systems where •NO and O₂•⁻ are co-generated, producing peroxyxynitrite *in situ* (Sikora et al., 2009). Also, it was verified that •NO₂ does not oxidize boronates to phenols (Sikora et al., 2009).

The proposed mechanism of the simple phenylboronates reaction with ONOO⁻, OCl⁻, and H₂O₂ is quite general and can be applied to other acidic hydroperoxides and hypohalous acids as well as to other boronates, including boronate-based profluorescent probes, erroneously described in the literature as selective for H₂O₂. Over the years, more oxidants have been demonstrated to be able to oxidize boronic compounds, including amino acid hydroperoxides (Michalski et al., 2014), peroxyxynitrate (O₂NOO⁻) (Huang et al., 2019), peroxyphosphonate (O₃POO³⁻) (LaButti and Gates, 2009), and peroxydicarbonate (O₂COO²⁻) (Truzzi and Augusto, 2017). Boronic acids and esters are organic compounds possessing trivalent, an sp²-hybridized boron atom that is linked to one alkyl or aryl substituent and two hydroxyl or ester groups. They are mild and hard Lewis acids that can easily coordinate hard nucleophilic bases. The pK_a-value for most arylboronic acids is in the range of 7–9, depending on the structure. The nucleophilic addition of peroxides (HOO⁻, ROO⁻, ONOO⁻, O₂NOO⁻, O₃POO³⁻, O₂COO²⁻) or hypohalite anions (OCl⁻, OBr⁻) to the boronate functional group is a facile reaction and the first step of the oxidation reaction. Based on available experimental and computational data, a general mechanism for arylboronates oxidation can be proposed (Scheme 4). The reaction occurs with the formation of the adduct of anionic oxidant to the boronic functional group, followed by the heterolytic cleavage of the O–O or O–halogen bond, resulting in the elimination of an anionic leaving group and formation of phenoxyboronic acid intermediate. This intermediate undergoes hydrolysis to form phenolic product and boric acid (Scheme 4). Isotope tracking experiments indicate that the oxygen atom in the phenolic product derives from the oxidant and not from the solvent (Rios et al., 2020).

The reported differences in the second-order rate constants for boronate oxidation by H₂O₂, HOCl, and ONOO⁻ at pH 7.4 (Sikora et al., 2009) can be partially explained by the differences in their pK_a-values: 11.7 (H₂O₂), 7.5 (HOCl), and 6.8 (ONOOH). The calculated fractions of the boronate-reactive anionic forms, HOO⁻, OCl⁻ and ONOO⁻, at pH 7.4 are 0.005, 46, and 80%, respectively. Other factors, including the type of the anionic leaving group and the extent of its solvation, also should be considered.

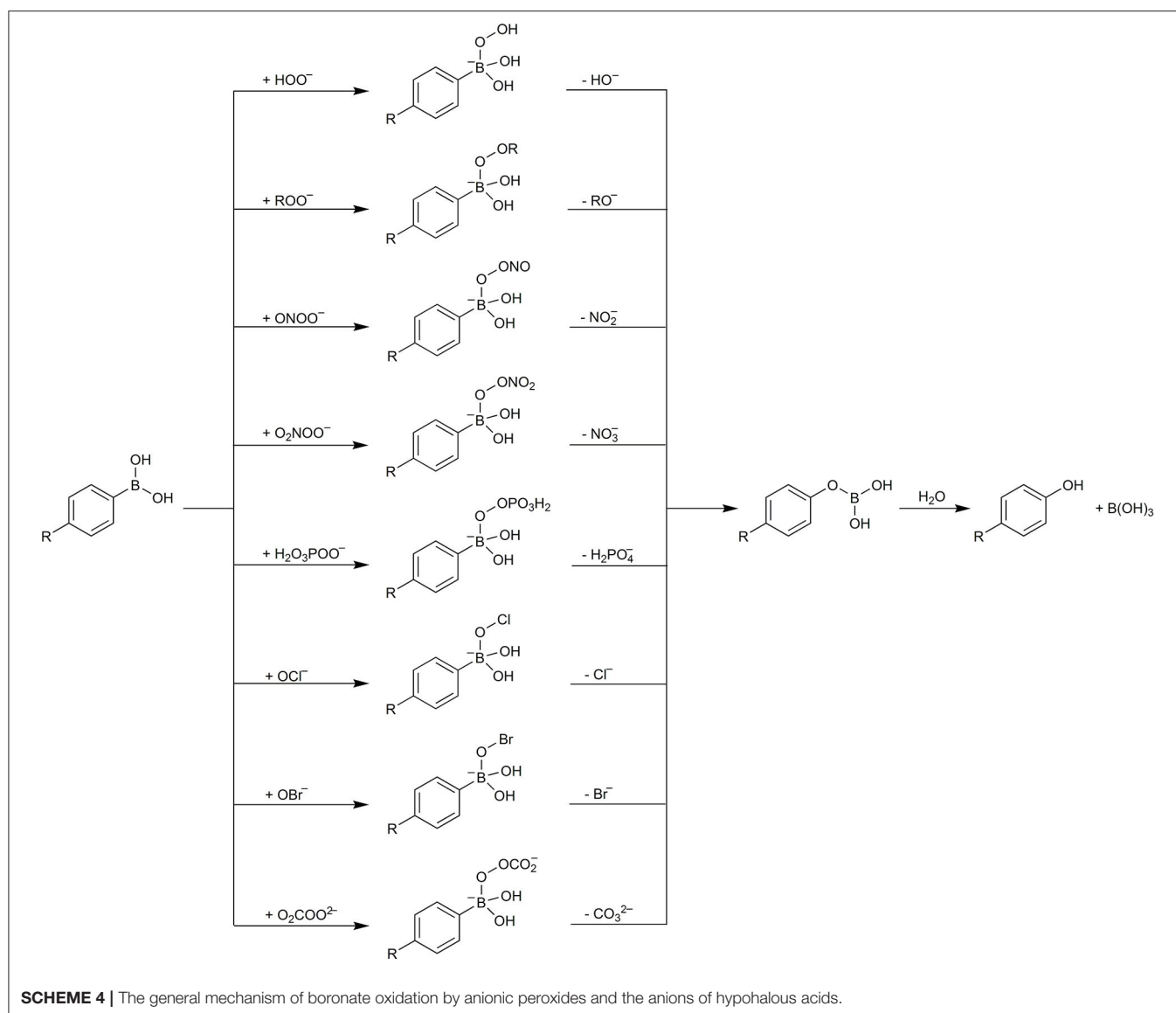
The effect of changes of pH on the reactivity of biological oxidants with boronates is complex and involves the acid-base equilibria of both the probe and the oxidant. Further studies are required, but based on the authors' experiences, two general assumptions can be made: (i) the higher the pH, the higher the amount of deprotonated oxidant is present, resulting in a faster oxidation process; and (ii) the higher the pH, the

higher the fraction of the boronate probe is present in the basic form, with the boron atom in sp³ hybridization, resulting in slower reaction kinetics. It can be anticipated that, for each specific probe and oxidant, there exists an optimal pH, with the highest rate constant of the oxidation reaction. Furthermore, for fluorescence-based detection, phenolic products may undergo acid-based equilibration within the physiological pH range, which will be reflected in the pH-dependent fluorescence signal.

Mechanism of Oxidation of Boronates by ONOO⁻

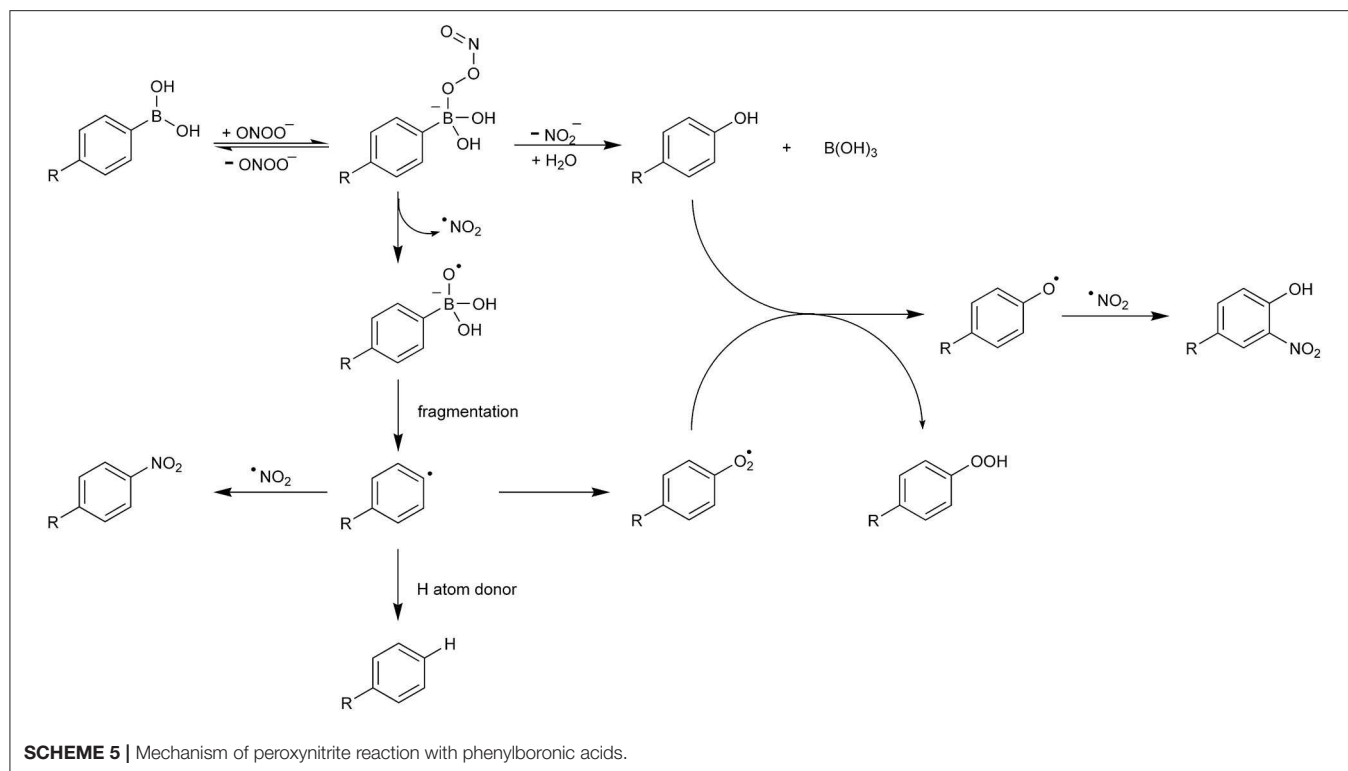
Product analyses and substrate consumption data, in combination with the kinetic data presented in the first two studies on the ONOO⁻-induced boronate oxidation (Sikora et al., 2009; Zielonka et al., 2010), indicate that all three oxidants tested (H₂O₂, HOCl, and ONOO⁻) react with boronates directly and stoichiometrically (with 1:1 stoichiometry), yielding the corresponding phenols as the sole (in the case of H₂O₂, HOCl) or major (yield of about 80–90% in the case of ONOO⁻) product. The formation and identity of other, minor products formed in the reaction of boronates with ONOO⁻ implicated the occurrence of a second, free radical pathway, involving the formation of phenoxy, phenyl, and •NO₂ radicals. This minor radical pathway was studied and described in detail in Sikora et al. (2011). The electron paramagnetic resonance (EPR) spin-trapping technique was used to trap and characterize the radical transient products formed in the reaction between boronic acids and peroxyxynitrite. The formation of phenyl radicals in the studied reaction was unequivocally confirmed with the use of two spin traps, 2-methyl-2-nitrosopropane (MNP) and 5-diethoxyphosphoryl-5-methyl-1-pyrroline-N-oxide (DEPMPO), based both on the spectral signatures and the inhibitory effects of 2-propanol, the scavenger and reductant of phenyl radical, on the yield of the spin adduct. Analogous spin-trapping experiments using H₂O₂ as the oxidant did not show formation of any radical intermediates, in agreement with the established yield of the phenolic product.

Based on these observations, the mechanism of ONOO⁻-induced boronate (PhB(OH)₂) oxidation was proposed (Scheme 5) (Sikora et al., 2011). The initial step of that reaction is the nucleophilic addition of ONOO⁻ to the electrophilic boron atom in PhB(OH)₂, resulting in the formation of an anionic adduct. This adduct undergoes further transformation into products *via* two mechanisms. In the major pathway, the O–O bond in the adduct undergoes heterolytic cleavage with the elimination of the nitrite anion, resulting in the formation of phenol and boric acid. In the minor pathway, the O–O bond in the adduct undergoes homolytic cleavage, resulting in the formation of •NO₂ and PhB(OH)₂O•⁻ transient radical products. The phenyl radical (Ph•) can be subsequently formed *via* the fragmentation of the PhB(OH)₂O•⁻ radical anion or of its protonated form, the PhB(OH)₃• radical. The latter can be regarded as an adduct of the phenyl radical Ph• to boric acid (B(OH)₃) and should be extremely unstable. Indeed, according to the reported results of density-functional theory quantum mechanical calculations, the energy barrier for the fragmentation



of the $\text{PhB(OH)}_2\text{O}^{\bullet-}$ radical anion leading to the formation of phenyl radical is very low (12–17 kJ/mol) (Sikora et al., 2011) and the dissociation of the $\text{PhB(OH)}_3^{\bullet}$ radical into Ph^{\bullet} and B(OH)_3 is barrierless. Once formed, the phenyl radical may undergo subsequent reactions with hydrogen atom donors, molecular oxygen, or the $\bullet\text{NO}_2$ radical (Scheme 5). The latter reaction, which may occur within the solvent cage, results in the formation of a stable ONOO^- -specific nitrobenzene product, PhNO_2 . Rapid reaction of Ph^{\bullet} with O_2 results in the formation of the highly oxidizing phenylperoxyl radical PhOO^{\bullet} , which can oxidize phenols, yielding phenoxyl radical PhO^{\bullet} and products derived from it. Inhibitory effects of hydrogen atom donors (e.g., 2-propanol) and radical scavengers (e.g., NADH, GSH, ascorbic acid) on the formation of phenoxyl radical-derived nitrophenolic product(s) confirmed that the phenoxyl radical is formed as the secondary transient radical species.

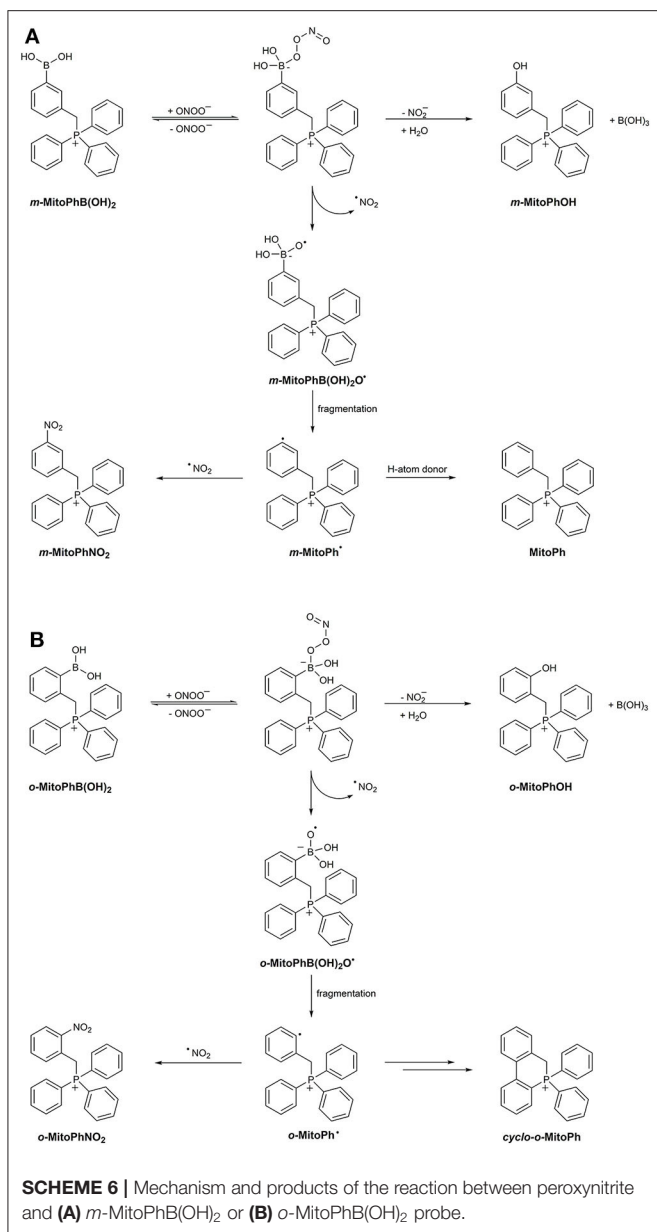
It has been proposed that the ONOO^- -specific products' profile of boronate oxidation reaction can be used in chemical, enzymatic, and cellular systems as a "peroxynitrite fingerprint" to confirm the presence of this oxidant. This is a significant advantage over the detection of protein nitration, which may occur via ONOO^- -independent pathways, as mentioned above. The peroxynitrite-specific products of *o*-MitoPhB(OH)₂ and PCL-1 oxidation have been detected in extracts of activated macrophages (Zielonka et al., 2016a,b). The relative contribution of the radical pathway during oxidation of boronate compounds by ONOO^- is, however, dependent on the chemical structure of the boronate. For example, it has been reported that the Fl-B probe undergoes conversion to the fluorescein product with a 99% yield (Rios et al., 2016). Therefore, for each new boronate probe developed for ONOO^- detection, the reaction mechanism should be determined and product distribution quantified.



The mechanism of ONOO^- -derived boronate oxidation was further explored in studies on the reaction of the mitochondria-targeted probe MitoB (*m*-MitoPhB(OH)₂) and its isomers *o*-MitoPhB(OH)₂ and *p*-MitoPhB(OH)₂ with ONOO^- (Sikora et al., 2013; Zielonka et al., 2015, 2016b; Rios et al., 2020). Similar to simple arylboronates, MitoB and its *para*- and *ortho*-isomers react rapidly with ONOO^- with the formation of the corresponding phenolic products at 90% reaction yield. The determined second-order rate constants for the reaction of ONOO^- with MitoPhB(OH)₂ isomers at pH 7.4 are equal to $(3.5 \pm 0.5) \times 10^5$, $(1.0 \pm 0.1) \times 10^6$, and $(1.0 \pm 0.1) \times 10^6 \text{ M}^{-1}\text{s}^{-1}$ for *ortho*-, *meta*-, and *para*-isomers, respectively (Sikora et al., 2013). All three isomers react with ONOO^- with the formation of additional, minor products *via* the radical pathway. EPR spin-trapping experiments showed that the phenyl radicals formed from the reaction between ONOO^- and *m*-MitoPhB(OH)₂ or *p*-MitoPhB(OH)₂ but not from the *ortho*-isomer could be trapped using the MNP and DEPMPO spin traps. In the case of *para*- and *meta*-isomers, the dominant minor product formed from the radical pathway in the presence of phenyl radical reductant, 2-propanol, is MitoPhH, formed by hydrogen atom abstraction from 2-PrOH by MitoPh• radicals. In case of the *ortho*-isomer, not only was the EPR spin trapping of the phenyl radical unsuccessful, but also the yield of MitoPhH in the presence of 2-PrOH was significantly lower. Nevertheless, for all three isomers, the additional minor nitration product, MitoPhNO₂, was detected (Sikora et al., 2013). This product was also detected in macrophages activated to produce ONOO^- in the presence of the *o*-MitoPhB(OH)₂ probe (Zielonka et al., 2015, 2016b). Mass spectrometric-based

investigation on the products formed in the reaction between *o*-MitoPhB(OH)₂ and ONOO^- led to the conclusion that the transient phenyl radical *o*-MitoPh• predominantly undergoes rapid intramolecular cyclization to form a peroxyxynitrite-specific product, cyclo-*o*-MitoPh (9,10-dihydro-9,9-diphenyl-9-phosphoniaphenanthrene) (**Scheme 6B**), in 10.5% yield while the nitrobenzene-type product, *o*-MitoPhNO₂, is formed in only 0.5% yield (Zielonka et al., 2016b).

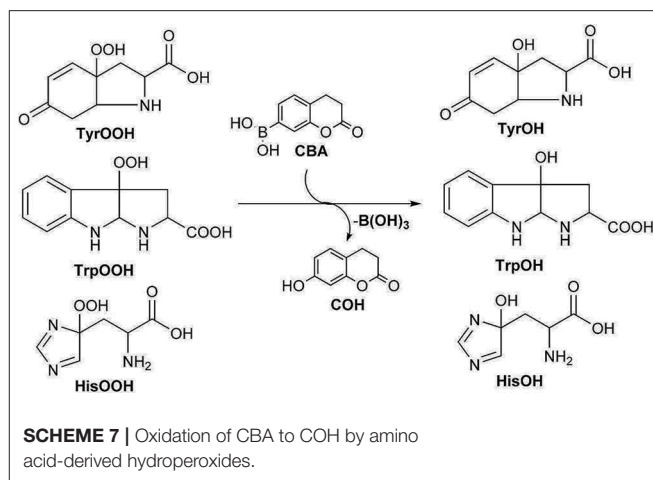
As with simple arylboronates, the formation of the observed products of the ONOO^- reaction with *o*-MitoPhB(OH)₂ can be rationalized assuming the mechanism where the ONOO^- adduct to the electrophilic boron atom decays on two pathways: *via* heterolytic or homolytic cleavage of the O–O bond (**Scheme 6**) (Sikora et al., 2013). The major, heterolytic cleavage pathway leads to the formation of the corresponding phenol, MitoPhOH, and NO_2^- . The minor, homolytic cleavage pathway results in the formation of a radical anion, MitoPhB(OH)₂O•⁻, and •NO₂. Subsequent fragmentation of MitoPhB(OH)₂O•⁻ to MitoPh• and its further reactions (including intramolecular cyclization in the case of *o*-MitoPh•, **Scheme 6B**) result in the formation of ONOO^- -specific minor products (Sikora et al., 2013; Zielonka et al., 2016b). The proposed mechanism has been further corroborated by tracking the O–18 atoms in the products formed during the reaction between *o*-MitoPhB(OH)₂ and $\text{ON}^{18}\text{O}^{18}\text{O}^-$ (Rios et al., 2020). Relative quantitative analyses of the non-radical and radical-derived products of MitoPhB(OH)₂ oxidation give insight into the kinetics of both pathways. The ratio of the rate constants of the radical and non-radical pathways $k_{\text{rad}}/k_{\text{non-rad}}$ can be estimated from the plot of sum of the minor products vs. the amount of major



product. The determined values of those ratios were equal to 0.1, 0.1, and 0.07 for *ortho*-, *meta*-, and *para*-isomers, respectively (Sikora et al., 2013).

Boronate-Based Molecular Probes in the Studies of HNO Reactivity

Boronate-based molecular probes have emerged as a valuable tool in studies on HNO reactivity. In 2014, coumarin-7-boronic acid (CBA, **26**) and *p*-MitoPhB(OH)₂ (**77**) probes were used to determine the chemical identity of the product of the HNO reaction with O₂ in aqueous solutions at physiological pH (Smulik et al., 2014).



HNO, commonly known as nitroxyl (IUPAC recommended name: azanone), formally is the protonated product of the one-electron reduction of nitric oxide. This reactive triatomic molecule remains one of the most enigmatic reactive nitrogen species, as its biological chemistry and physiological activity are still not completely understood. For many years, one of the most intriguing aspects of HNO chemistry was its reaction with O₂. It has been reported in the literature that the azanone anion (NO⁻) reacts rapidly with molecular oxygen ($k = 2.7 \times 10^9 \text{ M}^{-1}\text{s}^{-1}$), forming ONOO⁻ (Donald et al., 1986; Shafirovich and Lymar, 2002) (reaction 8).



Despite several studies on the reaction of HNO with O₂, the chemical identity of the oxidant that is formed in this reaction has been controversial (Miranda et al., 2001, 2002; Kirsch and De Groot, 2002). The possibility of ONOO⁻ formation has been proposed (Kirsch and De Groot, 2002), but it has also been questioned (Miranda et al., 2001, 2002). This was due, in part, to the lack of appropriate molecular probes that directly react with ONOO⁻ with the formation of ONOO⁻-specific products. As has been discussed, several boronate compounds have shown that their reaction with peroxyxynitrite leads to the formation of a major phenolic product and several peroxyxynitrite-specific minor products (Sikora et al., 2009, 2011, 2013; Smulik et al., 2014; Zielonka et al., 2015, 2016a,b; Rios et al., 2020). The generation of ONOO⁻ in the reaction of HNO with O₂ in aqueous solutions at pH 7.4 was confirmed based on the oxidation of the boronate probes used and the formation of ONOO⁻-specific products in the solutions of HNO donors (Smulik et al., 2014). The use of a set of HNO scavengers of known reactivity and the competition kinetics method allowed the second order rate constant for the HNO reaction with O₂ [$k = (1.8 \pm 0.3) \times 10^4 \text{ M}^{-1}\text{s}^{-1}$] to be determined (Smulik et al., 2014). This value is two times higher than previously reported ($k = 8 \times 10^3 \text{ M}^{-1}\text{s}^{-1}$) (Liochev and Fridovich, 2003) and ~5 times higher than the value proposed by Miranda et al. (2003) ($k = 3 \times 10^3 \text{ M}^{-1}\text{s}^{-1}$). The use of boronate redox probes, in combination with a competition

kinetics approach, was proposed to study the reactivity of HNO toward its scavengers, and the determination of the kinetics of HNO reaction with selected thiols was reported.

The same methodology, in combination with the use of the resorufin-based boronate probe, PC1 (15), was also used in a study on the reactivity of HNO toward selected scavengers (Smulik-Izydorczyk et al., 2017). The kinetic method was based on two parallel HNO reactions: one with the studied scavenger and the other with molecular oxygen [$k = (1.8 \pm 0.3) \times 10^4 \text{ M}^{-1}\text{s}^{-1}$ (Smulik et al., 2014)]. The latter led to the formation of ONOO⁻, which was detected fluorometrically with the use of the PC1 probe.

Recently, a kinetic study on HNO liberation from Piloxy's acid derivatives showed that boronate-based molecular probes can be a useful tool for the characterization of HNO donors (Smulik-Izydorczyk et al., 2019). Again, the indirect method of HNO detection was used, based on its reaction with O₂ to form peroxyxynitrite, and quantitation using boronate-based redox probe PC1.

Fluorescence-Based Monitoring of H₂O₂ and ONOO⁻ Formed *in situ* in Enzymatic and Cellular Systems

One of the first reported fluorogenic boronate probes, PF1 (3), was shown to undergo intracellular oxidation to a green-fluorescent product upon exposure of live cells to H₂O₂ (Chang et al., 2004). This report provides a proof of principle for the ability of boronate-based probes to respond to H₂O₂ in a cellular milieu. Building on this observation, a series of mono-boronated probes [e.g., PG1 (16)] have been synthesized and shown to respond to endogenously produced H₂O₂, demonstrating the potential of boronate-based redox reporters as a new generation of probes for redox biology (Miller et al., 2007). CBA (26) was the first boronate-based profluorescent probe applied for the real-time monitoring of ONOO⁻ formation in an enzymatic system (Zielonka et al., 2010) and in cultured cells (Zielonka et al., 2012b). Similar to simple arylboronates, CBA has been shown to react rapidly and stoichiometrically with ONOO⁻, yielding fluorescent 7-hydroxycoumarin (COH) as the major product ($\eta \approx 83\%$) and ONOO⁻-specific minor products: coumarin and 7-nitrocoumarin (Smulik et al., 2014). The observed reactivity of CBA toward biological oxidants is similar to what had been published for arylboronates: the second-order rate constants for the reaction of CBA with ONOO⁻ and H₂O₂ are equal to 1.1×10^6 and $1.5 \text{ M}^{-1}\text{s}^{-1}$, respectively (Zielonka et al., 2010). The CBA probe was used to demonstrate the formation of ONOO⁻ as the product of the reaction of O₂^{•-} and •NO, when used at different ratios (Zielonka et al., 2010) and as a product of the reaction of HNO with O₂ (Smulik et al., 2014). Following the CBA- and FLAmBE (22)-based detection of ONOO⁻ in RAW 264.7 macrophages stimulated to coproduce O₂^{•-} and •NO (Zielonka et al., 2012b), numerous boronate redox probes were developed and reported for the detection of cellular ONOO⁻ (Yu et al., 2012; Kim J. et al., 2014; Rios et al., 2016; Sedgwick et al., 2017; Murfin et al., 2019; Weber et al., 2020). CBA was also used in combination with the immuno-spin trapping technique

to demonstrate ONOO⁻-mediated protein radical formation in microglial cells exposed to lipopolysaccharide (Kumar et al., 2014).

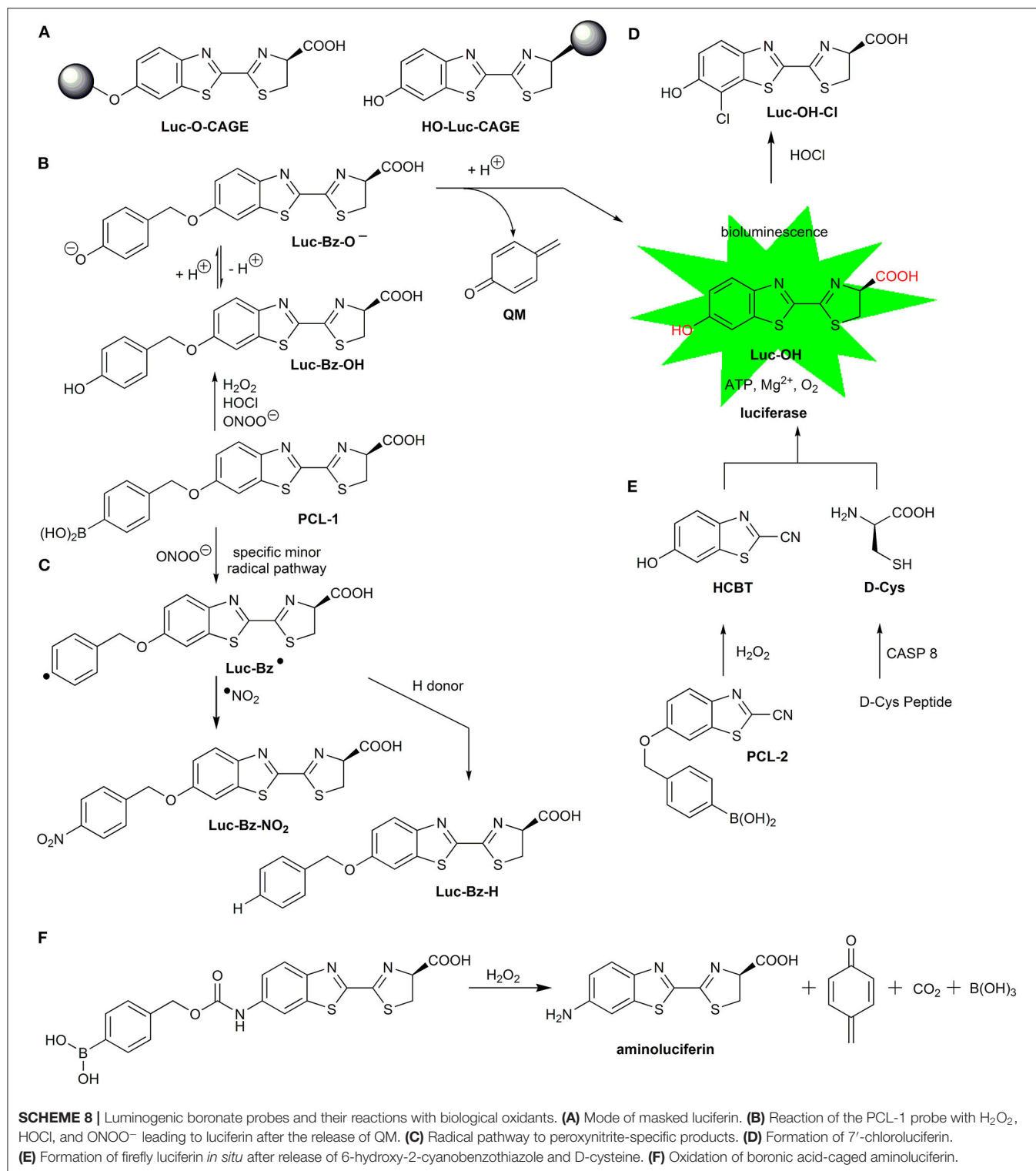
Fluorescence-Based Monitoring of Amino Acid and Protein-Bound Hydroperoxides

Boronate probes have been also proposed for the detection of amino acid, peptide, and protein hydroperoxides (Michalski et al., 2014). CBA (26) has been shown to react with enzymatically generated tyrosyl hydroperoxide to form the fluorescent COH product (Scheme 7).

Although the stoichiometry of the reaction between boronate probes and amino acid, peptide, and protein hydroperoxides has never been directly measured due to the lack of authentic standards of the corresponding hydroperoxides, it is reasonable to assume a 1:1 stoichiometry by analogy with the structurally related H₂O₂ and other tested oxidants (Sikora et al., 2009; Zielonka et al., 2010). The developed fluorometric assay for amino acid hydroperoxides has been adapted to a multi-well plate format and compared to the FOX assay, revealing several advantages, including a one-step detection process, a possibility of real time measurements, and superior assay quality as assessed by the Z' parameter (Michalski et al., 2014). Further studies using photochemically generated singlet oxygen enabled production of tyrosyl, tryptophan, and histidine hydroperoxides, and their reactivity toward the boronate probe was tested. These hydroperoxides have been shown to react with the CBA probe with rate constants at least 10 times higher as compared with H₂O₂. Finally, CBA has been successfully used for the detection of protein hydroperoxides generated on BSA and lysozyme and with those produced in lysates from cells exposed to visible light and the singlet oxygen-generating photosensitizer Rose Bengal. Subsequent studies on the reaction of boronated probes with amino acid hydroperoxides have shown that the high concentration of biothiols can affect the signal from the boronate probe (Debowska et al., 2016). The presence of a 0.3–3 mM concentration of GSH significantly decreased the fluorescence signal from probe oxidation (present at 10 μM), while 10 mM GSH completely abolished probe oxidation, indicating a direct reaction of GSH with tyrosyl hydroperoxide. On this basis, it can be concluded that detection of cellular hydroperoxides requires a relatively high concentration of the boronate probe to enable efficient competition with cellular scavengers of hydroperoxides. The CBA probe seems well-suited for this specific purpose due to its relatively high water solubility and superior chemical stability (Zielonka et al., 2010; Michalski et al., 2014).

Bioluminescence-Based Detection of Biological Oxidants

Bioluminescent imaging is commonly used for sensitive monitoring of various biomolecular processes in cells and living animals. The popularity of bioluminescence assays in biomedical research resulted in significant progress in the syntheses of luminogenic probes based on the firefly luciferin skeleton (Luc-OH, Scheme 8). The blocking (also referred to as "caging") of the hydroxyl or carboxyl group (Scheme 8A) by chemical



SCHEME 8 | Luminogenic boronate probes and their reactions with biological oxidants. **(A)** Mode of masked luciferin. **(B)** Reaction of the PCL-1 probe with H₂O₂, HOCl, and ONOO⁻ leading to luciferin after the release of QM. **(C)** Radical pathway to peroxynitrite-specific products. **(D)** Formation of 7'-chloroluciferin. **(E)** Formation of firefly luciferin *in situ* after release of 6-hydroxy-2-cyanobenzothiazole and D-cysteine. **(F)** Oxidation of boronic acid-caged aminoluciferin.

systems, which are capable of reacting specifically with the analyte of interest, makes recognizing the probe (Luc-O-CAGE, HO-Luc-CAGE) by luciferase impossible and thus blocks the formation of luminescence. The release of Luc-OH as a result of the dislodgement of the blocking group occurs during or after recognition of the analyte. Then, luciferase interacts with

Luc-OH and the required co-factors, and the bioluminescence signal is observed and recorded using luminescence reader or imaging system.

Several luciferin-based oxidant-sensitive probes have been developed and reported (Van De Bittner et al., 2010; Wu et al., 2014; Kojima et al., 2015; Chen et al., 2017). Among those probes,

all boronate-based luciferin derivatives contain self-immolative boronobenzyl moieties. Recently, a luciferin derivative, with the hydroxyl group directly substituted with the boronate group, was reported and shown to respond to activated macrophages (Szala et al., 2020). One of the first pro-luciferin bioluminescent probes designed for imaging H_2O_2 in live animals was peroxy-caged luciferin, PCL-1 (Van De Bittner et al., 2010) (**Scheme 8**). The second order rate constant for the reaction between PCL-1 and H_2O_2 was determined to be equal to $3.8 \pm 0.3 \text{ M}^{-1}\text{s}^{-1}$. In 2014, boronic acid-caged aminoluciferin (CAL) was synthesized and applied as a probe for real-time detection of H_2O_2 *in vitro*, *in cellulo*, and *in vivo* (Wu et al., 2014). In both PCL-1 and CAL, the boronobenzyl moiety is oxidized to intermediate phenol, which subsequently releases luciferin (**Schemes 8B,F**) or aminoluciferin Luc-NH₂, respectively, *via* a self-immolative reaction mechanism.

Follow-up studies determined that the PCL-1 probe also can be oxidized by ONOO⁻ [$k = (9.8 \pm 0.3) \times 10^5 \text{ M}^{-1}\text{s}^{-1}$] (Sieracki et al., 2013). Similar to simple arylboronates, the reaction of PCL-1 with ONOO⁻ proceeds *via* two pathways. The major pathway is the same as for H_2O_2 and involves the formation of the phenolic intermediate (Luc-Bz-OH), which after elimination of QM yields Luc-OH as the stable end product. Rapid HPLC analyses enabled the detection of the primary phenolic intermediate formed upon the reaction of PCL-1 with different oxidants (Zielonka et al., 2016a). The minor pathway of the reaction of PCL-1 with ONOO⁻ produces nitrated and reduced products, Luc-Bz-NO₂ and Luc-Bz-H, respectively (**Scheme 7C**). The formation of phenyl-type radical Luc-Bz• during oxidation of PCL-1 by ONOO⁻ was confirmed by EPR spin trapping combined with liquid chromatography-mass spectrometry (LC-MS)-based identification of the spin adduct (Zielonka et al., 2016a). Detection of ONOO⁻-specific Luc-Bz-NO₂, in combination with bioluminescence-imaging, was proposed for identification of this oxidant and its formation in activated macrophages has been demonstrated (Zielonka et al., 2016a).

Hypochlorite is another oxidant that is able to convert PCL-1 to Luc-OH (Sieracki et al., 2013). In a subsequent reaction with HOCl, Luc-OH produces 7'-chloroluciferin (Luc-OH-Cl, **Scheme 7D**) (Zielonka et al., 2016a). Therefore, Luc-OH-Cl detection in addition to bioluminescence *in vivo* may help identify HOCl as an oxidant responsible for the bioluminescence signal.

In 2013, the small-molecular-weight boronate pro-luciferin bioluminescent probe PCL-2 was proposed for dual-analyte *in vivo* imaging (Van De Bittner et al., 2013). This imaging system relies on *in situ* formation of luciferin in a condensation of 6-hydroxy-2-cyanobenzothiazole, which is uncaged by H_2O_2 , and D-cysteine is produced upon the action of caspase 8 on pentapeptide. The disadvantage of this system for the sole purpose of detecting biological oxidants is the need to simultaneously unmask the two partners necessary to produce luciferin.

The described pro-luciferin bioluminescent probes were successfully applied for the bioluminescent detection of ONOO⁻ in cell culture studies (Sieracki et al., 2013; Zielonka et al., 2016a)

and for the bioluminescent imaging of biological oxidants *in vivo* in mice (Van De Bittner et al., 2010, 2013; Cheng et al., 2020).

Selectivity of Boronate-Based Probes

Meaningful application of the probes to detect a specific analyte requires knowledge of the probe's chemistry and, thus, selectivity. Over the last two decades, hundreds of promising new redox probes have been reported and their selectivity toward a single oxidizing species claimed. This is also true for boronate-based redox probes, which initially were claimed as selective for H_2O_2 , while reports claiming their selectivity toward ONOO⁻ or HOCl were also published. Examples include the PF3 probe (**18**, also known as Fl-B, **Table 1**), which was proposed for selective detection of H_2O_2 (Dickinson et al., 2010) but later demonstrated to react with HOCl and ONOO⁻ and applied for monitoring ONOO⁻ in a cellular system (Rios et al., 2016). The PR1 probe (**8**, **Table 1**), proposed for the detection of H_2O_2 (Miller et al., 2005) and ONOO⁻ (Weber et al., 2018), represents an interesting case where initial oxidative deboronation of both boronate groups will result in the formation of dihydroresorufin, which in the presence of O_2 will generate H_2O_2 (Maeda et al., 2000), driving further oxidation of the probe. In such a case, ONOO⁻-initiated probe oxidation may lead to H_2O_2 formation, and partial sensitivity of the fluorescence signal to catalase, an enzymatic H_2O_2 scavenger. In another example, the TCF-BOR2 probe (**43**, **Table 1**) was proposed for selective detection of HOCl (Shu et al., 2015), ONOO⁻ (Sedgwick et al., 2017), and H_2O_2 (Choudhury et al., 2019). As discussed, most boronate probes will respond to all three oxidants, as well as other oxidants listed above, at least in pure chemical systems. Clearly, many claims of the selectivity of boronate redox probes toward a single oxidizing species were due to the lack of expertise/appreciation of the limitations and potential pitfalls in studying the reactivity of several members of ROS.

Following are some typical pitfalls/limitations in studies of the probes' responses to different oxidants. It is our hope that this will help the community characterize new redox probes.

- 1. Organic solvent.** Many cell-permeable probes are more soluble in organic solvents than in water. Therefore, their stock solutions are prepared in those solvents, typically DMSO or ethanol, due to their relatively low cytotoxicity. Those solvents may, however, scavenge the tested oxidant, resulting in false-negative. For example, the lack of response of the probe to the hydroxyl radical or HOCl may be due to scavenging of those species by DMSO. DMSO was shown to block oxidation of the CBA probe by HOCl (Zielonka et al., 2016a). When the use of organic solvents is necessary, their ability to compete for the oxidant of interest should be considered. One has to remember that even at 0.1% by vol., the organic solvent would equate to millimolar concentrations. For instance, 0.1% (by vol.) DMSO corresponds to a 14 mM concentration, three orders of magnitude higher than the typical concentration of the probe! When the use of an organic solvent cannot be avoided, to limit its interference and minimize the final concentration of the solvent, a high concentration stock solution (0.1 M or higher) of the probe

should be made and serially diluted in the assay medium. In addition, the choice of solvent should be based both on its compatibility with cells and on its minimal reactivity toward the species to be detected. Always, the final concentration of the probe and solvent should be calculated and the ability of the probe to outcompete the solvent for the species of interest should be established. The ability of other solution components (e.g., buffer, metal chelator) to compete for the oxidants tested should be also considered.

2. **Excess of the oxidant over the probe.** Studies of the oxidation of boronates by H_2O_2 can be conveniently carried out using an excess of this oxidant. This is because, in most cases, the phenolic product is not reactive toward H_2O_2 . This is not, however, the case for many other oxidants. As demonstrated for simple arylboronates, under the conditions of excess HOCl, the phenolic product undergoes chlorination, resulting in its consumption (Sikora et al., 2009). The same applies to many other oxidants, including HO^\bullet , $^\bullet\text{NO}_2$, and $\text{CO}_3^{\bullet-}$, which are also the products of the decomposition of ONOO^- or ONOOCO_2^- . The use of an excess of the probe over the oxidant should help avoid the product consumption and better mimic the conditions in cell-based experiments where oxidants are very rarely present in excess of the probe.
3. **Using a bolus addition of an unstable oxidant.** In many cases, the oxidizing species to be studied is not stable and decomposes within the time of mixing. This applies not only to highly unstable free radicals but also, for example, to ONOO^- . Efficient mixing of the probe with bolus ONOO^- requires good manual skills as well as some experience. Our typical protocol involves rapidly and vigorously mixing the solution of the probe placed in a 1.5 mL microcentrifuge tube with a small volume of ONOO^- solution placed inside the clean, dry tube cap. Another example is $\text{O}_2^{\bullet-}$: Although it can be prepared as a stable solution of potassium superoxide (KO_2) in an anhydrous DMSO, adding it to an aqueous buffer will result in rapid dismutation at the water-DMSO phase interface, the loss of $\text{O}_2^{\bullet-}$, and the potential formation of not-yet-characterized DMSO-derived oxidants. Similarly, directly adding grains of KO_2 powder to a buffered aqueous solution will result in efficient dismutation and loss of $\text{O}_2^{\bullet-}$ at the KO_2 solid/water interface. In the case of $\text{O}_2^{\bullet-}$, $^\bullet\text{NO}$, and ONOO^- , chemical or biochemical sources can alternatively (or complementarily) be used to produce a slow, steady, and homogenous flux of the species and enable rigorous characterization of the probe's reactivity (Sikora et al., 2009; Zielonka et al., 2010).
4. **The stoichiometry of the reaction is higher than expected.** The determined stoichiometry of the reaction of mono-boronated probes with H_2O_2 , HOCl, and ONOO^- is 1:1 (Zielonka et al., 2012a). It is expected that the stoichiometry may increase to 2:1 for a diboronated probe. A higher ratio of the oxidant to the probe may point to the loss of the oxidant by the interaction with a reaction mixture component, or a differential chemical reactivity. This may affect the probe's selectivity, and the reasons for the altered stoichiometry should be determined.

5. **Product formation is slower than the lifetime of the oxidant studied.** Direct reaction of the probe with the oxidant results in a decreased lifetime of the oxidant. Therefore, after the bolus addition, formation of the oxidation product should occur on a time scale shorter than the lifetime of the oxidant. Delayed formation of the product may occur when a self-immolative moiety is used in the probe design. In such case, the dynamics of elimination of the self-immolative moiety may control the kinetics of product formation. In other cases, delayed formation of the detectable product would bring into question the identity of the species responsible for probe oxidation. For example, ONOO^- decomposes within seconds. If the product formation is slower, it could indicate that ONOO^- is not the actual oxidant.

In addition to the points above, one must consider the effect of cellular milieu on the probe's reactivity. For example, in cells, the ability of boronate probes to intercept HOCl may be limited due to rapid HOCl reaction with thiols and amines, as discussed above. Conversely, strong one-electron oxidants, unreactive toward most boronate probes, may produce amino acid hydroperoxides, established oxidants of the boronate compounds. Clearly, knowledge of the chemical reactivity of boronates must be a pre-requisite of any studies of their fate and selectivity in cellular systems.

Although the rate constant of the reaction of boronate probes with different oxidants varies over several orders of magnitude, determining which oxidant is responsible for probe oxidation in a cell-based experiment may be not trivial, as all oxidants produce the same major product. Two complementary approaches have been proposed to identify the oxidants involved: (i) the use of species-specific enzymatic scavengers and inhibitors of the sources of the oxidants, and (ii) the profiling of the probe-derived products formed and identification of ONOO^- - and HOCl-specific products (Zielonka et al., 2013a; Hardy et al., 2018). To prevent H_2O_2 -mediated boronate oxidation, catalase may be used as an enzymatic scavenger, while inhibitors of the enzymatic sources of $\text{O}_2^{\bullet-}$ and H_2O_2 may block H_2O_2 formation. To prevent ONOO^- -mediated oxidation, superoxide dismutase (an enzymatic scavenger of $\text{O}_2^{\bullet-}$) and inhibitors of nitric oxide synthases or enzymatic $\text{O}_2^{\bullet-}$ sources may be used. In the case of HOCl-mediated oxidation, inhibitors of the MPO enzyme or of the enzymatic sources of $\text{O}_2^{\bullet-}$ and H_2O_2 may be used to prevent probe oxidation. It should be noted that inhibitors of $\text{O}_2^{\bullet-}$ sources are expected to inhibit the formation of all three mentioned oxidants, and thus may not be sufficient for identification purposes. However, they may help in establishing the source of the oxidant. Cell-permeable derivatives of antioxidant enzymes, or genetic manipulation of their cellular expression, may help in the modulation of intracellular oxidants. While using non-enzymatic, small-molecule scavengers would be a convenient route to identify the oxidizing species, the "inconvenient truth" is that, similar to redox probes, most small molecule chemical scavengers lack the sufficient selectivity to provide unequivocal assignment.

BORONATE-BASED REDOX PROBES IN THE STUDIES OF NADPH OXIDASES

In addition to mitochondrial electron transport chain, NADPH oxidases (or Nox enzymes) are regarded as the major source of cellular $O_2^{\bullet-}$ and H_2O_2 . While an array of probes and assays have been developed over the last 30 years, in order to monitor Nox activity, most probes suffer from serious limitations, including the potential to generate $O_2^{\bullet-}$ and H_2O_2 by the probes themselves (Zielonka et al., 2013b, 2017a; Kalyanaraman et al., 2016). Boronate redox probes have emerged as a new tool to study the activity and role of NADPH oxidases in cellular redox signaling and immune response (Dickinson et al., 2011a; Brewer et al., 2015; Zielonka et al., 2017a).

First application of boronate-based probes to study Nox-derived H_2O_2 was reported in the very first paper on the synthesis and use of monoboronated fluorogenic probes (Miller et al., 2007). Stimulation of the EGFR-mediated cellular signaling led to increased fluorescence signal from the PG1 probe, and the signal was inhibited by apocynin, used as a Nox inhibitor. As the ability of apocynin to inhibit NADPH oxidases is a subject of controversy (Heumüller et al., 2008), additional tests would be required to corroborate the involvement of Nox and determine the Nox isoform in EGFR-mediated H_2O_2 production.

The first identified Nox isoform, NADPH oxidase-2 (Nox2), is abundant in immune cells, including neutrophils and macrophages. With the use of CBA (**26**) and FlAmBE (**22**), boronate redox probes, it has been demonstrated that simultaneous activation of Nox2 and inducible nitric oxide synthase in macrophages results in production of ONOO⁻ (Zielonka et al., 2012b). These boronate probes have been used in parallel with the probes for $O_2^{\bullet-}$ and $\bullet NO$, establishing a platform for “global profiling” of ROS and reactive nitrogen species in cellular systems (Zielonka et al., 2012b, 2013a). CBA and Fl-B (**18**) probes also have been used to determine the production of ONOO⁻ by activated macrophages in the presence of erythrocytes (Prolo et al., 2015). Because erythrocytes contain a large amount of hemoglobin, they serve as a sink/scavenger of $\bullet NO$, preventing it from reacting with Nox2-derived $O_2^{\bullet-}$. Fl-B was also instrumental in demonstrating that *Trypanosoma cruzi* uses the Fe-superoxide dismutase enzyme to resist being killed by macrophages *via* removing phagosomal (Nox2-derived) $O_2^{\bullet-}$ and limiting ONOO⁻ formation (Martinez et al., 2019).

Also, CBA proved to be the probe of choice to monitor H_2O_2 produced in activated neutrophils. Activation of Nox2 by a phorbol ester (PMA) in differentiated HL60 cells led to production of H_2O_2 as a product of $O_2^{\bullet-}$ dismutation, and stimulation of CBA oxidation. This process was utilized in the design of a high-throughput screening campaign for the discovery of novel inhibitors of Nox2 (Zielonka et al., 2014, 2019). A combination of the CBA probe and hydroethidine was used for simultaneous monitoring of H_2O_2 and $O_2^{\bullet-}$, released from activated neutrophils. The assay is based on rapid HPLC analyses (90 s per injection) of the cell media, and quantitation of COH and 2-hydroxyethidium as the products of H_2O_2 and

$O_2^{\bullet-}$. With such a setup, quasi-real-time monitoring of $O_2^{\bullet-}$ and H_2O_2 was utilized to demonstrate the differences in the production of both species by different NADPH oxidase isoforms (Nox2, Nox4, and Nox5) (Zielonka et al., 2014). Following the design of the high-throughput screening workflow for Nox2 inhibitors, a medium-sized library of bioactive compounds (2029 compounds) was screened, and several candidates for Nox2 inhibitors have been identified (Zielonka et al., 2016b). With the use of the *o*-MitoPhB(OH)₂ probe (**76**) and establishment of cyclo-*o*-MitoPh as a specific marker for ONOO⁻ (**Scheme 6B**), it was shown that the compounds capable of blocking Nox2 activity decrease ONOO⁻ production in activated macrophages.

CONCLUDING REMARKS

Boronate probes represent a new class of redox probes with clear advantages over widely used probes based on reduced fluorescent dyes (e.g., DCFH, DHR). The reaction kinetics, stoichiometry, and mechanisms for many boronate probes have been established and reported, providing an opportunity for meaningful application of boronates in the area of redox biology research. Development of boronate probes for *in vivo* applications and determination of their pharmacokinetic behavior may yield novel tools for studying the role of biological oxidants in various pathological conditions, including cancer, neurodegeneration, and cardiovascular diseases.

AUTHOR CONTRIBUTIONS

All authors contributed to the review concept, design, and bibliographic research. AS, JZ, RM, RS-I, JP, and RP prepared the first version of the manuscript. AS, KD, and AA prepared the tables and AS, KD, KP, RP, and RM prepared the schemes and figures. AS, JZ, and BK critically reviewed and prepared the final version of the manuscript. All authors accepted the manuscript in its final form.

FUNDING

AS was supported by Polish National Science Center within the SONATA BIS program (Grant no. 2015/18/E/ST4/00235). JZ was supported in part by Institutional Research Grant #16-183-31 from the American Cancer Society and the Medical College of Wisconsin Cancer Center. RP was supported by a grant from the Polish National Science Center SONATA BIS program (Grant no. 2016/22/E/ST4/00549). RM was supported by a grant from the Polish National Science Center SONATA program (Grant no. 2018/31/D/ST4/03494).

SUPPLEMENTARY MATERIAL

The Supplementary Material for this article can be found online at: <https://www.frontiersin.org/articles/10.3389/fchem.2020.580899/full#supplementary-material>

REFERENCES

- Ainley, A. D., and Challenger, F. (1930). CCLXXX.—Studies of the boron-carbon linkage. Part I. The oxidation and nitration of phenylboric acid. *J. Chem. Soc.* 1, 2171–2180. doi: 10.1039/JR9300002171
- Akhavan-Tafti, H., Eickholt, R. A., Lauwers, K. S., and Handley, R. S. (2005). *Signalling Compounds for Use in Methods of Detecting Hydrogen Peroxide*. U.S. Patent No 6,919,463. Available online at: <https://patents.google.com/patent/US7704752B2/en>
- Albers, A. E., Dickinson, B. C., Miller, E. W., and Chang, C. J. (2008). A red-emitting naphthofluorescein-based fluorescent probe for selective detection of hydrogen peroxide in living cells. *Bioorg. Med. Chem. Lett.* 18, 5948–5950. doi: 10.1016/j.bmcl.2008.08.035
- Albers, A. E., Okreglak, V. S., and Chang, C. J. (2006). A FRET-based approach to ratiometric fluorescence detection of hydrogen peroxide. *J. Am. Chem. Soc.* 128, 9640–9641. doi: 10.1021/ja063308k
- Arnhold, J., Monzani, E., Furtmuller, P. G., Zederbauer, M., Casella, L., and Obinger, C. (2006). Kinetics and thermodynamics of halide and nitrite oxidation by mammalian heme peroxidases. *Eur. J. Inorg. Chem.* 19, 3801–3811. doi: 10.1002/ejic.200600436
- Augusto, O., Bonini, M. G., Amanso, A. M., Linares, E., Santos, C. C., and De Menezes, S. L. (2002). Nitrogen dioxide and carbonate radical anion: two emerging radicals in biology. *Free Radic. Biol. Med.* 32, 841–859. doi: 10.1016/S0891-5849(02)00786-4
- Augusto, O., Goldstein, S., Hurst, J. K., Lind, J., Lyman, S. V., Merenyi, G., et al. (2019). Carbon dioxide-catalyzed peroxynitrite reactivity - the resilience of the radical mechanism after two decades of research. *Free Radic. Biol. Med.* 135, 210–215. doi: 10.1016/j.freeradbiomed.2019.02.026
- Barrett, T. J., and Hawkins, C. L. (2012). Hypothiocyanous acid: benign or deadly? *Chem. Res. Toxicol.* 25, 263–273. doi: 10.1021/tx200219s
- Biswas, S., Das, J., Barman, S., Rao Pinninti, B., Maiti, T. K., and Singh, N. D. P. (2017). Environment activatable nanoprodug: two-step surveillance in the anticancer drug release. *ACS Appl. Mater. Interfaces* 9, 28180–28184. doi: 10.1021/acsami.7b05132
- Bonini, M. G., Rota, C., Tomasi, A., and Mason, R. P. (2006). The oxidation of 2',7'-dichlorofluorescein to reactive oxygen species: a self-fulfilling prophesy? *Free Radic. Biol. Med.* 40, 968–975. doi: 10.1016/j.freeradbiomed.2005.10.042
- Bou, R., Codony, R., Tres, A., Decker, E. A., and Guardicila, F. (2008). Determination of hydroperoxides in foods and biological samples by the ferrous oxidation-xylenol orange method: a review of the factors that influence the method's performance. *Anal. Biochem.* 377, 1–15. doi: 10.1016/j.ab.2008.02.029
- Branchaud, B. P., and Walsh, C. T. (1985). Functional group diversity in enzymic oxygenation reactions catalyzed by bacterial flavin-containing cyclohexanone oxygenase. *J. Am. Chem. Soc.* 107, 2153–2161. doi: 10.1021/ja00293a054
- Brewer, T. F., Garcia, F. J., Onak, C. S., Carroll, K. S., and Chang, C. J. (2015). Chemical approaches to discovery and study of sources and targets of hydrogen peroxide redox signaling through NADPH oxidase proteins. *Annu. Rev. Biochem.* 84, 765–790. doi: 10.1146/annurev-biochem-060614-034018
- Calabria, D., Guardigli, M., Mirasoli, M., Punzo, A., Porru, E., Zangheri, M., et al. (2020). Selective chemiluminescent TURN-ON quantitative bioassay and imaging of intracellular hydrogen peroxide in human living cells. *Anal. Biochem.* 600:113760. doi: 10.1016/j.ab.2020.113760
- Carroll, V., Michel, B. W., Blecha, J., Vanbrocklin, H., Keshari, K., Wilson, D., et al. (2014). A boronate-caged [(1)(8)F]FLT probe for hydrogen peroxide detection using positron emission tomography. *J. Am. Chem. Soc.* 136, 14742–14745. doi: 10.1021/ja509198w
- Chance, B., Sies, H., and Boveris, A. (1979). Hydroperoxide metabolism in mammalian organs. *Physiol. Rev.* 59, 527–605. doi: 10.1152/physrev.1979.59.3.527
- Chang, M. C., Pralle, A., Isacoff, E. Y., and Chang, C. J. (2004). A selective, cell-permeable optical probe for hydrogen peroxide in living cells. *J. Am. Chem. Soc.* 126, 15392–15393. doi: 10.1021/ja0441716
- Chen, P., Zheng, Z., Zhu, Y., Dong, Y., Wang, F., and Liang, G. (2017). Bioluminescent turn-on probe for sensing hypochlorite *in vitro* and in tumors. *Anal. Chem.* 89, 5693–5696. doi: 10.1021/acs.analchem.7b01103
- Cheng, G., Pan, J., Podsiadly, R., Zielonka, J., Garces, A. M., Dias Duarte Machado, L. G., et al. (2020). Increased formation of reactive oxygen species during tumor growth: *ex vivo* low-temperature EPR and *in vivo* bioluminescence analyses. *Free Radic. Biol. Med.* 147, 167–174. doi: 10.1016/j.freeradbiomed.2019.12.020
- Cheng, G., Zielonka, M., Dranka, B., Kumar, S. N., Myers, C. R., Bennett, B., et al. (2018). Detection of mitochondria-generated reactive oxygen species in cells using multiple probes and methods: potentials, pitfalls, and the future. *J. Biol. Chem.* 293, 10363–10380. doi: 10.1074/jbc.RA118.003044
- Choudhury, R., Ricketts, A. T., Molina, D. G., and Paudel, P. (2019). A boronic acid based intramolecular charge transfer probe for colorimetric detection of hydrogen peroxide. *Tetrahedron Lett.* 60:151258. doi: 10.1016/j.tetlet.2019.151258
- Chung, C., Srikun, D., Lim, C. S., Chang, C. J., and Cho, B. R. (2011). A two-photon fluorescent probe for ratiometric imaging of hydrogen peroxide in live tissue. *Chem. Commun.* 47, 9618–9620. doi: 10.1039/c1cc13583j
- Chung, T. H., Wu, Y. P., Chew, C. Y., Lam, C. H., and Tan, K. T. (2018). Imaging and quantification of secreted peroxynitrite at the cell surface by a streptavidin-biotin-controlled binding probe. *ChemBiochem* 19, 2584–2590. doi: 10.1002/cbic.201800542
- Cochemé, H. M., Logan, A., Prime, T. A., Abakumova, I., Quin, C., Mcquaker, S. J., et al. (2012). Using the mitochondria-targeted ratiometric mass spectrometry probe MitoB to measure H₂O₂ in living *Drosophila*. *Nat. Protoc.* 7, 946–958. doi: 10.1038/nprot.2012.035
- Cochemé, H. M., Quin, C., Mcquaker, S. J., Cabreiro, F., Logan, A., Prime, T. A., et al. (2011). Measurement of H₂O₂ within living *Drosophila* during aging using a ratiometric mass spectrometry probe targeted to the mitochondrial matrix. *Cell Metab.* 13, 340–350. doi: 10.1016/j.cmet.2011.02.003
- Cox, A. G., Peskin, A. V., Paton, L. N., Winterbourn, C. C., and Hampton, M. B. (2009). Redox potential and peroxide reactivity of human peroxiredoxin 3. *Biochemistry* 48, 6495–6501. doi: 10.1021/bi900558g
- Dai, F., Jin, F., Long, Y., Jin, X. L., and Zhou, B. (2018). A 1,8-naphthalimide-based turn-on fluorescent probe for imaging mitochondrial hydrogen peroxide in living cells. *Free Radic. Res.* 52, 1288–1295. doi: 10.1080/10715762.2018.1446530
- Daniel, K. B., Agrawal, A., Manchester, M., and Cohen, S. M. (2013). Readily accessible fluorescent probes for sensitive biological imaging of hydrogen peroxide. *ChemBiochem* 14, 593–598. doi: 10.1002/cbic.201200724
- Das, B. C., Mahalingam, S. M., and Evans, T. (2009). Design and synthesis of novel pinacolylboronate containing combretastatin 'antimitotic agent' analogues. *Tetrahedron Lett.* 50, 3031–3034. doi: 10.1016/j.tetlet.2009.04.003
- Davies, M. J. (2016). Protein oxidation and peroxidation. *Biochem. J.* 473, 805–825. doi: 10.1042/BJ20151227
- Davies, M. J., Hawkins, C. L., Pattison, D. I., and Rees, M. D. (2008). Mammalian heme peroxidases: from molecular mechanisms to health implications. *Antioxid. Redox Signal* 10, 1199–1234. doi: 10.1089/ars.2007.1927
- De Armas, M. I., Esteves, R., Viera, N., Reyes, A. M., Mastrogianni, M., Alegria, T. G. P., et al. (2019). Rapid peroxynitrite reduction by human peroxiredoxin 3: implications for the fate of oxidants in mitochondria. *Free Radic. Biol. Med.* 130, 369–378. doi: 10.1016/j.freeradbiomed.2018.10.451
- Debowska, K., Debski, D., Michalowski, B., Dybala-Defratyka, A., Wojcik, T., Michalski, R., et al. (2016). Characterization of fluorescein-based monoboronate probe and its application to the detection of peroxynitrite in endothelial cells treated with doxorubicin. *Chem. Res. Toxicol.* 29, 735–746. doi: 10.1021/acs.chemrestox.5b00431
- Demicheli, V., Moreno, D. M., Jara, G. E., Lima, A., Carballal, S., Rios, N., et al. (2016). Mechanism of the reaction of human manganese superoxide dismutase with peroxynitrite: nitration of critical tyrosine 34. *Biochemistry* 55, 3403–3417. doi: 10.1021/acs.biochem.6b00045
- Diao, Q., Guo, H., Yang, Z., Luo, W., Li, T., and Hou, D. (2019). Design of a Nile red-based NIR fluorescent probe for the detection of hydrogen peroxide in living cells. *Spectrochim. Acta A Mol. Biomol. Spectrosc.* 223:117284. doi: 10.1016/j.saa.2019.117284
- Dickinson, B. C., and Chang, C. J. (2008). A targetable fluorescent probe for imaging hydrogen peroxide in the mitochondria of living cells. *J. Am. Chem. Soc.* 130, 9638–9639. doi: 10.1021/ja802355u

- Dickinson, B. C., Huynh, C., and Chang, C. J. (2010). A palette of fluorescent probes with varying emission colors for imaging hydrogen peroxide signaling in living cells. *J. Am. Chem. Soc.* 132, 5906–5915. doi: 10.1021/ja1014103
- Dickinson, B. C., Lin, V. S., and Chang, C. J. (2013). Preparation and use of MitoPY1 for imaging hydrogen peroxide in mitochondria of live cells. *Nat. Protoc.* 8, 1249–1259. doi: 10.1038/nprot.2013.064
- Dickinson, B. C., Peltier, J., Stone, D., Schaffer, D. V., and Chang, C. J. (2011a). Nox2 redox signaling maintains essential cell populations in the brain. *Nat. Chem. Biol.* 7, 106–112. doi: 10.1038/nchembio.497
- Dickinson, B. C., Tang, Y., Chang, Z., and Chang, C. J. (2011b). A nuclear-localized fluorescent hydrogen peroxide probe for monitoring sirtuin-mediated oxidative stress responses *in vivo*. *Chem. Biol.* 18, 943–948. doi: 10.1016/j.chembiol.2011.07.005
- Donald, C. E., Hughes, M. N., Thompson, J. M., and Bonner, F. T. (1986). Photolysis of the nitrogen-nitrogen double bond in trioxodinitrate: reaction between triplet oxonitrate(1-) and molecular oxygen to form peroxonitrite. *Inorg. Chem.* 25, 2676–2677. doi: 10.1021/ic00236a004
- Du, L., Li, M., Zheng, S., and Wang, B. (2008). Rational design of a fluorescent hydrogen peroxide probe based on the umbelliferone fluorophore. *Tetrahedron Lett.* 49, 3045–3048. doi: 10.1016/j.tetlet.2008.03.063
- Ferrer-Sueta, G., Campolo, N., Trujillo, M., Bartesaghi, S., Carballal, S., Romero, N., et al. (2018). Biochemistry of peroxynitrite and protein tyrosine nitration. *Chem. Rev.* 118, 1338–1408. doi: 10.1021/acs.chemrev.7b00568
- Ferrer-Sueta, G., and Radi, R. (2009). Chemical biology of peroxynitrite: kinetics, diffusion, and radicals. *ACS Chem. Biol.* 4, 161–177. doi: 10.1021/cb800279q
- Folkes, L. K., Patel, K. B., Wardman, P., and Wrona, M. (2009). Kinetics of reaction of nitrogen dioxide with dihydrohodamine and the reaction of the dihydrohodamine radical with oxygen: implications for quantifying peroxynitrite formation in cells. *Arch. Biochem. Biophys.* 484, 122–126. doi: 10.1016/j.abb.2008.10.014
- Forman, H. J., Ursini, F., and Maiorino, M. (2014). An overview of mechanisms of redox signaling. *J. Mol. Cell. Cardiol.* 73, 2–9. doi: 10.1016/j.yjmcc.2014.01.018
- Fu, Y., Yao, J., Xu, W., Fan, T., Jiao, Z., He, Q., et al. (2016). Schiff base substituent-triggered efficient deboration reaction and its application in highly sensitive hydrogen peroxide vapor detection. *Anal. Chem.* 88, 5507–5512. doi: 10.1021/acs.analchem.6b01057
- Gallego-Villar, L., Rivera-Barahona, A., Cuevas-Martín, C., Guenzel, A., Pérez, B., Barry, M. A., et al. (2016). *In vivo* evidence of mitochondrial dysfunction and altered redox homeostasis in a genetic mouse model of propionic acidemia: implications for the pathophysiology of this disorder. *Free Radic. Biol. Med.* 96, 1–12. doi: 10.1016/j.freeradbiomed.2016.04.007
- Gao, P., Pan, W., Li, N., and Tang, B. (2019). Fluorescent probes for organelle-targeted bioactive species imaging. *Chem. Sci.* 10, 6035–6071. doi: 10.1039/C9SC01652J
- Gnaim, S., and Shabat, D. (2019). Activity-based optical sensing enabled by self-immolative scaffolds: monitoring of release events by fluorescence or chemiluminescence output. *Accounts Chem. Res.* 52, 2806–2817. doi: 10.1021/acs.accounts.9b00338
- Goldstein, S., and Czapski, G. (1995). The reaction of NO with O₂⁻ and HO₂: a pulse radiolysis study. *Free Radic. Biol. Med.* 19, 505–510. doi: 10.1016/0891-5849(95)00034-U
- Green, O., Eilon, T., Hananya, N., Gutkin, S., Bauer, C. R., and Shabat, D. (2017a). Opening a gateway for chemiluminescence cell imaging: distinctive methodology for design of bright chemiluminescent dioxetane probes. *ACS Cent. Sci.* 3, 349–358. doi: 10.1021/acscentsci.7b00058
- Green, O., Gnaim, S., Blau, R., Eldar-Boock, A., Satchi-Fainaro, R., and Shabat, D. (2017b). Near-infrared dioxetane luminophores with direct chemiluminescence emission mode. *J. Am. Chem. Soc.* 139, 13243–13248. doi: 10.1021/jacs.7b08446
- Guo, Y., Lu, G., Zhuo, J., Wang, J., Li, X., and Zhang, Z. (2018). A visible-near-infrared fluorescent probe for peroxynitrite with large pseudo-Stokes and emission shift via through-bond energy and charge transfers controlled by energy matching. *J. Mater. Chem. B* 6, 2489–2496. doi: 10.1039/C8TB00452H
- Han, J., Chu, C., Cao, G., Mao, W., Wang, S., Zhao, Z., et al. (2018). A simple boronic acid-based fluorescent probe for selective detection of hydrogen peroxide in solutions and living cells. *Bioorg. Chem.* 81, 362–366. doi: 10.1016/j.bioorg.2018.08.036
- Hardy, M., Zielonka, J., Karoui, H., Sikora, A., Michalski, R., Podsiadly, R., et al. (2018). Detection and characterization of reactive oxygen and nitrogen species in biological systems by monitoring species-specific products. *Antioxid. Redox Signal* 28, 1416–1432. doi: 10.1089/ars.2017.7398
- Hariri, A., Zhao, E., Jeevarathinam, A. S., Lemaster, J., Zhang, J., and Jokerst, J. V. (2019). Molecular imaging of oxidative stress using an LED-based photoacoustic imaging system. *Sci. Rep.* 9:11378. doi: 10.1038/s41598-019-47599-2
- Hawkins, C. L. (2009). The role of hypothiocyanous acid (HOSCN) in biological systems. *Free Radic. Res.* 43, 1147–1158. doi: 10.3109/10715760903214462
- He, C., Danes, J. M., Hart, P. C., Zhu, Y., Huang, Y., De Abreu, A. L., et al. (2019). SOD₂ acetylation on lysine 68 promotes stem cell reprogramming in breast cancer. *Proc. Natl. Acad. Sci. U.S.A.* 116, 23534–23541. doi: 10.1073/pnas.1902308116
- He, L., Liu, X., Zhang, Y., Yang, L., Fang, Q., Geng, Y., et al. (2018). A mitochondria-targeting ratiometric fluorescent probe for imaging hydrogen peroxide with long-wavelength emission and large Stokes shift. *Sens. Actuators B Chem.* 276, 247–253. doi: 10.1016/j.snb.2018.08.119
- Heumüller, S., Wind, S., Barbosa-Sicard, E., Schmidt, H. H., Busse, R., Schröder, K., et al. (2008). Apocynin is not an inhibitor of vascular NADPH oxidases but an antioxidant. *Hypertension* 51, 211–217. doi: 10.1161/HYPERTENSIONAHA.107.100214
- Hogg, N., Zielonka, J., and Kalyanaram, B. (2017). “Chapter 3 - detection of nitric oxide and peroxynitrite in biological systems: a state-of-the-art review,” in *Nitric Oxide (Third Edition)*, eds L. J. Ignarro and B. A. Freeman (London: Academic Press), 23–44. doi: 10.1016/B978-0-12-804273-1.00003-X
- Hu, J.-S., Shao, C., Wang, X., Di, X., Xue, X., Su, Z., et al. (2019). Imaging dynamic peroxynitrite fluxes in epileptic brains with a near-infrared fluorescent probe. *Adv. Sci.* 6:1900341. doi: 10.1002/advsc.201900341
- Huang, Y. Y., Rajda, P. J., Szweczyk, G., Bhayana, B., Chiang, L. Y., Sarna, T., et al. (2019). Sodium nitrite potentiates antimicrobial photodynamic inactivation: possible involvement of peroxynitrate. *Photochem. Photobiol. Sci.* 18, 505–515. doi: 10.1039/C8PP00452H
- Huie, R. E., and Padmaja, S. (1993). The reaction of NO with superoxide. *Free Radic. Res. Com.* 18, 195–199. doi: 10.3109/10715769309145868
- Jessup, W., Dean, R. T., and Gebicki, J. M. (1994). Iodometric determination of hydroperoxides in lipids and proteins. *Oxygen Radic. Biol. Syst. Pt C* 233, 289–303. doi: 10.1016/S0076-6879(94)33032-8
- Kalyanaram, B., Hardy, M., Podsiadly, R., Cheng, G., and Zielonka, J. (2017). Recent developments in detection of superoxide radical anion and hydrogen peroxide: Opportunities, challenges, and implications in redox signaling. *Arch. Biochem. Biophys.* 617, 38–47. doi: 10.1016/j.abb.2016.08.021
- Kalyanaram, B., Hardy, M., and Zielonka, J. (2016). A critical review of methodologies to detect reactive oxygen and nitrogen species stimulated by naph oxidase enzymes: implications in pesticide toxicity. *Curr. Pharmacol. Rep.* 2, 193–201. doi: 10.1007/s40495-016-0063-0
- Karton-Lifshin, N., Albertazzi, L., Bendikov, M., Baran, P. S., and Shabat, D. (2012). “Donor-two-acceptor” dye design: a distinct gateway to NIR fluorescence. *J. Am. Chem. Soc.* 134, 20412–20420. doi: 10.1021/ja308124q
- Kemp, D. S., and Roberts, D. C. (1975). New protective groups for peptide synthesis—II the Dobz group boron-derived affinity protection with the p-dihydroxyborylbenzyloxycarbonylamino function. *Tetrahedron Lett.* 16, 4629–4632. doi: 10.1016/S0040-4039(00)91037-2
- Kim, D., Kim, G., Nam, S. J., Yin, J., and Yoon, J. (2015). Visualization of endogenous and exogenous hydrogen peroxide using a lysosome-targetable fluorescent probe. *Sci. Rep.* 5:8488. doi: 10.1038/srep08488
- Kim, E. J., Bhuniya, S., Lee, H., Kim, H. M., Cheong, C., Maiti, S., et al. (2014). An activatable prodrug for the treatment of metastatic tumors. *J. Am. Chem. Soc.* 136, 13888–13894. doi: 10.1021/ja5077684
- Kim, H. M., and Cho, B. R. (2013). Mitochondrial-targeted two-photon fluorescent probes for zinc ions, H₂O₂, and thiols in living tissues. *Oxid. Med. Cell. Longev.* 2013:323619. doi: 10.1155/2013/323619

- Kim, J., Park, J., Lee, H., Choi, Y., and Kim, Y. (2014). A boronate-based fluorescent probe for the selective detection of cellular peroxynitrite. *Chem. Commun.* 50, 9353–9356. doi: 10.1039/C4CC02943G
- Kirsch, M., and De Groot, H. (2002). Formation of peroxynitrite from reaction of nitroxyl anion with molecular oxygen. *J. Biol. Chem.* 277, 13379–13388. doi: 10.1074/jbc.M108079200
- Kissner, R., Nauser, T., Bugnon, P., Lye, P. G., and Koppenol, W. H. (1997). Formation and properties of peroxynitrite as studied by laser flash photolysis, high-pressure stopped-flow technique, and pulse radiolysis. *Chem. Res. Toxicol.* 10, 1285–1292. doi: 10.1021/tx970160x
- Kobayashi, K., Miki, M., and Tagawa, S. (1995). Pulse-radiolysis study of the reaction of nitric oxide with superoxide. *J. Chem. Soc. Dalton Trans.* 17, 2885–2889. doi: 10.1039/dt9950002885
- Kojima, R., Takakura, H., Kamiya, M., Kobayashi, E., Komatsu, T., Ueno, T., et al. (2015). Development of a sensitive bioluminogenic probe for imaging highly reactive oxygen species in living rats. *Angew. Chem. Int. Ed. Engl.* 54, 14768–14771. doi: 10.1002/anie.201507530
- Koppenol, W. H., Moreno, J. J., Pryor, W. A., Ischiropoulos, H., and Beckman, J. S. (1992). Peroxynitrite, a cloaked oxidant formed by nitric oxide and superoxide. *Chem. Res. Toxicol.* 5, 834–842. doi: 10.1021/tx00030a017
- Kuivila, H. G. (1954). Electrophilic displacement reactions. III. Kinetics of the reaction between hydrogen peroxide and benzenboronic acid. *J. Am. Chem. Soc.* 76, 870–874. doi: 10.1021/ja01632a070
- Kuivila, H. G., Benjamin, L. E., Murphy, C. J., Price, A. D., and Polevy, J. H. (1962). Electrophilic displacement reactions. XIV. Two novel reactions involving areneboronic acids and halogens. *J. Org. Chem.* 27, 825–829. doi: 10.1021/jo01050a032
- Kumar, A., Chen, S. H., Kadiiska, M. B., Hong, J. S., Zielonka, J., Kalyanaram, B., et al. (2014). Inducible nitric oxide synthase is key to peroxynitrite-mediated, LPS-induced protein radical formation in murine microglial BV2 cells. *Free Radic. Biol. Med.* 73, 51–59. doi: 10.1016/j.freeradbiomed.2014.04.014
- LaButti, J. N., and Gates, K. S. (2009). Biologically relevant chemical properties of peroxymonophosphate (=O₃POOH). *Bioorg. Med. Chem. Lett.* 19, 218–221. doi: 10.1016/j.bmcl.2008.10.133
- Lampard, E. V., Sedgwick, A. C., Sun, X., Filer, K. L., Hewins, S. C., Kim, G., et al. (2018). Boronate-based fluorescence probes for the detection of hydrogen peroxide. *ChemistryOpen* 7, 262–265. doi: 10.1002/open.201700189
- Lee, J., Yoon, S. A., Chun, J., Kang, C., and Lee, M. H. (2019). A red-emitting styrylnaphthalimide-based fluorescent probe providing a ratiometric signal change for the precise and quantitative detection of H₂O₂. *Anal. Chim. Acta* 1080, 153–161. doi: 10.1016/j.aca.2019.07.008
- Li, G., Ji, D., Zhang, S., Li, J., Li, C., and Qiao, R. (2017). A mitochondria-targeting fluorescence turn-on probe for hypochlorite and its applications for *in vivo* imaging. *Sens. Actuators B Chem.* 252, 127–133. doi: 10.1016/j.snb.2017.05.138
- Li, K.-B., Dong, L., Zhang, S., Shi, W., Jia, W.-P., and Han, D.-M. (2017). Fluorogenic boronate-based probe-lactulose complex for full-aqueous analysis of peroxynitrite. *Talanta* 165, 593–597. doi: 10.1016/j.talanta.2017.01.028
- Li, Q., and Yang, Z. (2018). A boronate-based ratiometric fluorescent probe for fast selective detection of peroxynitrite. *Tetrahedron Lett.* 59, 125–129. doi: 10.1016/j.tetlet.2017.12.004
- Li, Z., Huang, S., He, Y., Duan, Q., Zheng, G., Jiang, Y., et al. (2020). AND logic gate based fluorescence probe for simultaneous detection of peroxynitrite and hypochlorous acid. *Spectrochim. Acta A Mol. Biomol. Spectrosc.* 230:118073. doi: 10.1016/j.saa.2020.118073
- Li, Z., Yu, C., Chen, Y., Liu, C., Jia, P., Zhu, H., et al. (2019). A novel ratiometric fluorescent probe for highly sensitive and selective detection of peroxynitrite and its application for tracing endogenous peroxynitrite in live cells. *Anal. Methods* 11, 5699–5703. doi: 10.1039/C9AY02069A
- Liang, X., Zhang, L., Xu, X., Qiao, D., Shen, T., Yin, Z., et al. (2019). An ICT-based mitochondria-targeted fluorescent probe for hydrogen peroxide with a large turn-on fluorescence signal. *ChemistrySelect* 4, 1330–1336. doi: 10.1002/slct.201803185
- Lim, C. S., Cho, M. K., Park, M. Y., and Kim, H. M. (2018). A two-photon ratiometric fluorescent probe for imaging of hydrogen peroxide levels in rat organ tissues. *ChemistryOpen* 7, 53–56. doi: 10.1002/open.201700155
- Liochev, S. I., and Fridovich, I. (2003). The mode of decomposition of Angeli's salt (Na₂N₂O₃) and the effects thereon of oxygen, nitrite, superoxide dismutase, and glutathione. *Free Radic. Biol. Med.* 34, 1399–1404. doi: 10.1016/S0891-5849(03)00111-4
- Lippert, A. R., Gschneidner, T., and Chang, C. J. (2010). Lanthanide-based luminescent probes for selective time-gated detection of hydrogen peroxide in water and in living cells. *Chem. Commun.* 46, 7510–7512. doi: 10.1039/c0cc01560a
- Lippert, A. R., Van De Bittner, G. C., and Chang, C. J. (2011). Boronate oxidation as a bioorthogonal reaction approach for studying the chemistry of hydrogen peroxide in living systems. *Acc. Chem. Res.* 44, 793–804. doi: 10.1021/ar200126t
- Liu, C., Shen, Y., Yin, P., Li, L., Liu, M., Zhang, Y., et al. (2014). Sensitive detection of acetylcholine based on a novel boronate intramolecular charge transfer fluorescence probe. *Anal. Biochem.* 465, 172–178. doi: 10.1016/j.ab.2014.08.003
- Liu, G. J., Long, Z., Lv, H. J., Li, C. Y., and Xing, G. W. (2016). A dialdehyde-diboronate-functionalized AIE luminogen: design, synthesis and application in the detection of hydrogen peroxide. *Chem. Commun.* 52, 10233–10236. doi: 10.1039/C6CC05116B
- Liu, J., Zhou, S., Ren, J., Wu, C., and Zhao, Y. (2017). A lysosome-locating and acidic pH-activatable fluorescent probe for visualizing endogenous H₂O₂ in lysosomes. *Analyst* 142, 4522–4528. doi: 10.1039/C7AN01280B
- Liu, Y., Zhu, J., Xu, Y., Qin, Y., and Jiang, D. (2015). Boronic acid functionalized aza-bodipy (azaBDPBA) based fluorescence optodes for the analysis of glucose in whole blood. *ACS Appl. Mater. Interfaces* 7, 11141–11145. doi: 10.1021/acsami.5b00265
- Lo, L. C., and Chu, C. Y. (2003). Development of highly selective and sensitive probes for hydrogen peroxide. *Chem. Commun.* 9, 2728–2729. doi: 10.1039/b309393j
- Logan, A., Shabalina, I. G., Prime, T. A., Rogatti, S., Kalinovich, A. V., Hartley, R. C., et al. (2014). *In vivo* levels of mitochondrial hydrogen peroxide increase with age in mtDNA mutator mice. *Aging Cell* 13, 765–768. doi: 10.1111/acel.12212
- Lu, C. P., Lin, C. T., Chang, C. M., Wu, S. H., and Lo, L. C. (2011). Nitrophenylboronic acids as highly chemoselective probes to detect hydrogen peroxide in foods and agricultural products. *J. Agric. Food Chem.* 59, 11403–11406. doi: 10.1021/jf202874r
- Lymar, S. V., and Hurst, J. K. (1995). Rapid reaction between peroxynitrite ion and carbon dioxide: implications for biological activity. *J. Am. Chem. Soc.* 117, 8867–8868. doi: 10.1021/ja00139a027
- Maeda, H., Matsu-Ura, S., Senba, T., Yamasaki, S., Takai, H., Yamauchi, Y., et al. (2000). Resorufin as an electron acceptor in glucose oxidase-catalyzed oxidation of glucose. *Chem. Pharm. Bull.* 48, 897–902. doi: 10.1248/cpb.48.897
- Maghzal, G. J., Cergol, K. M., Shengule, S. R., Suarna, C., Newington, D., Kettle, A. J., et al. (2014). Assessment of myeloperoxidase activity by the conversion of hydroethidine to 2-chloroethidium. *J. Biol. Chem.* 289, 5580–5595. doi: 10.1074/jbc.M113.539486
- Martinez, A., Prolo, C., Estrada, D., Rios, N., Alvarez, M. N., Pineyro, M. D., et al. (2019). Cytosolic Fe-superoxide dismutase safeguards *Trypanosoma cruzi* from macrophage-derived superoxide radical. *Proc. Natl. Acad. Sci. U.S.A.* 116, 8879–8888. doi: 10.1073/pnas.1821487116
- Masanta, G., Heo, C. H., Lim, C. S., Bae, S. K., Cho, B. R., and Kim, H. M. (2012). A mitochondria-localized two-photon fluorescent probe for ratiometric imaging of hydrogen peroxide in live tissue. *Chem. Commun.* 48, 3518–3520. doi: 10.1039/c2cc00034b
- McCord, J. M., and Fridovich, I. (1969). Superoxide dismutase. An enzymic function for erythrocyte (hemocuprein). *J. Biol. Chem.* 244, 6049–6055.
- McQuaker, S. J., Quinlan, C. L., Caldwell, S. T., Brand, M. D., and Hartley, R. C. (2013). A prototypical small-molecule modulator uncouples mitochondria in response to endogenous hydrogen peroxide production. *Chembiochem* 14, 993–1000. doi: 10.1002/cbic.201300115
- Merenyi, G., Lind, J., and Engman, L. (1994). One-electron and 2-electron reduction potentials of peroxy radicals and related species. *J. Chem. Soc. Perkin Trans. 2*, 2551–2553. doi: 10.1039/P29940002551
- Michalski, R., Zielonka, J., Gapys, E., Marcinek, A., Joseph, J., and Kalyanaram, B. (2014). Real-time measurements of amino acid and protein hydroperoxides using coumarin boronic acid. *J. Biol. Chem.* 289, 22536–22553. doi: 10.1074/jbc.M114.553727
- Miller, E. W., Albers, A. E., Pralle, A., Isacoff, E. Y., and Chang, C. J. (2005). Boronate-based fluorescent probes for imaging cellular hydrogen peroxide. *J. Am. Chem. Soc.* 127, 16652–16659. doi: 10.1021/ja054474f

- Miller, E. W., Dickinson, B. C., and Chang, C. J. (2010). Aquaporin-3 mediates hydrogen peroxide uptake to regulate downstream intracellular signaling. *Proc. Natl. Acad. Sci. U.S.A.* 107, 15681–15686. doi: 10.1073/pnas.1005776107
- Miller, E. W., Tulyathan, O., Isacoff, E. Y., and Chang, C. J. (2007). Molecular imaging of hydrogen peroxide produced for cell signaling. *Nat. Chem. Biol.* 3, 263–267. doi: 10.1038/nchembio871
- Miranda, K. M., Espey, M. G., Yamada, K., Krishna, M., Ludwick, N., Kim, S., et al. (2001). Unique oxidative mechanisms for the reactive nitrogen oxide species, nitroxyl anion. *J. Biol. Chem.* 276, 1720–1727. doi: 10.1074/jbc.M006174200
- Miranda, K. M., Paolucci, N., Katori, T., Thomas, D. D., Ford, E., Bartberger, M. D., et al. (2003). A biochemical rationale for the discrete behavior of nitroxyl and nitric oxide in the cardiovascular system. *Proc. Natl. Acad. Sci. U.S.A.* 100, 9196–9201. doi: 10.1073/pnas.1430507100
- Miranda, K. M., Yamada, K., Espey, M. G., Thomas, D. D., Degraff, W., Mitchell, J. B., et al. (2002). Further evidence for distinct reactive intermediates from nitroxyl and peroxynitrite: effects of buffer composition on the chemistry of Angeli's salt and synthetic peroxynitrite. *Arch. Biochem. Biophys.* 401, 134–144. doi: 10.1016/S0003-9861(02)00031-0
- Mohapatra, H., and Phillips, S. T. (2012). Using smell to triage samples in point-of-care assays. *Angew. Chem. Int. Ed. Engl.* 51, 11145–11148. doi: 10.1002/anie.201207008
- Morris, J. C. (1966). The acid ionization constant of HOCl from 5 to 35°. *J. Phys. Chem. A* 70, 3798–3805. doi: 10.1021/j100884a007
- Murfin, L. C., Weber, M., Park, S. J., Kim, W. T., Lopez-Alled, C. M., McMullin, C. L., et al. (2019). Azulene-derived fluorescent probe for bioimaging: detection of reactive oxygen and nitrogen species by two-photon microscopy. *J. Am. Chem. Soc.* 141, 19389–19396. doi: 10.1021/jacs.9b09813
- Narayanaswamy, N., Narra, S., Nair, R. R., Saini, D. K., Kondaiah, P., and Govindaraju, T. (2016). Stimuli-responsive colorimetric and NIR fluorescence combination probe for selective reporting of cellular hydrogen peroxide. *Chem. Sci.* 7, 2832–2841. doi: 10.1039/C5SC03488D
- Niki, E. (2014). Biomarkers of lipid peroxidation in clinical material. *BBA-Gen. Subjects* 1840, 809–817. doi: 10.1016/j.bbagen.2013.03.020
- Odyniec, M. L., Han, H. H., Gardiner, J. E., Sedgwick, A. C., He, X. P., Bull, S. D., et al. (2019). Peroxynitrite-activated drug conjugate systems based on a coumarin scaffold toward the application of theranostics. *Front. Chem.* 7:775. doi: 10.3389/fchem.2019.00775
- Odyniec, M. L., Sedgwick, A. C., Swan, A. H., Weber, M., Tang, T. M. S., Gardiner, J. E., et al. (2018). AND⁺-based fluorescence scaffold for the detection of ROS/RNS and a second analyte. *Chem. Commun.* 54, 8466–8469. doi: 10.1039/C8CC04316G
- Palanisamy, S., Wu, P. Y., Wu, S. C., Chen, Y. J., Tzou, S. C., Wang, C. H., et al. (2017). *In vitro* and *in vivo* imaging of peroxynitrite by a ratiometric boronate-based fluorescent probe. *Biosens. Bioelectron.* 91, 849–856. doi: 10.1016/j.bios.2017.01.027
- Peskin, A. V., Cox, A. G., Nagy, P., Morgan, P. E., Hampton, M. B., Davies, M. J., et al. (2010). Removal of amino acid, peptide and protein hydroperoxides by reaction with peroxiredoxins 2 and 3. *Biochem. J.* 432, 313–321. doi: 10.1042/BJ20101156
- Prolo, C., Alvarez, M. N., Rios, N., Peluffo, G., Radi, R., and Romero, N. (2015). Nitric oxide diffusion to red blood cells limits extracellular, but not intraphagosomal, peroxynitrite formation by macrophages. *Free Radic. Biol. Med.* 87, 346–355. doi: 10.1016/j.freeradbiomed.2015.06.027
- Pryor, W. A., and Squadrito, G. L. (1995). The chemistry of peroxynitrite: a product from the reaction of nitric oxide with superoxide. *Am. J. Physiol.* 268, 699–722. doi: 10.1152/ajplung.1995.268.5.L699
- Purdey, M. S., Connaughton, H. S., Whiting, S., Schartner, E. P., Monro, T. M., Thompson, J. G., et al. (2015). Boronate probes for the detection of hydrogen peroxide release from human spermatozoa. *Free Radic. Biol. Med.* 81, 69–76. doi: 10.1016/j.freeradbiomed.2015.01.015
- Qian, Y.-Y., Xue, L., Hu, D.-X., Li, G.-P., and Jiang, H. (2012). Quinoline-based fluorescent probe for ratiometric detection of hydrogen peroxide in aqueous solution. *Dyes Pigm.* 95, 373–376. doi: 10.1016/j.dyepig.2012.05.013
- Quin, C., Robertson, L., Mcquaker, S. J., Price, N. C., Brand, M. D., and Hartley, R. C. (2010). Caged mitochondrial uncouplers that are released in response to hydrogen peroxide. *Tetrahedron* 66, 2384–2389. doi: 10.1016/j.tet.2010.01.103
- Rayner, B. S., Love, D. T., and Hawkins, C. L. (2014). Comparative reactivity of myeloperoxidase-derived oxidants with mammalian cells. *Free Radic. Biol. Med.* 71, 240–255. doi: 10.1016/j.freeradbiomed.2014.03.004
- Ren, M., Deng, B., Kong, X., Tang, Y., and Lin, W. (2017). Preparation of a two-photon fluorescent probe for imaging H₂O₂ in lysosomes in living cells and tissues. *Methods Mol. Biol.* 1594, 129–139. doi: 10.1007/978-1-4939-6934-0_7
- Rezende, F., Brandes, R. P., and Schröder, K. (2018). Detection of hydrogen peroxide with fluorescent dyes. *Antioxid. Redox Signal* 29, 585–602. doi: 10.1089/ars.2017.7401
- Rios, N., Piacenza, L., Trujillo, M., Martínez, A., Demicheli, V., Prolo, C., et al. (2016). Sensitive detection and estimation of cell-derived peroxynitrite fluxes using fluorescein-boronate. *Free Radic. Biol. Med.* 101, 284–295. doi: 10.1016/j.freeradbiomed.2016.08.033
- Rios, N., Radi, R., Kalyanaram, B., and Zielonka, J. (2020). Tracking isotopically labeled oxidants using boronate-based redox probes. *J. Biol. Chem.* 295, 6665–6676. doi: 10.1074/jbc.RA120.013402
- Rota, C., Chignell, C. F., and Mason, R. P. (1999). Evidence for free radical formation during the oxidation of 2'-7'-dichlorofluorescein to the fluorescent dye 2'-7'-dichlorofluorescein by horseradish peroxidase: possible implications for oxidative stress measurements. *Free Radic. Biol. Med.* 27, 873–881. doi: 10.1016/S0891-5849(99)00137-9
- Royall, J. A., Gwin, P. D., Parks, D. A., and Freeman, B. A. (1992). Responses of vascular endothelial oxidant metabolism to lipopolysaccharide and tumor necrosis factor- α . *Arch. Biochem. Biophys.* 294, 686–694. doi: 10.1016/0003-9861(92)90742-F
- Salin, K., Auer, S. K., Rudolf, A. M., Anderson, G. J., Cairns, A. G., Mullen, W., et al. (2015). Individuals with higher metabolic rates have lower levels of reactive oxygen species *in vivo*. *Biol. Lett.* 11:20150538. doi: 10.1098/rsbl.2015.0538
- Salin, K., Auer, S. K., Villasevil, E. M., Anderson, G. J., Cairns, A. G., Mullen, W., et al. (2017). Using the MitoB method to assess levels of reactive oxygen species in ecological studies of oxidative stress. *Sci. Rep.* 7:41228. doi: 10.1038/srep41228
- Salin, K., Villasevil, E. M., Anderson, G. J., Auer, S. K., Selman, C., Hartley, R. C., et al. (2018). Decreased mitochondrial metabolic requirements in fasting animals carry an oxidative cost. *Funct. Ecol.* 32, 2149–2157. doi: 10.1111/1365-2435.13125
- Santas, J., Guardiola, F., Rafecas, M., and Bou, R. (2013). Determination of total plasma hydroperoxides using a diphenyl-1-pyrenylphosphine fluorescent probe. *Anal. Biochem.* 434, 172–177. doi: 10.1016/j.ab.2012.11.021
- Sedgwick, A. C., Han, H. H., Gardiner, J. E., Bull, S. D., He, X. P., and James, T. D. (2017). Long-wavelength fluorescent boronate probes for the detection and intracellular imaging of peroxynitrite. *Chem. Commun.* 53, 12822–12825. doi: 10.1039/C7CC07845E
- Sedgwick, A. C., Han, H. H., Gardiner, J. E., Bull, S. D., He, X. P., and James, T. D. (2018). The development of a novel AND logic based fluorescence probe for the detection of peroxynitrite and GSH. *Chem. Sci.* 9, 3672–3676. doi: 10.1039/C8SC00733K
- Sedgwick, A. C., Sun, X., Kim, G., Yoon, J., Bull, S. D., and James, T. D. (2016). Boronate based fluorescence (ESIPT) probe for peroxynitrite. *Chem. Commun.* 52, 12350–12352. doi: 10.1039/C6CC06829D
- Seven, O., Sozmen, F., and Simsek Turan, I. (2017). Self immolative dioxetane based chemiluminescent probe for H₂O₂ detection. *Sensor Actuat. B Chem.* 239, 1318–1324. doi: 10.1016/j.snb.2016.09.120
- Shafirovich, V., and Lyman, S. V. (2002). Nitroxyl and its anion in aqueous solutions: spin states, protic equilibria, and reactivities toward oxygen and nitric oxide. *Proc. Natl. Acad. Sci. U.S.A.* 99, 7340–7345. doi: 10.1073/pnas.112202099
- Shen, Y., Zhang, X., Zhang, Y., Wu, Y., Zhang, C., Chen, Y., et al. (2018). A mitochondria-targeted colorimetric and ratiometric fluorescent probe for hydrogen peroxide with a large emission shift and bio-imaging in living cells. *Sensor Actuat. B Chem.* 255, 42–48. doi: 10.1016/j.snb.2017.08.020
- Shu, W., Wu, Y., Duan, Q., Zang, S., Su, S., Jing, J., et al. (2020a). A highly selective fluorescent probe for monitoring exogenous and endogenous ONOO⁻ fluctuations in HeLa cells. *Dyes Pigm.* 175:108069. doi: 10.1016/j.dyepig.2019.108069
- Shu, W., Wu, Y., Zang, S., Su, S., Kang, H., Jing, J., et al. (2020b). A mitochondria-targeting highly specific fluorescent probe for fast sensing of endogenous peroxynitrite in living cells. *Sensor Actuat. B Chem.* 303:127284. doi: 10.1016/j.snb.2019.127284

- Shu, W., Yan, L., Wang, Z., Liu, J., Zhang, S., Liu, C., et al. (2015). A novel visual and far-red fluorescent dual-channel probe for the rapid and sensitive detection of hypochlorite in aqueous solution and living cells. *Sensor Actuat. B Chem.* 221, 1130–1136. doi: 10.1016/j.snb.2015.07.066
- Sieracki, N. A., Gantner, B. N., Mao, M., Horner, J. H., Ye, R. D., Malik, A. B., et al. (2013). Bioluminescent detection of peroxynitrite with a boronic acid-caged luciferin. *Free Radic. Biol. Med.* 61, 40–50. doi: 10.1016/j.freeradbiomed.2013.02.020
- Sies, H., and Chance, B. (1970). The steady state level of catalase compound I in isolated hemoglobin-free perfused rat liver. *FEBS Lett.* 11, 172–176. doi: 10.1016/0014-5793(70)80521-X
- Sikora, A., Zielonka, J., Adamus, J., Debski, D., Dybala-Defratyka, A., Michalowski, B., et al. (2013). Reaction between peroxynitrite and triphenylphosphonium-substituted arylboronic acid isomers: identification of diagnostic marker products and biological implications. *Chem. Res. Toxicol.* 26, 856–867. doi: 10.1021/tx300499c
- Sikora, A., Zielonka, J., Lopez, M., Dybala-Defratyka, A., Joseph, J., Marcinek, A., et al. (2011). Reaction between peroxynitrite and boronates: EPR spin-trapping, HPLC Analyses, and quantum mechanical study of the free radical pathway. *Chem. Res. Toxicol.* 24, 687–697. doi: 10.1021/tx100439a
- Sikora, A., Zielonka, J., Lopez, M., Joseph, J., and Kalyanaraman, B. (2009). Direct oxidation of boronates by peroxynitrite: mechanism and implications in fluorescence imaging of peroxynitrite. *Free Radic. Biol. Med.* 47, 1401–1407. doi: 10.1016/j.freeradbiomed.2009.08.006
- Smulik, R., Debski, D., Zielonka, J., Michalowski, B., Adamus, J., Marcinek, A., et al. (2014). Nitroxyl (HNO) reacts with molecular oxygen and forms peroxynitrite at physiological pH. *Biol. Impl. J. Biol. Chem.* 289, 35570–35581. doi: 10.1074/jbc.M114.597740
- Smulik-Izidorczyk, R., Mesjasz, A., Gerbich, A., Adamus, J., Michalski, R., and Sikora, A. (2017). A kinetic study on the reactivity of azanone (HNO) toward its selected scavengers: insight into its chemistry and detection. *Nitric Oxide* 69, 61–68. doi: 10.1016/j.niox.2017.05.003
- Smulik-Izidorczyk, R., Rostkowski, M., Gerbich, A., Jarmoc, D., Adamus, J., Leszczyńska, A., et al. (2019). Decomposition of Piloty's acid derivatives - toward the understanding of factors controlling HNO release. *Arch. Biochem. Biophys.* 661, 132–144. doi: 10.1016/j.abb.2018.11.012
- Srikun, D., Albers, A. E., Nam, C. I., Iavarone, A. T., and Chang, C. J. (2010). Organelle-targetable fluorescent probes for imaging hydrogen peroxide in living cells via SNAP-Tag protein labeling. *J. Am. Chem. Soc.* 132, 4455–4465. doi: 10.1021/ja100117u
- Srikun, D., Miller, E. W., Domaille, D. W., and Chang, C. J. (2008). An ICT-based approach to ratiometric fluorescence imaging of hydrogen peroxide produced in living cells. *J. Am. Chem. Soc.* 130, 4596–4597. doi: 10.1021/ja711480f
- Sun, X., Xu, Q., Kim, G., Flower, S. E., Lowe, J. P., Yoon, J., et al. (2014). A water-soluble boronate-based fluorescent probe for the selective detection of peroxynitrite and imaging in living cells. *Chem. Sci.* 5, 3368–3373. doi: 10.1039/C4SC01417K
- Szala, M., Grzelakowska, A., Modrzejewska, J., Siarkiewicz, P., Słowiński, D., Swierczyńska, M., et al. (2020). Characterization of the reactivity of luciferin boronate - a probe for inflammatory oxidants with improved stability. *Dyes Pigm.* 18:108693. doi: 10.1016/j.dyepig.2020.108693
- Talib, J., Maghzal, G. J., Cheng, D., and Stocker, R. (2016). Detailed protocol to assess *in vivo* and *ex vivo* myeloperoxidase activity in mouse models of vascular inflammation and disease using hydroethidine. *Free Radic. Biol. Med.* 97, 124–135. doi: 10.1016/j.freeradbiomed.2016.05.004
- Tang, L., Tian, M., Chen, H., Yan, X., Zhong, K., and Bian, Y. (2018). An ESIPt-based mitochondria-targeted ratiometric and NIR-emitting fluorescent probe for hydrogen peroxide and its bioimaging in living cells. *Dyes Pigm.* 158, 482–489. doi: 10.1016/j.dyepig.2017.12.028
- Tong, H., Zhang, Y., Ma, S., Zhang, M., Wang, N., Wang, R., et al. (2018). A pinacol boronate caged NIAD-4 derivative as a near-infrared fluorescent probe for fast and selective detection of hypochlorous acid. *Chin. Chem. Lett.* 29, 139–142. doi: 10.1016/j.ccl.2017.07.007
- Trujillo, M., Carballal, S., Zeida, A., and Radi, R. (2017). "Comparative analysis of hydrogen peroxide and peroxynitrite reactivity with thiols," in *Hydrogen Peroxide Metabolism in Health and Disease*, eds M. C. M. Visser, M. Hampton, and A. J. Kettle (Boca Raton, FL: CRC Press), 49–79. doi: 10.1201/9781315154831-3
- Truzzi, D. R., and Augusto, O. (2017). "Influence of CO₂ on hydroperoxide metabolism," in *Hydrogen Peroxide Metabolism in Health and Disease*, eds M. C. Visser, M. Hampton, and A. J. Kettle (Boca Raton, FL: CRC Press), 81–99. doi: 10.1201/9781315154831-4
- Van De Bittner, G. C., Bertozzi, C. R., and Chang, C. J. (2013). Strategy for dual-analyte luciferin imaging: *in vivo* bioluminescence detection of hydrogen peroxide and caspase activity in a murine model of acute inflammation. *J. Am. Chem. Soc.* 135, 1783–1795. doi: 10.1021/ja309078t
- Van De Bittner, G. C., Dubikovskaya, E. A., Bertozzi, C. R., and Chang, C. J. (2010). *In vivo* imaging of hydrogen peroxide production in a murine tumor model with a chemoselective bioluminescent reporter. *Proc. Natl. Acad. Sci. U.S.A.* 107, 21316–21321. doi: 10.1073/pnas.1012864107
- Wang, C., Wang, Y., Wang, G., Huang, C., and Jia, N. (2020). A new mitochondria-targeting fluorescent probe for ratiometric detection of H₂O₂ in live cells. *Anal. Chim. Acta* 1097, 230–237. doi: 10.1016/j.aca.2019.11.024
- Wang, G., Wang, Y., Wang, C., Huang, C., and Jia, N. (2020). A new long-wavelength fluorescent probe for tracking peroxynitrite in live cells and inflammatory sites of zebrafish. *Analyst* 145, 828–835. doi: 10.1039/C9AN01934K
- Wang, H., He, Z., Yang, Y., Zhang, J., Zhang, W., Zhang, W., et al. (2019). Ratiometric fluorescence imaging of Golgi H(2)O(2) reveals a correlation between Golgi oxidative stress and hypertension. *Chem. Sci.* 10, 10876–10880. doi: 10.1039/C9SC04384E
- Wang, Q., Liu, C., Chang, J., Lu, Y., He, S., Zhao, L., et al. (2013). Novel water soluble styrylquinolinium boronic acid as a ratiometric reagent for the rapid detection of hypochlorite ion. *Dyes Pigm.* 99, 733–739. doi: 10.1016/j.dyepig.2013.06.019
- Wang, Z., Wu, L., Wang, Y., Zhang, M., Zhao, Z., Liu, C., et al. (2019). A highly selective and ultrasensitive ratiometric fluorescent probe for peroxynitrite and its two-photon bioimaging applications. *Anal. Chim. Acta* 1049, 219–225. doi: 10.1016/j.aca.2018.05.064
- Wardman, P. (2007). Fluorescent and luminescent probes for measurement of oxidative and nitrosative species in cells and tissues: progress, pitfalls, and prospects. *Free Radic. Biol. Med.* 43, 995–1022. doi: 10.1016/j.freeradbiomed.2007.06.026
- Weber, M., Mackenzie, A. B., Bull, S. D., and James, T. D. (2018). Fluorescence-based tool to detect endogenous peroxynitrite in M1-polarized murine J774.2 macrophages. *Anal. Chem.* 90, 10621–10627. doi: 10.1021/acs.analchem.8b03035
- Weber, M., Yamada, N., Tian, X., Bull, S. D., Minoshima, M., Kikuchi, K., et al. (2020). Sensing peroxynitrite in different organelles of murine RAW264.7 macrophages with coumarin-based fluorescent probes. *Front. Chem.* 8:39. doi: 10.3389/fchem.2020.00039
- Wen, Y., Liu, K., Yang, H., Li, Y., Lan, H., Liu, Y., et al. (2014). A highly sensitive ratiometric fluorescent probe for the detection of cytoplasmic and nuclear hydrogen peroxide. *Anal. Chem.* 86, 9970–9976. doi: 10.1021/ac502909c
- Wen, Y., Liu, K., Yang, H., Liu, Y., Chen, L., Liu, Z., et al. (2015). Mitochondria-directed fluorescent probe for the detection of hydrogen peroxide near mitochondrial DNA. *Anal. Chem.* 87, 10579–10584. doi: 10.1021/acs.analchem.5b03326
- Winterbourn, C. C. (2002). Biological reactivity and biomarkers of the neutrophil oxidant, hypochlorous acid. *Toxicology* 181–182, 223–227. doi: 10.1016/S0300-483X(02)00286-X
- Winterbourn, C. C. (2013). The biological chemistry of hydrogen peroxide. *Meth. Enzymol.* 528, 3–25. doi: 10.1016/B978-0-12-405881-1.00001-X
- Winterbourn, C. C. (2014). The challenges of using fluorescent probes to detect and quantify specific reactive oxygen species in living cells. *Biochim. Biophys. Acta* 1840, 730–738. doi: 10.1016/j.bbagen.2013.05.004
- Wrona, M., Patel, K., and Wardman, P. (2005). Reactivity of 2',7'-dichlorodihydrofluorescein and dihydrodichlorodamine 123 and their oxidized forms toward carbonate, nitrogen dioxide, and hydroxyl radicals. *Free Radic. Biol. Med.* 38, 262–270. doi: 10.1016/j.freeradbiomed.2004.10.022
- Wrona, M., Patel, K. B., and Wardman, P. (2008). The roles of thiol-derived radicals in the use of 2',7'-dichlorodihydrofluorescein as a probe for oxidative stress. *Free Radic. Biol. Med.* 44, 56–62. doi: 10.1016/j.freeradbiomed.2007.09.005
- Wu, D., Chen, L. Y., Xu, Q. L., Chen, X. Q., and Yoon, J. Y. (2019). Design principles, sensing mechanisms, and applications of highly specific

- fluorescent probes for HOCl/OCI-. *Acc. Chem. Res.* 52, 2158–2168. doi: 10.1021/acs.accounts.9b00307
- Wu, L., Han, H. H., Liu, L., Gardiner, J. E., Sedgwick, A. C., Huang, C., et al. (2018a). ES IPT-based fluorescence probe for the rapid detection of peroxynitrite 'AND' biological thiols. *Chem. Commun.* 54, 11336–11339. doi: 10.1039/C8CC06917D
- Wu, L., Tian, X., Han, H.-H., Wang, J., Groleau, R. R., Tosuwan, P., et al. (2019). A simple near-infrared fluorescent probe for the detection of peroxynitrite. *ChemistryOpen* 8, 1407–1409. doi: 10.1002/open.201900301
- Wu, L., Wang, Y., Weber, M., Liu, L., Sedgwick, A. C., Bull, S. D., et al. (2018b). ES IPT-based ratiometric fluorescence probe for the intracellular imaging of peroxynitrite. *Chem. Commun.* 54, 9953–9956. doi: 10.1039/C8CC04919J
- Wu, W., Li, J., Chen, L., Ma, Z., Zhang, W., Liu, Z., et al. (2014). Bioluminescent probe for hydrogen peroxide imaging *in vitro* and *in vivo*. *Anal. Chem.* 86, 9800–9806. doi: 10.1021/ac502396g
- Wu, Y. P., Chew, C. Y., Li, T. N., Chung, T. H., Chang, E. H., Lam, C. H., et al. (2018). Target-activated streptavidin-biotin controlled binding probe. *Chem. Sci.* 9, 770–776. doi: 10.1039/C7SC04014H
- Xia, L., Tong, Y., Li, L., Cui, M., Gu, Y., and Wang, P. (2019). A selective fluorescent turn-on probe for imaging peroxynitrite in living cells and drug-damaged liver tissues. *Talanta* 204, 431–437. doi: 10.1016/j.talanta.2019.06.032
- Xiao, H., Li, P., Hu, X., Shi, X., Zhang, W., and Tang, B. (2016). Simultaneous fluorescence imaging of hydrogen peroxide in mitochondria and endoplasmic reticulum during apoptosis. *Chem. Sci.* 7, 6153–6159. doi: 10.1039/C6SC01793B
- Xu, J., Li, Q., Yue, Y., Guo, Y., and Shao, S. (2014). A water-soluble BODIPY derivative as a highly selective "Turn-On" fluorescent sensor for H₂O₂ sensing *in vivo*. *Biosens. Bioelectron.* 56, 58–63. doi: 10.1016/j.bios.2013.12.065
- Xu, J., Zhang, Y., Yu, H., Gao, X., and Shao, S. (2016). Mitochondria-Targeted Fluorescent Probe for Imaging Hydrogen Peroxide in Living Cells. *Anal. Chem.* 88, 1455–1461. doi: 10.1021/acs.analchem.5b04424
- Xu, W., Zeng, Z., Jiang, J. H., Chang, Y. T., and Yuan, L. (2016). Discerning the chemistry in individual organelles with small-molecule fluorescent probes. *Angew. Chem. Int. Ed. Engl.* 55, 13658–13699. doi: 10.1002/anie.201510721
- Yik-Sham Chung, C., Timblin, G. A., Saijo, K., and Chang, C. J. (2018). Versatile histochemical approach to detection of hydrogen peroxide in cells and tissues based on puromycin staining. *J. Am. Chem. Soc.* 140, 6109–6121. doi: 10.1021/jacs.8b02279
- Yin, H. Y., Xu, L. B., and Porter, N. A. (2011). Free radical lipid peroxidation: mechanisms and analysis. *Chem. Rev.* 111, 5944–5972. doi: 10.1021/cr200084z
- Yu, F., Song, P., Li, P., Wang, B., and Han, K. (2012). A fluorescent probe directly detect peroxynitrite based on boronate oxidation and its applications for fluorescence imaging in living cells. *Analyst* 137, 3740–3749. doi: 10.1039/c2an35246j
- Yuan, L., Lin, W., Zhao, S., Gao, W., Chen, B., He, L., et al. (2012). A unique approach to development of near-infrared fluorescent sensors for *in vivo* imaging. *J. Am. Chem. Soc.* 134, 13510–13523. doi: 10.1021/ja305802v
- Zeida, A., Trujillo, M., Ferrer-Sueta, G., Denicola, A., Estrin, D. A., and Radi, R. (2019). Catalysis of peroxide reduction by fast reacting protein thiols. *Chem. Rev.* 119, 10829–10855. doi: 10.1021/acs.chemrev.9b00371
- Zhan, X. Q., Su, B. Y., Zheng, H., and Yan, J. H. (2010). Sensing hydrogen peroxide involving intramolecular charge transfer pathway: a boronate-functioned styryl dye as a highly selective and sensitive naked-eye sensor. *Anal. Chim. Acta* 658, 175–179. doi: 10.1016/j.aca.2009.11.013
- Zhang, J., Li, Y., Zhao, J., and Guo, W. (2016). An arylboronate-based fluorescent probe for selective and sensitive detection of peroxynitrite and its applications for fluorescence imaging in living cells. *Sensor Actuat. B Chem.* 237, 67–74. doi: 10.1016/j.snb.2016.06.054
- Zhang, J., Shi, L., Li, Z., Li, D., Tian, X., and Zhang, C. (2019). Near-infrared fluorescence probe for hydrogen peroxide detection: design, synthesis, and application in living systems. *Analyst* 144, 3643–3648. doi: 10.1039/C9AN00385A
- Zhang, K., Wu, W., Li, Y., Sun, M., Yu, H., and Wong, M. S. (2016). Carbazole-based two-photon fluorescent probe for selective imaging of mitochondrial hydrogen peroxide in living cells and tissues. *RSC Adv.* 6, 115298–115302. doi: 10.1039/C6RA21260C
- Zhang, R., Song, B., and Yuan, J. L. (2018). Bioanalytical methods for hypochlorous acid detection: recent advances and challenges. *Trac. Trends Anal. Chem.* 99, 1–33. doi: 10.1016/j.trac.2017.11.015
- Zhang, W., Liu, W., Li, P., Huang, F., Wang, H., and Tang, B. (2015). Rapid-response fluorescent probe for hydrogen peroxide in living cells based on increased polarity of C–B bonds. *Anal. Chem.* 87, 9825–9828. doi: 10.1021/acs.analchem.5b02194
- Zhou, J., Li, Y., Shen, J., Li, Q., Wang, R., Xu, Y., et al. (2014). A ratiometric fluorescent probe for fast and sensitive detection of peroxynitrite: a boronate ester as the receptor to initiate a cascade reaction. *RSC Adv.* 4, 51589–51592. doi: 10.1039/C4RA10048D
- Zhu, B., Jiang, H., Guo, B., Shao, C., Wu, H., Du, B., et al. (2013). A highly selective ratiometric fluorescent probe for hydrogen peroxide displaying a large emission shift. *Sensor Actuat. B Chem.* 186, 681–686. doi: 10.1016/j.snb.2013.06.058
- Zhu, B., Wu, L., Wang, Y., Zhang, M., Zhao, Z., Liu, C., et al. (2018). A highly selective and ultrasensitive ratiometric far-red fluorescent probe for imaging endogenous peroxynitrite in living cells. *Sensor Actuat. B Chem.* 259, 797–802. doi: 10.1016/j.snb.2017.12.135
- Zhu, D., Li, G., Xue, L., and Jiang, H. (2013). Development of ratiometric near-infrared fluorescent probes using analyte-specific cleavage of carbamate. *Org. Biomol. Chem.* 11, 4577–4580. doi: 10.1039/c3ob40932e
- Zhu, H., Fan, J., Du, J., and Peng, X. (2016). Fluorescent probes for sensing and imaging within specific cellular organelles. *Acc. Chem. Res.* 49, 2115–2126. doi: 10.1021/acs.accounts.6b00292
- Zielonka, J., Cheng, G., Zielonka, M., Ganesh, T., Sun, A., Joseph, J., et al. (2014). High-throughput assays for superoxide and hydrogen peroxide: design of a screening workflow to identify inhibitors of NADPH oxidases. *J. Biol. Chem.* 289, 16176–16189. doi: 10.1074/jbc.M114.548693
- Zielonka, J., Hardy, M., Michalski, R., Sikora, A., Zielonka, M., Cheng, G., et al. (2017a). Recent developments in the probes and assays for measurement of the activity of NADPH oxidases. *Cell Biochem. Biophys.* 75, 335–349. doi: 10.1007/s12013-017-0813-6
- Zielonka, J., Joseph, J., Sikora, A., Hardy, M., Ouari, O., Vasquez-Vivar, J., et al. (2017b). Mitochondria-targeted triphenylphosphonium-based compounds: syntheses, mechanisms of action, and therapeutic and diagnostic applications. *Chem. Rev.* 117, 10043–10120. doi: 10.1021/acs.chemrev.7b00042
- Zielonka, J., Joseph, J., Sikora, A., and Kalyanaraman, B. (2013a). "Chapter nine - real-time monitoring of reactive oxygen and nitrogen species in a multiwell plate using the diagnostic marker products of specific probes," in *Methods in Enzymology*, eds E. Cadenas and L. Packer (San Diego, CA: Academic Press), 145–157. doi: 10.1016/B978-0-12-405883-5.00009-0
- Zielonka, J., Lambeth, J. D., and Kalyanaraman, B. (2013b). On the use of L-012, a luminol-based chemiluminescent probe, for detecting superoxide and identifying inhibitors of NADPH oxidase: a reevaluation. *Free Radic. Biol. Med.* 65, 1310–1314. doi: 10.1016/j.freeradbiomed.2013.09.017
- Zielonka, J., Podsiadly, R., Zielonka, M., Hardy, M., and Kalyanaraman, B. (2016a). On the use of peroxy-caged luciferin (PCL-1) probe for bioluminescent detection of inflammatory oxidants *in vitro* and *in vivo* - identification of reaction intermediates and oxidant-specific minor products. *Free Radic. Biol. Med.* 99, 32–42. doi: 10.1016/j.freeradbiomed.2016.07.023
- Zielonka, J., Sikora, A., Adamus, J., and Kalyanaraman, B. (2015). Detection and differentiation between peroxynitrite and hydroperoxides using mitochondria-targeted arylboronic acid. *Methods Mol. Biol.* 1264, 171–181. doi: 10.1007/978-1-4939-2257-4_16
- Zielonka, J., Sikora, A., Hardy, M., Joseph, J., Dranka, B. P., and Kalyanaraman, B. (2012a). Boronate probes as diagnostic tools for real time monitoring of peroxynitrite and hydroperoxides. *Chem. Res. Toxicol.* 25, 1793–1799. doi: 10.1021/tx300164j
- Zielonka, J., Sikora, A., Joseph, J., and Kalyanaraman, B. (2010). Peroxynitrite is the major species formed from different flux ratios of co-generated nitric oxide and superoxide: direct reaction with boronate-based fluorescent probe. *J. Biol. Chem.* 285, 14210–14216. doi: 10.1074/jbc.M110.110080

- Zielonka, J., Zielonka, M., Cheng, G., Hardy, M., and Kalyanaraman, B. (2019). High-throughput screening of NOX inhibitors. *Methods Mol. Biol.* 1982, 429–446. doi: 10.1007/978-1-4939-9424-3_25
- Zielonka, J., Zielonka, M., Sikora, A., Adamus, J., Joseph, J., Hardy, M., et al. (2012b). Global profiling of reactive oxygen and nitrogen species in biological systems: high-throughput real-time analyses. *J. Biol. Chem.* 287, 2984–2995. doi: 10.1074/jbc.M111.309062
- Zielonka, J., Zielonka, M., Verplank, L., Cheng, G., Hardy, M., Ouari, O., et al. (2016b). Mitigation of NADPH oxidase 2 activity as a strategy to inhibit peroxynitrite formation. *J. Biol. Chem.* 291, 7029–7044. doi: 10.1074/jbc.M115.702787

Conflict of Interest: The authors declare that the research was conducted in the absence of any commercial or financial relationships that could be construed as a potential conflict of interest.

Copyright © 2020 Sikora, Zielonka, Dębowska, Michalski, Smulik-Izydorzyc, Pięta, Podsiadły, Artelska, Pierzchała and Kalyanaraman. This is an open-access article distributed under the terms of the Creative Commons Attribution License (CC BY). The use, distribution or reproduction in other forums is permitted, provided the original author(s) and the copyright owner(s) are credited and that the original publication in this journal is cited, in accordance with accepted academic practice. No use, distribution or reproduction is permitted which does not comply with these terms.